Ethylene Production by Oxidative Coupling of Methane: New Process Flow Diagram Based on Adsorptive Separation

vorgelegt von
M.Sc.
Xuan Son Nghiem
aus Hanoi, S. R. Vietnam

von der Fakultät III – Prozesswissenschaften
der Technischen Universität Berlin
zur Erlangung des akademischen Grades
Doktor der Ingenieurwissenschaften
- Dr.-Ing -

genehmigte Dissertation

Promotionsausschuss:

Vorsitzender:	Prof. Dr.-Ing. habil. George Tsatsaronis
Gutachter:	Prof. Dr.-Ing. habil. Günter Wozny
Gutachter:	Prof. Dr.-Ing. habil. Jens-Uwe Repke

Tag der wissenschaftlichen Aussprache: 14. 03. 2014

Berlin 2014

D 83

Abstract

Ethylene is the most produced petrochemical with about 140 million tonnes annual production and nearly 300 million tonnes annual carbon dioxide emission. In recent years, record price of crude oil – the origin of more than 50% ethylene worldwide – has put naphtha-based producers in a very tough position, especially the ones in region with strict emission regulation such as Europe. Meanwhile 150 billion cubic meters of methane are flared or vented every year due to transport and store difficulty, emitting about 400 million tonnes of carbon dioxide. In this situation, oxidative coupling of methane (OCM), the reaction directly converts methane into ethylene, seems to be a sustainable solution for both short-term oil price and long-term environment preservation.

Unfortunately, OCM process in present state of the art is still considered inadequate for industrial application. Most researches in this topic have been focusing on improving the performance of OCM reactor, which is only a part (though important) of a plant. This work aims at a comprehensive development of the whole process which, in combination with available OCM reactors, can make this technology a decent choice for commercial ethylene production.

The diversity of ethylene plants (naphtha cracking, ethane cracking, coal-to-olefin…) means there is no universally superior option. Finding an application for OCM requires comparing it with other technologies, pointing out the condition under which OCM can bring relative improvement. Since OCM is not a mature technology yet, it is only mentioned briefly in reviews of ethylene production alternatives while researches on OCM tend to focus on this process alone rather than comparison with others. Hence, the first chapter of this thesis reviews different means of ethylene production and methane conversion. The gap

between their limitations is the place where OCM can be employed for a better use of natural resource.

Despite the abundant supply of methane, OCM is still not selected because ethylene produced by this technology is more expensive than by other alternatives. In the second chapter, production cost of ethylene by OCM is estimated as a function of ethylene yield and selectivity as well as prices of raw material and utilities required for plant operation. The estimated production cost can be compare with the production cost by other technologies to decide if OCM should be considered for a new ethylene plant or not. The attained function can be used to analyse the sensitivity of production cost against reactor performance, raw material and energy prices. Cost estimation also revealed cryogenic distillation as the bottle-neck in process flow diagram. Different substitutes are reviewed and a new process flow diagram based on adsorptive separation is synthesised conceptually. Also proposed in this chapter are solutions for by products and unreacted methane. The amount of these substances is significant due to low conversion and selectivity of OCM reactor.

In the next chapter, the proposal is analysed quantitatively by simulation. Two representative sorbents are tested: zeolite and activated carbon. Simulation result provides information for sorbent selection, process operation and final decision on process flow diagram.

The proposal is finally validated by experiment. Calculation based on scaling up experiment result proves that when combines with state of the art OCM reactors the proposal can be competitive enough to replace naphtha cracking in region with low-priced natural gas supply such as North America.

Zusammenfassung

Äthylen ist die am meisten produzierte Petrochemie mit ungefähr 140 Millionen Tonnen Jahresproduktion und fast 300 Millionen Tonnen jährlich Kohlendioxid-Emissionen. In den letzten Jahren hat der Rekordpreis von Rohöl – die Herkunft von mehr als 50 % Äthen weltweit ist Naphtha basierend – die Hersteller wie zum Beispiel die in Europa in eine sehr schwierigen Lage gesetzt. Inzwischen werden jedes Jahr 150 Milliarden Kubikmeter Methan wegen Transportschwierigkeiten abgefackelt oder abgelassen und etwa 400 Millionen Tonnen Kohlendioxid emittieren. In dieser Situation scheint Oxydative Kupplung von Methan (OCM), die Reaktion die Methan in Äthylen direkt umwandelt, eine nachhaltige Lösung des kurzfristigen hohen Ölpreises und der langfristige Erhaltung der Umwelt zu sein.

Leider ist der OCM Prozess im derzeitigen Stand der Technik noch unzureichend für die industrielle Anwendung. Die meisten Untersuchungen zu diesem Thema haben sich auf die Verbesserung des OCM Reaktors, der zwar ein wichtiger aber nicht alleinbestimmender Teil der Anlage ist, konzentriert. Diese Arbeit zielt auf eine umfassende Entwicklung des ganzen Prozesses, die zusammen mit verfügbaren OCM Reaktoren eine gute Wahl für die kommerzielle Äthylenherstellung sein kann.

Die Vielfalt der Äthylen-Anlagen (Naphtha-Cracken, Ethan-Cracken, Kohle-zu-Olefin...) bedeutet, dass es keine allgemeine überlegene Option gibt. Die Suche nach einem Übergang auf OCM zur Äthylenherstellung erfordert einen Vergleich mit anderen Technologien und den Hinweis auf die Bedingung, unter der OCM eine bessere Lösung erzielen kann. OCM wird derzeitig nur kurz in Bewertungen von modernen Äthylen Produktionsalternativen erwähnt, weil es noch keine ausgereifte Technologie ist. Forschungen zu OCM neigen dazu, sich auf diesen Prozess allein aber nicht im Vergleich zu Alternativen zu konzentrieren. Daher bewerten die ersten Kapitel in der vorgelegten Arbeit verschiedene Varianten zur

Äthylenherstellung und Methanumwandlung. OCM kann die bestehenden Technologien ergänzen, um in Zukunft zur besseren Nutzung der natürlichen Ressourcen beizutragen.

Trotz großer Vorkommen und Reserven von Methan ist OCM noch nicht kommerzialisiert worden, weil die Äthylenherstellung durch diese Technologie teurer als durch andere Alternativen ist. Im zweiten Kapitel werden die Produktionskosten von Äthylen durch OCM als Funktion von Äthylen Ausbeute und Selektivität sowie Rohstoffpreise und Betriebsmedienpreise geschätzt. Die geschätzten Produktionskosten können mit den aktuellen Produktionskosten verglichen werden, um zu entscheiden, ob OCM für eine neue Äthylen-Anlage berücksichtigt werden sollte. Die entwickelt Kostenfunktionen können verwendet werden, um die Empfindlichkeit der Produktionskosten gegen Reaktorleistung, Rohstoff- und Energiepreise zu analysieren. Die Kostenschätzung ergab auch, dass die kryogene Destillation der Hauptkostentreiber ist. Verschiedene Alternativen für die Kryotechnik werden berücksichtigt und ein neues Verfahrensfließbild mit adsorptiver Trennung wurde konzeptioniert und anschließend analysiert. In diesem Kapitel werden auch Lösungen für die Verwendung der Nebenprodukte und des nicht umgewandelten Methans vorgeschlagen. Die Menge dieser Stoffe ist bedeutsam aufgrund des niedrigen Umsatzes und Selektivität des OCM Reaktors.

In dem nächsten Kapitel wird der entwickelte Lösungsvorschlag durch Simulation quantitativ detailliert analysiert. Zwei repräsentative Adsorptionsmittel wurden getestet: Zeolith und Aktivkohle. Simulationsergebnisse liefern detaillierte Informationen für die Adsorptionsmittelauswahl, den Prozessbetrieb und führen zu einer Entwicklung eines neuen Verfahrensfließbildes.

Der Prozessvorschlag wurde schließlich durch Experimente bestätigt. Das Versuchsergebnis beweist, dass der Vorschlag zusammen mit neuen OCM Reaktoren das Naphtha-Cracken in der Region mit preisgünstiger Erdgasversorgung wirtschaftlich ersetzen kann.

Acknowledgement

I would like to express the deepest gratitude to my supervisor, Prof. Günter Wozny for his continual support and guidance throughout this work.

I am especially indebted to Prof. Tran Trung Kien and Prof. Harvey Arellano-Garcia for introducing me to the group of Prof. Wozny and my research topic.

I am deeply grateful to my dear friends Daniel, Duc, Hamid, Setareh, Shankui, Stanislav and Xiaodan for their encouragement in hard times and the excellent working atmosphere during my study in Berlin.

I also want to thank all other members of DBTA without whom I could not complete this thesis, especially Dietmar, Max, Philipp and Steffen for the great experimental setup.

The financial assistance from Deutscher Akademischer Austauschdienst is sincerely appreciated.

Contents

List of Figures

List of Tables

Nomenclature

Symbol	Unit	Dimension	Description
		Latin letters	
a			Decaying factor
b_1	1/Pa	$M^{-1}L^{1}T^{2}$	Langmuir coefficient of first site
b_2	1/Pa	$M^{-1}L^{1}T^{2}$	Langmuir coefficient of second site
B	m^2	L^2	Permeability coefficient
c	mol/m^3	L^{-3}	Gas phase concentration
Cp	J/(mol.K)	$ML^2T^{-2}\Theta^{-1}$	Gas specific heat capacity
Cp_s	J/(kg.K)	$L^2T^{-2}\Theta^{-1}$	Sorbent specific heat capacity
d_p	m	L	Particle diameter
D_{bed}	m	L	Bed diameter
D	m^2/s	L^2T^{-1}	Diffusion coefficient
f	mol/m^2s	$L^{-2}T^{-1}$	Flux
k_V	m^3/h	L^3T^{-1}	Flow coefficient
l	m	L	Bed length
m	kg/m^3	ML^{-3}	Sorbent density
M	g/mol	M	Molecular weight
n_c			Number of components
p	Pa	$ML^{-1}T^{-2}$	Pressure
s	1/s	T^{-1}	Adsorption rate
t	s	T	Time
u	m/s	LT^{-1}	Gas velocity

x	m	L	Dimension x along adsorption bed
q	mol/m^3	L^{-3}	Solid phase concentration
Q_1	mol/m^3	L^{-3}	Saturated solid phase concentration of site 1
Q_2	mol/m^3	L^{-3}	Saturated solid phase concentration of site 2
r	m	L	Crystal radius
r_p	m	L	Particle radius
R	J/(mol.K)	ML^{2}T^{-2}Θ^{-1}	Gas constant
S			Selectivity based on number of carbon
T	K	T	Temperature
X			Conversion based on number of carbon
Y			Yield based on number of carbon
		Greek letters	
α	1/K	Θ^{-1}	Thermal expansion coefficient
ΔH	J/mol	ML^{2}T^{-2}	Adsorption enthalpy
ε			Void fraction
μ	Pa.s	ML^{-1}T^{-1}	Gas viscosity
		Subscripts	
i			Component i
		Superscripts	
k			Node k of spatial mesh
in			Inlet
		Abbreviations	
ASU			Air Separation Unit
bpd			Barrel Per Day

C_2	Ethane and ethylene
C_{2+}	Ethane, ethylene and higher hydrocarbons
CE PCI	Chemical Engineering Plant Cost Index
COP	Coefficient Of Performance
CTO	Coal-To-Olefins
DEA	DiEthanolAmine
DRI	Direct Reduced Iron
GGFR	Global Gas Flaring Reduction
GTL	Gas-To-Liquids
IR	InfraRed
MEA	MonoEthanolAmine
MFC	Mass Flow Controller
MFM	Mass Flow Meter
MMbpd	Million barrels per day
MTO	Methanol-To-Olefins
OCM	Oxidative Coupling of Methane
PSA	Pressure Swing Adsorption
PWM	Pulse Width Modulation
RPSA	Rapid Pressure Swing Adsorption
TPD	Temperature Program Desorption
TSA	Thermal Swing Adsorption

Chapter 1. Introduction

The author started this project in 2009, one year after the national recession of United States spread worldwide. By now it still lasts in some big economies such as Italy, Spain while others are struggling with recovering. Although financial sector is more concerned, petroleum industry also involved as both victim and culprit: oil price increase has been argued as a significant cause of United States recession (Hamilton, 2009) while fifteen refineries have been shutdown in Western Europe since 2008 (Kent & Werber, 2013). This is not a surprise as the importance of petroleum in modern world is well-known. We have learnt a lot from the first and second oil crises and since then many efforts have been made to mitigate the next one by finding substitutes for petroleum products, both fuels and petrochemicals. Thanks to the promotion from both manufacturers and law makers, renewable energy is gaining bigger share in both electricity generation and transport fuels. On the other hand, petrochemicals are still largely from fossil resources as 60% global feedstock of ethylene – the most produced petrochemical – is from oil (2008).

Through crisis, each country has its own way to survive the oil price. For example, Braskem run a 200 000 t/y green ethylene plant in Brazil since 2010, taking the advantage of the surplus supplies of sugarcane. China – the largest coal producer in the world – set a goal of producing 20% of their ethylene from diversified sources, which practically means coal, by 2015. In China UOP alone has licensed their advanced methanol-to-olefins (MTO) technology to four plants with total capacity at ca. 2 Mt/y. The shale gas boom in United States, thanks to advances in hydraulic fracturing, encourages ethylene producers to switch from naphtha to natural gas liquid – mainly ethane cracking. By 2008, ethane was already the biggest ethylene feedstock in US (Seddon, 2010).

All solutions above have however their own limitations.

Green ethylene from ethanol meets both economic and ecologic criteria but is hardly applicable outside Brazil, the only sustainable bio-fuel economy with vast cultivable land, suitable climate and advanced technology.

Coal-to-olefin (CTO) technology is opposite. It produces much pollution while large energy consumption and initial investment make the economic viability doubtful without high oil price. The property in common with bio-ethanol dehydration is that it also requires at the same time some exclusive conditions: very high coal supply, very high ethylene demand but low emission standard.

Compare to the others ethane cracking is more widely applicable with the increasing share of ethane in global feedstock. Although the carbon footprint of ethane crackers is larger than naphtha crackers, their limitation comes from another problem: the source of ethane. Shale gas and natural gas in general consist of mostly methane while ethane only makes up 10 %wt. or less. With typical cracking selectivity at 80%, this means one tonne of ethylene production requires more than ten tonnes of methane extraction from underground. Methane is the cleanest fossil fuel but also most expensive in term of transportation, which practically requires pipelines. In US only, ethane production grew 40% in 1984 – 2008 period and another 40% to nearly 1 MMbpd in 2008 – 2012 period (Cantrell, et al., 2013), which means natural gas production is about 10 MMbpd. The consequence is natural gas is flared in many areas due to the lack of pipeline capacity. For example over half a million m^3/day STP was flared in North Dakota in June 2012 (Curtis & Ware, 2012). According to Global Gas Flaring Reduction (GGFR) partnership, a World Bank-led initiative, 150 billion m^3/y of natural gas are being flared or vented (World Bank, 2013). This is equivalent to 25% of United States' gas consumption, 30% of European Union's gas consumption and more than the combined gas consumption of Central and South America. It is not only a huge waste of resource but also a tremendous harm to environment with about 400 Mt/y of carbon dioxide emission.

Technically the simplest solution for over mined methane is building more pipelines. Pipeline network expansion however meets many obstacles because it requires lots of land spreading in a long distance and thus raises serious concern about environment and safety. A famous example is the case of Keystone XL: the pipeline extension through North Dakota was proposed in 2008 (Lincoln Journal-Star, 2008) but has not been started until now (Trans Canada, 2013), making the doubt among relevant companies that it will ever be built (Lefebvre, 2013).

The other solution is onsite conversion of methane into ethylene or other higher value hydrocarbon. There are two ways to do this: direct or indirect. Indirect technologies such as gas-to-liquids (GTL) also convert raw material into syngas like CTO then from syngas produce methanol, dimethyl ether and higher hydrocarbons. An example of salvation effort with GTL is the mega project of Sasol in Louisiana: a 1.5 Mt/y ethane cracker combine with a 96 000 bpd (4 Mt/y) GTL plant (Sasol, 2013). The cracker is under construction but the final decision on the GTL plant will only be made in 2014, the estimated building cost has risen from $8 – $9 billion at the beginning to $11 – $14 billion. Meanwhile the plan to build a 48 000 bpd GTL plant in Alberta has been put on hold (Sasol Canada, 2013). Talisman Energy – their Canadian partner – exited the project after participating in the feasibility study in 2012 (Talisman Energy, 2012). Another example is Pearl plant, the largest GTL plant in the world owned by Shell and Government of the State Qatar. The 140 000 bpd plant costs $19 billion and is considered profitable with free gas supply from North Field – the world's largest single non-associated gas field according to Shell (Shell, 2012). Despite this success, they still announce that the company will stop pursuing the proposed 140 000 bpd GTL project in Louisiana (Royal Dutch Shell plc, 2013). The reasons are "development cost of such a project" and "uncertainties on long-term oil and gas prices and differentials". These obstacles also hold true for any other company and make GTL a risky investment.

Direct conversion of methane requires fewer steps and therefore less capital cost. The simplest reaction is thermal dehydrogenation but the high stability of methane molecule makes the process difficult. Yet no feasible result on methane thermal dehydrogenation has been reported. The newest attempt is the joint project between BASF, The Linde Group and ThyssenKrupp (The Linde Group, 2013). They aimed at thermally decomposing methane into hydrogen and solid carbon and later using hydrogen to produce syngas and consume carbon dioxide from other processes. The project started on July 1, 2013 and is expected to last three years.

Another alternative of direct conversion is oxidative dehydrogenation, which is better known as oxidative coupling of methane (OCM). With the presence of oxidant, methane reacts at lower temperature and produces different products depend on reaction condition and the availability of oxidant. So far carbon dioxide and oxygen are two oxidants that get the most attention. Using carbon dioxide prevents full combustion of methane and opens the chance to reduce carbon footprint from other processes. Useful products are higher hydrocarbon such as ethylene or syngas in dry reforming process. Unfortunately achieved results (Asami, et al., 1995) (Chen, et al., 1996) (Asami, et al., 1997) (Wang, et al., 1998) (Wang, et al., 1998) (Wang, et al., 1999) (Wang & Ohtsuka, 2000) (Wang & Ohtsuka, 2001) (Cai, et al., 2003) (Wang & Zhu, 2004) are not good enough to be applied in commercial production.

Compare to carbon dioxide, oxygen is the stronger oxidant and can convert methane more effectively. Since Keller et al. pioneered in this area (Keller & Bhasin, 1982), much effort has been spent on developing the suitable catalysts and reactors for producing ethylene from methane and oxygen:

$$2CH_4 + O_2 \rightarrow C_2H_4 + 2H_2O \qquad (1.1)$$

Although there are different explanations about mechanism, the common is the formation of ethane via methane coupling follow by the formation of ethylene via ethane dehydrogenation:

$$4CH_4 + O_2 \rightarrow 2C_2H_6 + 2H_2O \quad (1.2)$$

$$C_2H_6 \rightarrow C_2H_4 + H_2 \quad (1.3)$$

The draw back of using oxygen is the combustion of methane and products:

$$CH_4 + 2O_2 \rightarrow CO_2 + 2H_2O \quad (1.4)$$

$$2C_2H_6 + 7O_2 \rightarrow 4CO_2 + 6H_2O \quad (1.5)$$

$$C_2H_4 + 3O_2 \rightarrow 2CO_2 + 2H_2O \quad (1.6)$$

$$2H_2 + O_2 \rightarrow 2H_2O \quad (1.7)$$

Carbon monoxide is also produced via partial oxidation or water-gas shift reaction. Coke formation can also happen and deactivate catalyst but it is mitigate by the presence of steam. Other products such as acetylene, propylene, benzene, methanol,… are also produced at small rates. Since OCM process involves ethane dehydrogenation, its performance cannot surpass ethane cracking and is actually much inferior because of undesired reactions (1.4) – (1.6). State of the art performance, ~50% ethylene selectivity at ~40% methane conversion (in a recent publication (Godini, et al., 2014) 20.3% ethylene yield and 52.5% ethylene selectivity were achieved), is no match to the typical performance of ethane cracker: ~80% ethylene yield at 60 – 75% ethane conversion. OCM therefore cannot compete with ethane cracking as an economic method of ethylene production. When considering as a methane salvation method, in combination with ethane cracking, it still cannot compete with GTL technology despite the lower capital cost as the large amount of carbon dioxide and unconverted methane impose a big cost in separation steps. After more than three decades of development, OCM catalysts seem to reach the performance limit, losing the initial attention from researchers (Zavyalova, et al.,

2011). It is a pity that such a promising idea is missing from the portfolio of ethylene producers amid the big trend toward natural gas feedstock.

Based on the review of OCM, we believe that its challenges cannot be overcome solely by catalyst or reactor development but require a comprehensive development of the whole process, in particular the downstream section. The typical separation methods, which spend nearly 60% plant net work on demethanization (Zimmermann & Walzl, 2012), are not appropriate to the unique composition of OCM reactor effluent. Researches on improving hydrocarbon fractionation have not taken into account the presence of carbon dioxide, which is small in conventional ethylene plant. In this work, we intended to draw a new downstream scheme for OCM process, based on adsorptive separation. The goal of the work is to make OCM competitive with naphtha cracking or other ethylene production from oil-based feedstock. The competitiveness should not be restricted in remote areas where stranded gas is very cheap or even free as the case of GTL process. If this goal is achieved, OCM can be used as methane salvation process in combination with ethane cracker or standalone process in the region where ethane content in natural gas is too low for separation. The smaller scale of OCM plants, in comparison with GTL plants, will make it suitable for small gas reserves and shorten the time to market. The method to complete this job is firstly analysing OCM process, identifying its challenges and conceptually deriving solution. Simulation is then used to quantify the solution, reveal problems which cannot be noticed at the first glance and screen out unsuitable options. Later, experimentation is used to judge the achievement. From experiment results, conclusions are drawn as well as future steps to bring OCM from laboratory to industry. It is worthy notice that this work is only a step in the long way for OCM to develop into a mature technology.

Chapter 2. OCM: Challenges and solutions

2.1. Cost estimation

Producing ethylene by OCM is obviously challenging: at high temperature (500 – 1000^{O}C) and the presence of oxygen, methane and ethylene tend to be oxidized to carbon dioxide. This tendency reduces ethylene selectivity and persists as long as gas phase exists, no matter which catalyst is used. Because carbon dioxide is a valueless green house gas, a low selectivity toward C_{2+} is clearly a waste of raw material and an environmental problem, especially when carbon dioxide emission regulations are tightening worldwide. Low selectivity also raises problems in downstream and right at the reaction section: it increases both carbon dioxide removal and reactor cooling duty. Since combusting to carbon dioxide releases six times more heat than producing ethylene, one percent decrement from typical selectivity results in about one percent cooling duty and two percents carbon dioxide removal duty increment. All these potential problems mean high selectivity is crucial to the success of OCM application. Impractical solutions such as very low oxygen partial pressure can give very high selectivity by sacrificing methane conversion due to the lack of oxygen. The low conversion then raises other problems: reactor size and catalyst inventory increase, compressor and separation section also get more duty because of lower conversion as unconverted methane must be separated for recycling. Therefore low conversion is also very unfavourable although methane is not wasted and carbon dioxide emission is not a problem. The trade off between selectivity and conversion thus leads to yield limitation at about 20%, which is usually not attractive enough to ethylene producers.

Another challenge is temperature control. OCM process is highly exothermic with standard enthalpies of desired reaction (1.1) and methane combustion (1.4) are -280 kJ/mol and -890 kJ/mol respectively. There may be no problem if such

exothermic reactions take place in empty tubes such as in case of steam crackers. However, handling them in a very hot catalytic bed with limited heat transfer area is another challenge and it is quite common to observe hotspot around $100^{O}C$ or even more in fixed bed OCM reactors (Kooh, et al., 1990) (Dautzenberg, et al., 1992) (Schweer, et al., 1994) (Hoebink, et al., 1994) (Mleczko & Baerns, 1995) (Taniewski, et al., 1996) (Pak & Lunsford, 1998) (Jaso, 2012). A slightly unbalanced heating/cooling when the temperature is close to the limit of materials can lead to severe problems. Because cooling through reactor wall alone is not enough in case of large reactors, additional gas is essential for heat dissipation. In reported experiments, nitrogen was usually used for this purpose as it also helps prevent explosive methane/oxygen mixture. This practice, however, should not be applied in real production since it is difficult to separate nitrogen later. More economical solutions are using methane, steam or carbon dioxide as heat carrier. When methane is used, not only we avoid extra component in the streams but selectivity is also improved as methane/oxygen ratio is increased. The drawback is more methane need to be separated and recycled. Steam is also a potential diluent that can be used to control excess heat as it seems to improve selectivity and can be easily removed by cooling. There are studies on effect of steam on OCM reaction (Zhusheng, et al., 1996) with some focus on heat control (Liu, et al., 2008). Carbon dioxide may be a good diluent since it can react with methane to produce ethylene at lower rate and absorb some heat from the main reaction (Aika & Nishiyama, 1988). In that case, the cost of carbon dioxide removal in downstream must be considered.

With the mentioned difficulties, there is a wonder whether OCM process can find an application in industry (Labinger, 1988) (Ren, et al., 2008). Techno-economic studies on OCM feasibility with different schemes have been conducted and criteria have been given in term of selectivity and conversion. For example, Suzuki et al. (Suzuki, et al., 1996) concluded that “the optimal performance of the OCM catalyst is 30% methane conversion and 80% C_{2+} selectivity under some

inverse correlation of conversion and selectivity". Hoebink et al. also confirmed that OCM as an add-on unit to naphtha cracker is economically feasible at this reactor performance (Hoebink, et al., 1995). However, these numbers should be updated as technology advances and market changes. In this chapter, a quick calculation is presented to estimate the profitability of OCM process based on comparing revenue and operating cost. Although does not cover all financial matters, it is a good indicator for choosing among alternatives and finding out which part of the process should be improved. For simplification we only focus on raw material and utility cost of major steps in OCM process. With the exclusion of minor costs and financial terms, we do not expect a full techno-economic assessment of OCM process as it is out of the scope of this thesis. Instead, lower limits of ethylene price produced by OCM or minimal performance of profitable OCM are estimated. Readers interested in more comprehensive economic evaluation of OCM combining with different productions such as formaldehyde can find information in (Salerno, 2013).

Many schemes combining OCM with ethane cracking, naphtha cracking, oligomerization… were proposed. Their common steps, which form the basic OCM process, are: reaction, compression, carbon dioxide removal and ethylene separation as depicted in Figure 2-1. Operating costs per weight unit ethylene of these steps are calculated based on conversion and ethylene selectivity with the following assumptions:

- Carbon dioxide removal and ethylene separation utilise typical technology: absorption and cryogenic distillation, respectively.
- For simplification, only two main reactions are considered at the beginning: OCM reaction to ethylene (1.1) and combustion to carbon dioxide (1.4). Later, ethane production (1.2) as well as the influence of hydrogen and carbon monoxide will be considered.

- Oxygen reacts completely: Oxygen conversion is between 90% and 100% in most reported experiments. This assumption therefore makes calculation simpler without losing much accuracy. If more accurate calculation is desired, oxygen can be treated like other non-condensing gas such as nitrogen.
- Water is condensed completely after reactor: Desiccation before cryogenic distillation is required but its cost is not accounted here.
- No heat integration between sections: This is certainly untrue in commercial plans. However, it separates sections and gives a clearer view of cost structure. Otherwise, an expensive step can be hidden behind a sophisticated heat coupling. Possible energy saving solution will be discussed later.

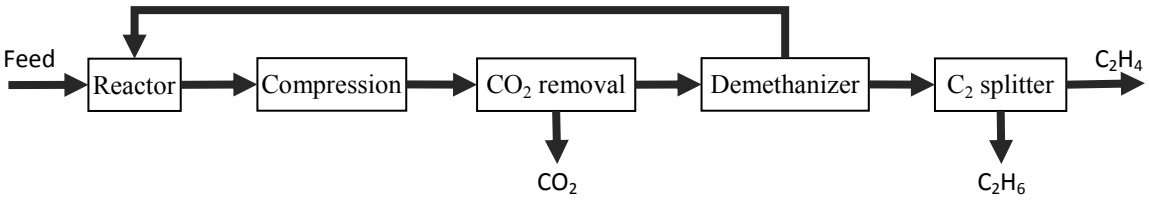

Figure 2-1: Major sections of OCM process

With above assumptions, the outlet composition of the reactor (% mol) is: $\frac{200-200X_{CH_4}}{2-Y_{C_2H_4}}$ % methane, $\frac{100Y_{C_2H_4}}{2-Y_{C_2H_4}}$ % ethylene, $\frac{200X_{CH_4}-200Y_{C_2H_4}}{2-Y_{C_2H_4}}$ % carbon dioxide (see Appendix A). Utility costs are estimated according to (Ulrich & Vasudevan, 2006) with CE PCI = 588.8 (December 2011) (Chemical Engineering, 2013) and fuel price at 2 $/GJ (April 2012) (U.S. Energy Information Administration, 2013) (see Appendix C). The costs are first calculated in US dollars then converted into Euro for convenient; exchange rate is fixed at 1.3.

- Reaction:
  - Raw material: Reaction needs methane and oxygen. $\frac{2}{S_{C_2H_4}}$ mol of methane and $\frac{4-3S_{C_2H_4}}{S_{C_2H_4}}$ mol of oxygen react to produce 1 mol of

ethylene, $\frac{2-2S_{C_2H_4}}{S_{C_2H_4}}$ mol of carbon dioxide and $\frac{4-2S_{C_2H_4}}{S_{C_2H_4}}$ mol of water. On weight basis, $\frac{8}{7S_{C_2H_4}}$ tonnes of methane and $\frac{32-24S_{C_2H_4}}{7S_{C_2H_4}}$ tonnes of oxygen are consumed to produce 1 tonne of ethylene (see Appendix A). Methane price in April 2012 is approximately 140 €/t (U.S. Energy Information Administration, 2013) and the price of oxygen from pipeline is about 30 €/t (Rameshni, 2002). Pure oxygen is chosen over air because OCM process with nitrogen dilution is economically inferior (Eng & Chiang, 1995). Depending on particular situation building Air Separation Unit (ASU) may be more economical than buying oxygen, that option will be considered later.

- Utilities: Feed gas must reach reaction temperature before entering reactor. Heating is partly done by hot reactor outlet in a waste heat exchanger and then completed in a furnace, which requires additional fuel. The amount of fuel depends on design, which must balance between fuel cost and capital cost of the waste heat exchanger. It is reasonable, though may not optimal, to let waste heat exchanger to heat the feed up to half of reaction temperature ($300^{O}C$ – $400^{O}C$) and furnace do the rest. With the feed consists of $\frac{8}{7Y_{C_2H_4}}$ tonnes of methane and $\frac{32-24S_{C_2H_4}}{7S_{C_2H_4}}$ tonnes of oxygen for each tonne of ethylene (see Appendix A), fuel consumption of the furnace is approximately $\frac{1+2X_{CH_4}-1.5Y_{C_2H_4}}{Y_{C_2H_4}}$ GJ for each tonne of ethylene, assuming 90% efficiency (see Appendix B). If inert gas is added, this additional gas also needs heating. About $\frac{1780-1500S_{C_2H_4}}{S_{C_2H_4}}$ MJ is released by reactor when producing 1 kmol of ethylene. On weight basis, cooling duty is $\frac{63.6-53.6S_{C_2H_4}}{S_{C_2H_4}}$ GJ for each tonne of ethylene produced (see Appendix B). Suppose that

reaction heat is utilized to produce high pressure steam, the cost of each GJ transferred is 0.05 € (see Appendix C).

- Compression: Most OCM experiments were conducted at atmospheric pressure. Cryogenic demethanizers operate between 10 and 30 bar (Zimmermann & Walzl, 2012), with higher pressure means more compressing cost but less chilling cost. Carbon dioxide absorption works in a wide range of pressure, from near atmospheric for flue gas treatment to more than 70 bar as in LNG plants. Higher pressure usually has good effect at absorption process and can help saving steam used in striper reboiler (at the cost of compressing). However, in case of OCM, too high pressure leads to significant loss of ethylene. When compressor is driven by electric motor with 90% efficiency, electricity consumption varies from 0.08 kWh/Nm^3 gas (compress to 10 bar, polytropic head = 24km) to 0.12 kWh/Nm^3 gas (compress to 30 bar, polytropic head = 36km). Electricity price is 0.075 €/kWh (see Appendix C). For 1 tonne of ethylene production, totally $800\frac{2-Y_{C_2H_4}}{Y_{C_2H_4}}$ Nm^3 need to be compressed (see Appendix B). If inert gas is added, this additional gas must be compressed too.

- Carbon dioxide removal: $\frac{22-22S_{C_2H_4}}{7S_{C_2H_4}}$ tonnes of carbon dioxide are co-produced along with 1 tonne of ethylene (see Appendix A). Carbon dioxide is removed from reaction product by regenerative solvent (alkanolamines) and once-through (caustic wash) scrubbing. Operating alkanolamines absorption system requires steam, make-up water and electricity for solvent pump (solvent loss is not accounted). Make-up water account for a minor portion of operating cost. Electricity and steam consumptions depend on technology. Amine Guard FS technology by UOP is claimed to be able to achieve carbon dioxide level below 50 ppm with reboiler duty at 1 tonne steam/tonne carbon dioxide (UOP, 2009). Electricity consumption ranges

between 0.3 and 0.4 kWh/t carbon dioxide for each bar difference between absorber and stripper. Steam price is 5.67 €/t and electricity price is 0.075 €/kWh (see Appendix C). It is impossible with alkanolamines alone to lower the concentration of carbon dioxide to ppm level, which is required for cryogenic process. In any case a fine purification consisting of a caustic wash unit is needed to reach the required carbon dioxide specification. Assuming regenerative scrubbing can reduce carbon dioxide concentration to less than 50 ppm, each Nm^3 of hydrocarbon needs about 0.1 g of caustic soda for fine carbon dioxide removal. In undiluted cases, $\frac{0.16-0.16X_{C_2H_4}+0.08Y_{C_2H_4}}{Y_{C_2H_4}}$ kg of caustic soda is spent for each tonne of ethylene produced (see Appendix B). The amount increase in case of non-condensing gases dilution. Caustic soda price is approximately 3 €/kg.

- Ethylene separation: 1 tonne of ethylene must be separated from $\frac{8-8X_{CH_4}}{7Y_{C_2H_4}}$ tonnes of methane. Cryogenic distillation requires refrigerant for condenser while reboiler is usually coupled with a gas cooler. Refrigerant price depends on dilution as well as operating pressure. Utility requirement can be estimated from a distillation design based on desired ethylene purity and recovery. In the Table 2-1 are calculations of utilities required for each tonne of ethylene with examples from literature when the column operates at 30 bar, purity and recovery are both 99%. The calculation based on Aspen Plus® simulation, any other tool for distillation design can be used instead.

The operating costs of 10 cases are demonstrated in Figure 2-2. The figure shows that large amount of non-condensing gas (cases 5, 7 – 10) makes operating cost higher than ethylene price while operating cost is less than 1000 € in most undiluted cases. Once again, we can see that nitrogen/helium dilution is not a choice for commercial OCM. It also worthy notice that reactor cooling does not impose much operating cost, its technical difficulty reflects more in capital expense.

Table 2-1: Cryogenic distillation utilities*

No.	Reference	X_{CH4} %	S_{C2H4} %	CH_4/C_2H_4 w/w	Inert/CH_4 w/w	Scale	Refrigerant GJ	Refrigerant Price €/GJ
1	(Murata, et al., 1997)	30.7	56.8	4.54	No	Lab	2.62	38
2	(Otsuka & Komatsu, 1987)	32	35.3	6.88	No	Lab	3.60	38
3	(Pan, et al., 2010)	38.2	43.3	4.27	No	Lab	2.53	38
4	(Liu, et al., 2008)	39	46.7	3.83	Steam	Pilot	2.29	38
5	(Jaso, 2012)	46.7	35	3.73	N2 = 4.2	Pilot	7,30662	38
6	(Zarrinpashne, et al., 2006)	34.9	55.8	3.82	He = 0.45	Lab	4.23	38
7	(Machida & Enyo, 1987)	52.6	36.1	2.85	He = 1.5	Lab	9.86	68
8	(Bhatia, et al., 2009)	51.6	39.3	2.73	N_2 = 2.3 He = 0.28	Lab	5.08	38
9	(Barghezadeh, et al., 2004)	52	25	4.22	N_2 = 3.5	Pilot	7.11	38
10	(Chu & Landis, 1990)	50	39.5	2.89	N_2 = 31.5	Lab	33.83	68

* Reactor performances are taken from literature; refrigerant duty required for these cases are calculated with Aspen Plus

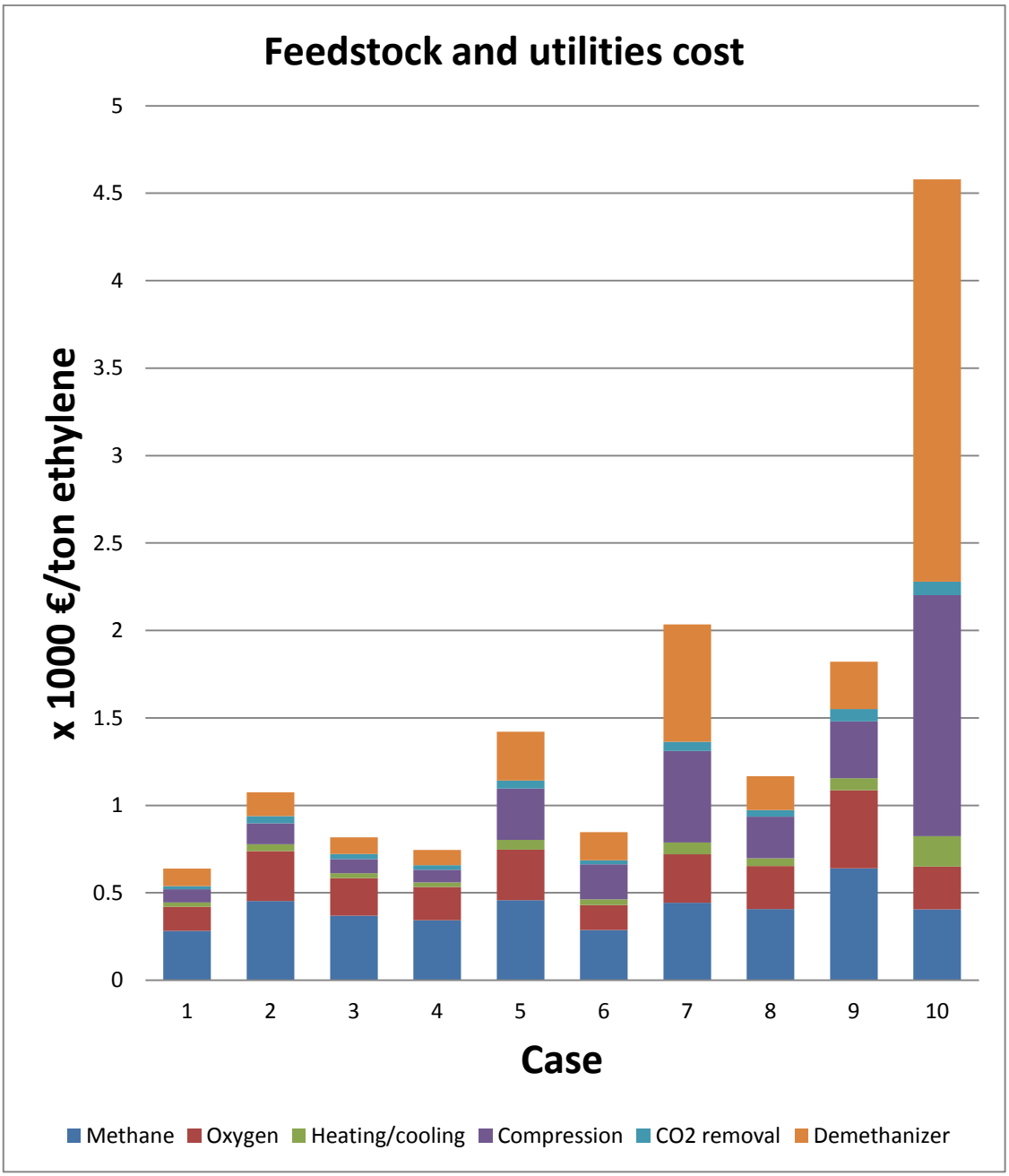

Figure 2-2: Operating cost per tonne of ethylene

When reactor feed is undiluted or steam diluted, the distillate is practically pure methane. Within typical range of conversion and selectivity, cooling duty is proportional to methane flow rate. As operating pressure and temperature are fixed, a simple equation for estimating operating cost can be drawn. For example, cooling duty is about 0.6 GJ for each tonne of methane when

distillation operates at 30 bar. Table 2-2 shows operating cost per tonne ethylene of each section depend on selectivity and yield when operating pressure in downstream section is 30 bar:

Table 2-2: Operating cost summary

Item	Price*	Amount	Total price, €
Reaction			
Methane	140 €/t	$\frac{8}{7S_{C_2H_4}}$	$\frac{160}{S_{C_2H_4}}$
Oxygen	30 €/t	$\frac{32-24S_{C_2H_4}}{7S_{C_2H_4}}$	$\frac{137}{S_{C_2H_4}}-103$
Heating	2 €/GJ	$\frac{1+2X_{CH_4}-1.5Y_{C_2H_4}}{Y_{C_2H_4}}$	$\frac{2}{Y_{C_2H_4}}+\frac{4}{S_{C_2H_4}}-3$
Cooling	0.05 €/GJ	$\frac{63.6-53.6S_{C_2H_4}}{S_{C_2H_4}}$	$\frac{3.18}{S_{C_2H_4}}-2.68$
Compression	0,009 €/Nm^3	$\frac{1600-800Y_{C_2H_4}}{Y_{C_2H_4}}$	$\frac{14.4}{Y_{C_2H_4}}-7.2$
CO_2 removal			
Pump**	0,9 €/t	$\frac{22-22S_{C_2H_4}}{7S_{C_2H_4}}$	$\frac{2.83}{S_{C_2H_4}}-2.83$
Steam	5.67 €/t	$\frac{22-22S_{C_2H_4}}{7S_{C_2H_4}}$	$\frac{17.8}{S_{C_2H_4}}-17.8$
Caustic soda	3 €/kg	$\frac{0.16-0.16X_{C_2H_4}+0.08Y_{C_2H_4}}{Y_{C_2H_4}}$	$\frac{0.48}{Y_{C_2H_4}}-\frac{0.48}{S_{C_2H_4}}+0.24$
Demethanizer			
Refrigerant	38 €/GJ	$\frac{4.8-4.8X_{CH_4}}{7Y_{C_2H_4}}$	$\frac{26}{Y_{C_2H_4}}-\frac{26}{S_{C_2H_4}}$
Total			$\mathbf{\frac{43}{Y_{C_2H_4}}+\frac{299}{S_{C_2H_4}}-136}$

* Utilities prices are calculated according to (Ulrich & Vasudevan, 2006) at CE PCI = 588.8 and fuel price at 2 $/GJ

** Pumping cost per tonne carbon dioxide

The total operating cost in this case can be estimated according to the equation:

$$Operating\ cost = \frac{43}{Y_{C_2H_4}} + \frac{299}{S_{C_2H_4}} - 136 \quad €/t\ ethylene \tag{2.1}$$

So far, only methane, ethylene and carbon dioxide are considered. Other components such as carbon monoxide, hydrogen, oxygen,… are less important but also affect plan operation. Their effects are discussed shortly here:

- Water: Water is condensed right after reactor and does not affect downstream process significantly. Gas stream must be completely dry before enter cryogenic section. There are many techniques for this purpose: absorption, adsorption, for instance. Water adds some operating cost but not significantly.
- Carbon monoxide, hydrogen, oxygen and non-condensing gases: These gases add to gas flow rate through all downstream sections and increase equipment size as well as compression duty, heat transfer duty,… They are removed at the top of demethanizer column along with methane. There they reduce the partial pressure of methane and thus reduce distillate temperature and increase refrigerant price. Precise calculation requires exact amount of these gases, which is not always available, especially hydrogen. Approximate numbers can be estimated from conversions of methane and oxygen and selectivity of ethylene, ethane and carbon dioxide.
- Ethane: Ethane and ethylene have similar properties and can be considered the same in carbon dioxide absorption and demethanizer sections. Therefore operating cost per unit C_2 can be obtained by replacing S_{C2H4} and Y_{C2H4} by S_{C2} and Y_{C2} in the calculation above. The operating cost per unit ethylene is then obtained by dividing the result by C_2H_4/C_2 ratio and added with cost of C_2-fractionation. The operating cost of C_2-fractionation can be estimated by distillation design, similar to demethanizer. Equation is modified considering ethane formation:

$$Operating\ cost = \frac{43}{Y_{C_2H_4}} + \frac{299}{S_{C_2H_4}} - 136\frac{S_{C_2}}{S_{C_2H_4}} + cost\ of\ C_2\ fractionation \quad €/t\ ethylene \tag{2.2}$$

When fractionation takes place at 30 bar, condenser duty can be up to 40 GJ/t ethane depends on feed composition and particular design. With the price of refrigerant at -30^{O}C is 2 €/GJ, operating cost can be estimate from equation (2.2):

$$Operating\ cost = \frac{43}{Y_{C_2H_4}} + \frac{299}{S_{C_2H_4}} - 136\frac{S_{C_2}}{S_{C_2H_4}} + 80\frac{S_{C_2H_6}}{S_{C_2H_4}} \quad €/t\ ethylene \tag{2.3}$$

Equation (2.3) can be shortened to:

$$Operating\ cost = \frac{43}{Y_{C_2H_4}} + \frac{299}{S_{C_2H_4}} - 136 - 56\frac{S_{C_2H_6}}{S_{C_2H_4}} \quad €/t\ ethylene \tag{2.4}$$

The formation of ethane reduces compression and carbon dioxide removal cost because volumetric flow rate and carbon dioxide are reduced, but cost of C_2 fractionation is added. Overall producing additional ethane saves around $56\frac{S_{C_2H_6}}{S_{C_2H_4}}$ €/t ethylene.

- Acetylene: Acetylene is produced by OCM reaction (0.62 % selectivity in case 1). The amount is too small to be considered as a valuable product but it leads to some difficulties in alternative separation techniques as described in the later part. In conventional ethylene plants, acetylene is hydrogenated to ethylene.
- Higher hydrocarbons: The amount of higher hydrocarbons is insignificant and should be only considered in more detailed calculations.

Equation (2.1) shows that operating cost depends mostly on yield and selectivity. The importance of selectivity is at the same level with yield or even higher although the later is more concerned in literature. For example, operating cost increase 215 €/t ethylene when yield decreases from 20% to 10% and 499 €/t ethylene when selectivity decreases from 60% to 30%. The reason is raw material

(methane and oxygen), of which cost depends solely on selectivity, constitute the major of operating cost in undiluted/steam diluted cases. This fact is clearly demonstrated in Figure 2-2: All cases with selectivity less than 40% require more than 1000 €/t operating cost although yield can be high (cases 2, 5, 7 – 9); operating cost of case 1, the one with highest selectivity, is significantly lower than the others although best yield is not achieved in this case. However, even in this case, the OCM process is still not attractive enough in comparison with other technologies. If a limit of the operating cost in equation (2.1) is set, requirement of selectivity can be calculated from given yield or vice versa. This limit varies with region and time. For example, average cost of ethylene production in Southeast Asia, where naphtha is main raw material, in 2011 is about 580 €/t (Source: Dow). In order to be considered by ethylene producers in this region, operating cost of OCM process should not excess 580 €/t. If ethylene yield is 20% (almost the best experimental result reported), the selectivity must be at least 60%. On selectivity – conversion (S – X) or selectivity – yield (S – Y) planes, the real performance of OCM reactors can be represented by points while minimum required performance is represented by hyperbolic curves. All points under the requirement curve are disqualified for profitable ethylene production. In Figure 2-3 are the minimum required conversion and yield versus selectivity with the limit of 580 €/t and case 1 – the best case in Table 2-1. When ethane production is taken into account, more accurate analysis can be conducted in a similar way using equation (2.4). As ethylene/ethane ratios are usually more than 2 in undiluted results, the difference between equation (2.1) and (2.4) is less than 30 €. It is clear that none of the listed cases meets the requirement, even though we did not count the cost of non-condensing gases yet.

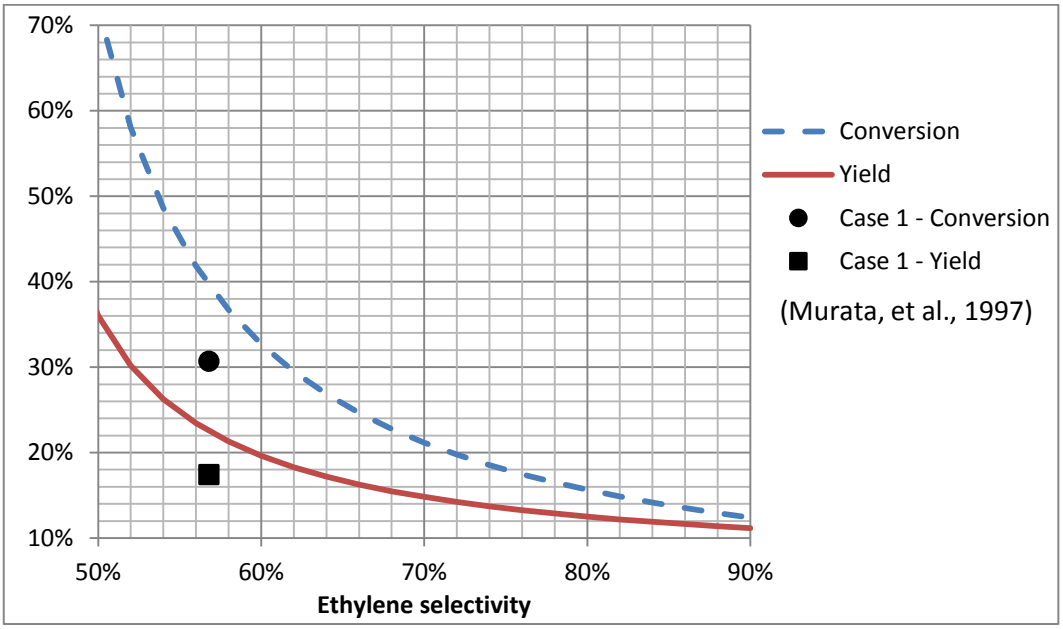

Figure 2-3: Required conversion and yield versus selectivity

After three decades of development, it seems that the limit of catalyst has been approached. In the near future, we cannot find a performance point higher than the requirement curves in Figure 2-3. Instead, it is more feasible to make these curves lower than the existing performance points. This can be done in two ways. The first way is raising ethylene price and/or lowering methane and utilities prices, which is totally out of the scope of this work. The second way is redesigning the whole process to save utilities and reduce production cost. In this way, the first option to be considered is heat integration. In conventional ethylene plant, combining cracking furnace with turbine and process steam generator and other sophisticated heat integration led to nearly 50% reduction of energy consumption compared to the early 1970s (Zimmermann & Walzl, 2012). Waste heat from furnace is almost enough to drive the whole downstream process (Zimmermann & Walzl, 2012). In OCM, reactor is also the most energy intensive unit. Assuming methane conversion and ethylene selectivity are 40% and 50% respectively, energy released by reaction and utilities required in downstream sections for producing 1 tonne of ethylene (30 bar downstream) are given in Table 2-3.

Table 2-3: Energy requirement

Equipment	Duty		Energy needed, GJ		Assumption
	Amount	Type	Amount	Form	
Reactant heater			7.5	Heat	90% furnace efficiency
Reactor			-73.6	Heat	
Compressor	7200 Nm^3	Gas	3.2	Work	Polytropic head = 36km
Solvent pump	17 kWh	Electricity	0.0612	Work	
Stripper reboiler	3.2 tonne	Steam	6.5	Heat	
Distillation condenser	2.1 GJ	Refrigerant	7	Work	COP = 0.3

Heat coupling between reactor and reboiler will be quite cheap and easy since reactor operates at a much higher temperature than reboiler. On the other hand, utilisation of reaction energy to compress gas and refrigerant is not so straightforward. Energy in the form of high pressure steam produced from reactor can be converted into work by steam turbine. Although large scale turbines in power plant can reach 30% efficiency, about 10% efficiency should be expected in case of waste heat recovery from reactor. Because work required by compressors is in excess of 10% of reaction heat, extra fuel is necessary although energy produced by reactor is far more than required in downstream processing. Beside energy, capital cost is also a big burden: Steam turbines cost hundreds €/kW while chilling under -100^{O}C usually needs two or three refrigerants in cascade which means more compressors are needed. Totally, investment in turbomachinery can exceed hundreds million Euros.

Another option of redesigning process is adding an Air Separation Unit (ASU) and avoiding paying for oxygen. Although air is free, ASU requires huge initial investment and energy to operate – 245 kWh/t oxygen according to Linde (Beysel, 2009). Hence the saving is only remarkable if free energy in the form of mechanical work – approximately 5 GJ/t ethylene – is available. Unfortunately, downstream processing already consumed all of this precious energy as calculated above. To summarise, the most possible way of reducing ethylene production cost is saving energy by utilisation of waste heat. However, since

mechanical work requirement is too much, the cost will be still high. When depreciation and financial costs like loan interest are taken into account, conventional OCM process will be definitely screened out of any business plan.

2.2. Alternatives Overview

So far OCM has not made its way into industry. The reason is that OCM reaction performance is far inferior to other ethylene producing reaction: The best yield of OCM reaction is about 20% with less than 60% selectivity while commercial ethane crackers convert more than 65% ethane with 80% selectivity. The results is ethylene makes up more than half of ethane cracking product while it is only 10% in case of OCM. In downstream of ethane cracker, less than one tonne of gases needs removing from one tonne of ethylene but this number is nine in case of OCM. With the same technologies used in conventional ethylene plant, there is no way OCM process can deliver ethylene at a competitive price. The analysis above shows that the most problematic step is cryogenic distillation. It is not only costly, both capital and operating costs, but also sensitive to non-condensing gas dilution as can be seen in Figure 2-2. Although nitrogen dilution will not be implemented, non-condensing gases such as hydrogen, carbon monoxide and nitrogen as impurity is unavoidable and significantly increase the cost of separation. In order to produce ethylene economically by OCM, cryogenic distillation needs to be replaced by another technology. Three technologies have been considered:

- Absorption: Large cost of low hydrocarbon distillation comes from very low temperature and high pressure condition, which is required for the occurrence of liquid phase. In absorption, liquid phase is artificially added and components dissolve or form chemical bond with the solvent in normal condition. Solvent is later regenerated in stripper which also works at normal condition. A solvent that selectively dissolves or reacts with hydrocarbons is the key of success. Early attempts utilised liquid

hydrocarbon such as gas naphtha (Eldred, 1923) but later ones focused on transition metallic salts which can form complex with ethylene or other molecules contain π bonds. Among them silver and cuprous solutions are considered the best (Keller, et al., 1992). Silver salts such as silver nitrate soon caught the attention (Davis & Francis, 1937) (Francis, 1949) thanks to their solubility and availability in laboratory. High price and the fact that silver ion – Ag^+ is easily reduced by reducing agents, e. g. hydrogen or even construction material of the equipments, hamper their large scale applications. Common contaminants also affect the operability: hydrogen sulphide reacts irreversibly with Ag^+ to form silver sulphide and lead to silver loss; acetylene reacts with Ag^+ regardless of the anion present (Keller, et al., 1992) and forms silver acetylides, which is extremely unstable and present a detonation hazard when dry (Safarik & Eldridge, 1998). Thorough removal of these contaminants before olefins separation is necessary but even 1 ppm acetylene is still dangerous because silver acetylides will continuously build up. Many efforts have been made to overcome these difficulties. For example, organic solvent such as ethylene glycol or aceto-nitrile can be used instead of water to reduce the hydration of silver ions, freeing them to complex with olefins (Friedman & Stedman, 1945). The improvement however did not reach “the extent desired for commercial operations” (Strand, 1950). Other ways are using aqueous solution with additives: monobutylamine nitrate (Strand, 1950) and phenol (Cole, 1950) increase absorptivity; ferric nitrate (Shaw, 1949) (Pirovano, et al., 2002) and hydrogen peroxide (Marcinkowsky, et al., 1979) prevent silver reduction while acetylene can be dealt with by using mercuric nitrate (Shaw, 1949) or silver permanganate (Marcinkowsky, et al., 1979). Other silver salts such as fluoborate and fluosilicate (Van Raay & Schwenk, 1959), hexafluorophosphate and hexafluoroantimonate (Quinn, 1965), trifluoroacetate (Alter & Bruns, 1982) with additives such as nitric acid

(Baxter, 1965), hydrogen fluoride or fluoboric acid (Baxter, 1963) were also considered. Bimetallic salt was report to have both higher absorptivity and stability (Baker & Knaack, 1961). Although there are different ways to cover the disadvantages of silver salt solution, they are laborious and negatively impact the process economic (Nijmeijer, 2003). In contrast to silver, cuprous (Cu^{+}) salts are cheap, for example $AgBF_4$ solution is over 60 times more expensive than $CuNO_3$/ethanolamine (Miller, 1969), but insoluble in water so hydrochloric acid (Gilliland, 1945) (Bernard & Bond, 1948), ammonia (Robey, 1941) or organic solvents such as pyridine (Robey, 1941), methanol/ethanolamine mixture (Evans & Scheibli, 1945), orthophenetidine (Ray, 1952), MEA (Cobb, 1958), acetic anhydride (Uebele, et al., 1970), xylene (Cymbaluk, et al., 1992) are used. Unfortunately, these solvents degrade in the presence of contaminants or pose serious problem with corrosion (acid) or high volatility (ammonia). The addition of pre-treatment steps makes the technology economically impractical (Eldridge, 1993). Copper acetylides are also dangerous like silver acetylides (Safarik & Eldridge, 1998). Another problem with cuprous salt, which does not occur in case of silver salt, is disproportionation which converts Cu(I) into Cu(II) and metallic copper and leads to absorbent degradation. As in the case of silver, different cuprous salts were investigated: chloride (Joshua & Stanley, 1935) (Francis & Reid, 1948), benzenesulfonate (Robey, 1941), nitrate (Cooper & Small, 1997), dodecylbenzenesulfonate (Tabler & Johnson, 1977) (Brown & Hair, 1993), diketonate (Ho, et al., 1988), carboxylate (Cymbaluk, et al., 1996) or bimetallic salt (Long, et al., 1972). The common problem with all cuprous salts is the co-absorption of carbon monoxide. Thus absorption with cuprous salt cannot produce high purity required in polymer grade (Barchas, et al., 1999). Up to now olefin separation based on absorption is limited to “very few examples” (Pirovano, et al., 2002). More detail on olefin/paraffin separation by absorption can be found in (Reine, 2004).

- Membrane: Membrane separation operates at high pressure but normal temperature. Hence major investment and running costs on cold-box are saved. Different types of membrane like polyimide (Hayashi, et al., 1996) (Staudt-Bickel & Koros, 2000) (Okamoto, et al., 1999), polyphenylene oxide (Ilinich & Zamaraev, 1993), polysulfone (Park, et al., 2000) or cellulose acetate (Ryu, et al., 2001) have been used but separation factors are too low to be attractive for industrial purposes. Silver impregnated membranes were developed, trying to improve selectivity via complexation (Steigelmann & Hughes, 1973) (Hsiue & Yang, 1993) (Yang & Hsiue, 1997) (Hong, et al., 2001) (Pinnau & Toy, 2001) (Morisato, et al., 2002) (Kang, et al., 2009). They face similar problems as with absorption counterpart. More detail on olefin/paraffin separation by membrane can be found in (Nijmeijer, 2003).
- Adsorption: Adsorption was considered for olefin separation seventy years ago (Kiesskalt, 1944) (Kiesskalt, 1944). Thermal swing adsorption (TSA) had been the favourable process due to limitation of compression technology but pressure swing adsorption (PSA) has been getting more preferred because of smaller bed inventory. The most suitable sorbents for physical adsorption are zeolitic while π-complexation sorbents are the best choice for chemical adsorption. Zeolite 4A was used in commercial PSA process (Petrofin process) for recovery of propylene. However this process has been discontinued because the low selectivity of zeolite limits purity and recovery of single step separation (Rege, et al., 1998) while low capacity renders multi-steps separation impractical. Chemical adsorption processes can achieve better performance owes to higher selectivity of π-complexation sorbents (Yang, 2003). However, those sorbents also met the problem of contaminant like in the case of absorption and membrane technology. In addition, irreversible degradation of Cu^{+} sorbents when exposure to both water and oxidizing agents make them unsuitable for OCM process (Miltenburg, 2007). Regeneration is more difficult due to higher bond energy

compare to physical adsorption. Several attempts to apply adsorption to the downstream of OCM reactor have been made (Tonkovich, et al., 1993) (Baronskaya, et al., 1996) (Kruglov, et al., 1996) (Machocki, 1996) (Bjorklund, et al., 2001) (Kundu, et al., 2009) (Schwittay, et al., 2001). Since they also met the problems as with general olefin separation, the improvements were limited.

In all alternative methods, a third agent (solvent, adsorbent or membrane) is introduced so that separation can take place without extreme condition. Agents based on π-complexation (more details on π-complexation adsorbent can be found in (Yang, 2003)) show the best performance regardless of method thanks to the moderate bond energy: strong enough to give high selectivity but weak enough for the process to be reversible (agent regeneration). Unfortunately, the activeness of transition metal ions (Ag^+ and Cu^+) makes these agents easy to degrade in the presence of contaminants. This is the reason why traditional cryogenic distillation still dominates chemical and refining industry despite numerous optimistic outlooks on non-distillation processes. There are two ways to improve these processes. The first one is developing stable materials based on π-complexation, for example by adding inhibitor to prevent degradation. The second is developing high performance process based on less selective but stable materials. In this work, the second approach is chosen for adsorption process.

2.3. Conceptual development

When third agent is utilized for separation, components are selectively bound to the agents (absorbed, adsorbed…) and then released. These two processes can happen at the same time in different places, e. g. absorber/striper in absorption technique or two sides of membrane in membrane technique. In adsorption these processes usually happen in the same place but at different time due to problem with handling solid material. In physical processes, bound components are released by pressure decrease and/or temperature increase. If no other

measure is taken, pressure or temperature change must be very big to achieve a reasonable mass transfer rate. For example, pressure difference is 100 bar in Separex, the membrane technology by UOP to remove carbon dioxide. To accelerate releasing process without such a big change, extra manipulation is necessary. It can be either partial solvent vaporization in absorption technique or using sweep gas in adsorption technique. In most cases, unbound components are collected during binding process (raffinate) and bound components are collected during the reversed one (extract). Separation performance therefore depends heavily on the selectivity of binding process. If selectivity is low, more stages are required for high purity and recovery. As selectivity of two components A and B can be defined as $\frac{Q_A}{Q_B}$ with Q is adsorption capacity, a sorbent with $Q_A >> Q_B$ is desired. Big Q_A also means less sorbent is needed. There are several ways to increase selectivity for a given material:

- Pressure change: Adsorption capacities decrease along with pressure at different rates depends on the component. For olefin/paraffin, selectivity is highest in Henry region where absolute pressure is less than 10 kPa. Such a low pressure is unacceptable because of difficulties with vacuum technology and too large volumetric flow rate.
- Temperature change: Adsorption capacities increase when temperature decreases, also at different rates depends on the component. Lowering temperature can help increasing both selectivity and capacity at the cost of cooling. Lowering temperature also slows down mass transfer, which is not desired. In practice, there is a critical temperature below which refrigeration must be used instead of simple cooling methods by air or water.
- Kinetic adsorption: When retention time is short, the adsorbed amount is less than maximum capacity. In that case selectivity can be written as $\frac{k_A Q_A}{k_B Q_B}$ where k_A and k_B are less than 1 and proportional to the adsorption

rates of the components. Selectivity increases if $k_A > k_B$ but more sorbent is required as the trade-off. Rege et al. (Rege, et al., 1998) demonstrated that kinetic adsorption with zeolite 4A is not good enough for commercial olefin/paraffin separation.

- Competitive adsorption: Since cryogenic condition can be avoided by adding sorbent as a third agent, one can think about introducing more components into the system to modify adsorption behaviour. Competitive adsorption is an usual mechanism that can explain the effect of additional components: Since total capacity for all components are limited (due to finite surface area, pore volume,…), components compete with others to occupy adsorption sites. Hence extra components reduce adsorption capacity of the main components to a certain extent depends on affinity. Higher affinity of the main components means less reduction and selectivity, $\frac{Q_A}{Q_B}$, increase if A is more strongly adsorbed than B. This idea has been successfully applied in analytic chemistry when A needs to be separated from B. For example, tailoring fluid phase composition is a common practice to improve performance of HPLC separation. However, in production, when A needs to be separated from all other components, this technique may lead to more separation steps and the selectivity improvement does not pay out. In case of OCM process, this problem can be solved by choosing carbon dioxide as the extra component. As carbon dioxide removal is already required, adding carbon dioxide does not impose any new separation step, only the sequence of gas treatment need changing: carbon dioxide removal takes place after demethanization. This is the key idea of the proposed solution.

Solving selectivity problem is only half the way to a successful separation, desorption process also needs careful design to ensure efficiency. Other than

high purity and recovery, short time and low energy consumption are desired because of economic reason. An important point which is usually ignored in academic research is simple operation. The simpler the more robust a process is. For example, some Temperature Program Desorption (TPD) processes perform well in laboratory but cannot be scaled up as a result of limitation on heat transfer which is only remarkable in large bulk.

As mentioned above, sweep gas is necessary to speed up desorption. For this purpose, feed or 'light'products (less adsorbed gases) are typically used. Although convenient, this choice tends to lower the purity of 'heavy' product (more adsorbed gases). To overcome this, extra gases can be used but introducing new components into system means more separation steps are required to remove them later. Nitrogen and C_4 – C_5 hydrocarbons were considered as sweep gas for adsorptive olefin/paraffin separation (Jarvelint & Fair, 1993) (Thomas & Crittenden, 1998). In those cases, two distillation columns are added for olefin/sweep gas and paraffin/sweep gas separation: we come back to distillation solution. In this work, we proposed to use carbon dioxide as sweep gas to avoid such extra separation step. More over, using carbon dioxide give a chance to purge column without compressor as shown later. Since carbon dioxide is adsorbed, ethylene will desorb faster and outlet concentration will be higher than using inert sweep gas. However, if carbon dioxide is adsorbed too strongly, there will be trouble desorbing it later. With these ideas, a new scheme for OCM downstream is drawn in Figure 2-4.

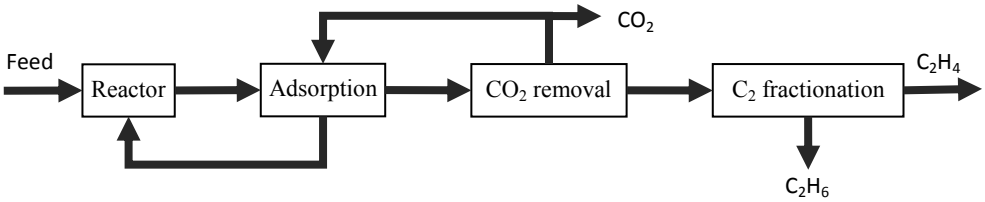

Figure 2-4: New scheme of OCM process

2.4. Process flow development

Based on the scheme in Figure 2-4, more detailed process flow diagrams (PFD) are developed, focusing on adsorption, carbon dioxide removal and utilisation of unconverted methane. In order to avoid costly compression, adsorption and carbon dioxide removal are performed at pressure similar to reactor.

2.4.1. Adsorption

Adsorption cycle essentially consists of two steps:

1. Ethylene adsorption: The dried, cooled downstream of reactor is fed to adsorption column. Cooling temperature is chosen to balance adsorption capacity and rate. Degree of dryness depends on adsorbent: hydrophilic ones need desiccation while hydrophobic ones require only conventional drying. During this step, the outlet of adsorption column comprises methane, carbon monoxide, hydrogen,… and a part of ethane. The amount of carbon dioxide in the outlet depends on particular design.
2. Ethylene desorption: Carbon dioxide is fed to adsorption column. At the beginning, the outlet still comprises methane, carbon monoxide, hydrogen,… and will be mixed with the outlet from the first step. The outlet later contains carbon dioxide, ethylene and a part of ethane. It is put through carbon removal section to retrieve ethylene. This step take place until all ethylene is desorbed.

In case carbon dioxide is strongly adsorbed, an extra step to desorb carbon dioxide is necessary:

3. Carbon dioxide desorption: When carbon dioxide is adsorbed too strongly, it must be desorbed using sweep gas and/or increasing temperature. Air can be chosen as it is free but air blower is needed. When this step is employed, carbon dioxide can be desorbed completely and the outlet of the first step is

free of carbon dioxide. Otherwise carbon dioxide concentration in that outlet will be high.

For continuous production, multiple columns are implemented.

2.4.2. Carbon dioxide removal

Carbon dioxide removal section separates carbon dioxide from the outlet of the second step in adsorption process. Carbon dioxide is recycled to purge adsorption column and the remaining is put to C_2 fractionation section to separate ethylene and ethane. In order to recycle carbon dioxide without any booster, the stripper is operated at higher pressure than absorber. The elevated pressure required for circulation is achieved by solvent pump instead of gas compressor. The cycle of carbon dioxide is similar to Rankine cycle. Caustic wash is necessary for fine carbon dioxide removal. Additionally, carbon dioxide may be removed from one of these streams:

- If adsorption process consists of only two essential steps then the outlet of the first step contains large amount of carbon dioxide and need carbon dioxide removing before recirculation. Carbon dioxide removal may be not necessary if this outlet is put to another process instead of circulated back to OCM reactor.
- If adsorption process consists of three steps then the outlet of the third step is a mixture of carbon dioxide and air. It can be vented directly or carbon dioxide can be separated and stored to reduce emission if it is possible, e.g. in oil field or coal seam.

These additional removals do not need caustic wash because a certain carbon dioxide contamination can be tolerated.

2.4.3. Unconverted methane utilisation

Unconverted methane is separated along with carbon monoxide, hydrogen, ethane,… After removing carbon dioxide (if necessary), it can be mixed with fresh methane and circulated back to OCM reactor. When methane is received from high pressure pipeline (> 50 bar), an injector can be used to compensate pressure drop and methane can be circulated without any other booster. Unconverted methane can also be used in other processes instead of recirculation. There are many processes consume methane and can be combined with OCM, at least one of them should be implemented to prevent inert gas accumulation. Below are some potential choices which require neither further separation nor compression:

- Combustion: The mixture of hydrocarbons, hydrogen, and carbon monoxide can be burned to produce energy. This energy can be used for: heating the feed of OCM reactor up to reaction temperature – ~800^{O}C; driving compressors for air separation unit or C_2 fractionation section; producing electricity.
- Methane reforming: When adsorption process consists of only two steps the outlet of the first step comprises large amount of methane and carbon dioxide along with carbon monoxide and hydrogen. Methane and carbon dioxide can react with each other to produce carbon monoxide and hydrogen, which are intermediary for various productions. For this purpose, Midrex technology can be used. As shown in Table 2-4, the feed composition of Midrex reformer (Mobarakeh plant (Vakhshouri & Hashemi, 2008)) is compatible with the adsorption outlet. The technology was commercialised since 1969 and – as claimed by the company – employed for 60% of global Direct Reduced Iron (DRI) production. A problem with this option is many important applications of syngas like methanol or ammonia production are high pressure. In order to avoid expensive compression, only low pressure

application such as direct iron reduction or Fischer-Tropsch process should be considered (Fischer-Tropsch process can be operated at either low or high pressure). This limitation lowers the chance of combining OCM with syngas consuming process. Moreover, some of them, Fischer-Tropsch for instance, are already economically challenging. However this option still worth investigate from the environmental aspect because it consumes carbon dioxide produced by OCM and reduces emission.

Table 2-4: Feed composition of Midrex reformer, % mol

CH_4	C_2H_6	C_3H_8	C_4H_{10}	H_2	H_2O	CO	CO_2	N_2
14.99	1.4	0.53	0.19	35.02	13.64	18.95	14.24	1.03

2.4.4. Process flow diagram

In Figure 2-5 is process flow diagram with two steps adsorption. Oxygen feed, reactor outlet cooling and drying as well as waste heat recovery from reactor and C_2 distillation column are not shown for clearer view. Two columns in adsorption section represent two steps; actual number of columns is calculated in quantitative design. It can be seen from the diagram that investment on compressor is greatly reduced. Since C_2 only add up to 10 %mol of reactor outlet, the compressor in C_2 fractionation section is ten times smaller than the mainstream compressor required in conventional downstream scheme. When using heat-pumped C_2 fractionation technique, only one three stages compressor is employed: C_2 mixture is compressed in two stages to 8 bar, ethylene from top of the column – after heating to ambient temperature in feed-effluent exchanger – is compressed to 20 bar in third stage then condensed in reboiler and circulated to the column as reflux. Compare to conventional downstream processing, three or four mainstream and refrigerant compressors working up to 40 bar are replaced by only one compressor at 20 bar. Lower reflux ratio and less column trays are required because ethane is partly removed in adsorption section. Saving on investment and energy consumption is therefore remarkable.

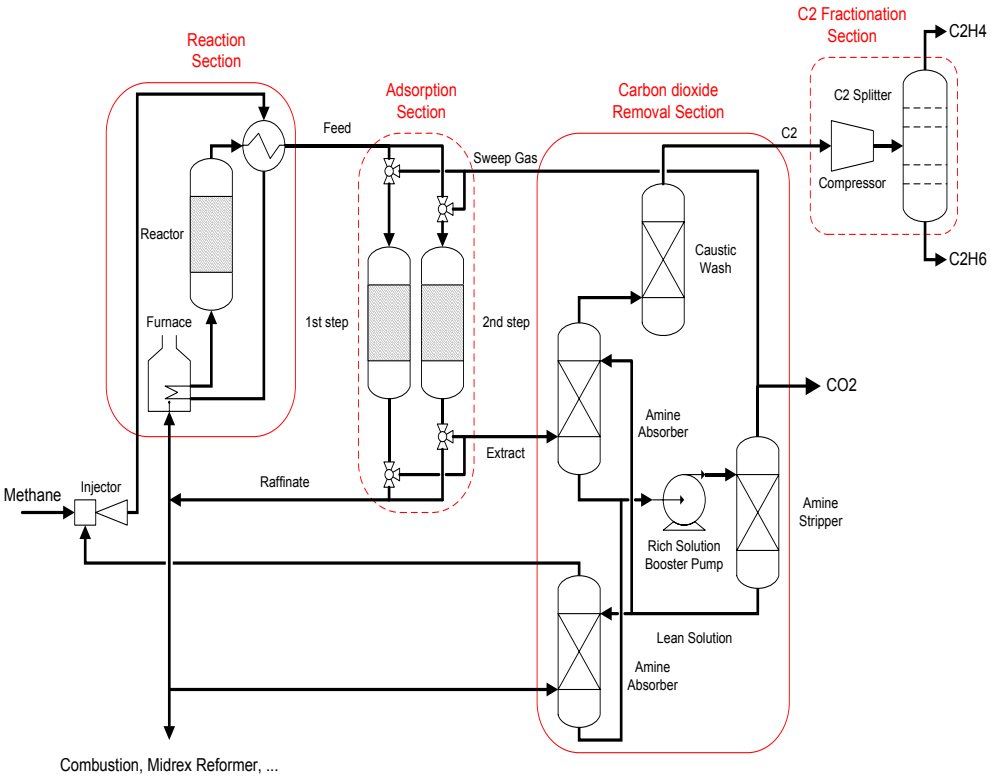

Figure 2-5: Process flow diagram with two steps adsorption

Chapter 3. Simulation of adsorption process

Chemical engineers are always curious about what happen during processes. This information is necessary for designing, operating processes and can be obtained via either experimentation or calculation. Well designed experiments are useful and crucial to process development. However, they are usually time consuming, expensive and may raise safety concern in particular when approaching process limits. Calculation based on mathematic models can compensate these disadvantages and speed up process development, bring it from a kind of art to a real branch of engineering. Models vary from simple algebraic equations as in case of double-pipe heat exchanger to complicated partial differential equations (PDEs) as in case of fluidized bed reactor. Simple but effective methods exist for traditional applications such as distillation and allow designing workable units within a short time calculation giving sufficient thermodynamic information. In case of adsorption, where processes operate in transient state rather than steady state, it is more difficult to predict process behaviour from thermodynamic characteristic. Computer-based simulations are often required, especially for challenging tasks such as olefin/paraffin separation. Due to unsteady nature, adsorption processes design requires not only calculating spatial dimensions but also timing operating actions such as switching inlet and outlet flows. Modelling then usually involves PDEs, which may be converted into ordinary differential equation (ODE) or differential algebraic equation (DAE) system depend on particular mathematic tools. Precise estimation leads to large number of equations while simultaneous processes with very different rates make these equations stiff. Adsorption process simulation thus becomes a challenging problem. Despite many efforts and progresses in this area, a compromise between details, accuracy and computing cost is still needed. In this work, simulation is used to study zeolite 4A – the best candidate reported in literature for olefin/paraffin separation by physical adsorption and activated

carbon – the most popular sorbent. In the following are major considerations when simulating adsorption processes and the choices for this work:

3.1. Modelling

3.1.1. Dimension

Four-dimensional space (three-dimensional Euclidean space plus time) is enough to mathematically model any process include adsorption. Nonetheless, since chemical processes usually consist of multi phases with distinctive characteristic, it is a common practice to model each phase with a separate space. Interaction between phases is then modelled by interface mass/heat transfer equations. Hence a model with n phases may have up to $3n+1$ dimensions. More dimensions complicate model but do not always bring more benefit. The number of dimension is therefore usually reduced to a few whenever it is possible:

- Taking advantage of symmetry: When the space is symmetric, a symmetric set of points may have one common value for a physical property and can be represented by a single point. The number of dimensions then can be decreased without losing the amount and quality of information. Typical example are cylindrical vessel which can be modelled with two dimensions – radius and length – or spherical particle which can be modelled with one dimesion – radius. In this work cylindrical vessel is chosen as adsorber so the number of dimensions is reduced by one.
- Lumping: Physical properties of points along one dimension can be considered to have the same value which is determined by conservation laws. By doing this, the dimension can be taken out of calculation. The number of dimensions as well as model complexity is then reduced at the cost of losing details and accuracy. The accuracy can be later improved by fitting experiment result or adding modification factors. In this work lumping is applied to both fluid phase and solid phase. For solid phase lumping is applied to all dimensions of sorbent particle and to radius of sorbent bed. By

this choice, intraparticle process is simplified. Information such as influence of pore length or pore diameter to separation process is unknown. Such information is needed to tailor material but detailed modelling of intraparticle process requires huge computation effort (Lopez-Isunza, 2013). As the aim of this work is developing separation process based on available material, we chose to simplify intraparticle process be cause the lost of information is not crucial to process design and simulation time must be short enough for optimisation. Lumping is applied to bed radius for fluid phase. Mixing effect due to the present of particles makes velocity and concentration along bed radius more even than the case when gases flow through empty pipe. Wall effect still affects accuracy but it is ignorable when bed diameter is sufficiently bigger than particle diameter, $\frac{d_{bed}}{d_{particle}} > 10$, which is typical in industry and will be considered in experiment setup design. On the other hand, too large bed diameter imposes difficulties upon fluid distribution and renders part of the bed underutilised. This problem is however less severe in gas application and only remarkable in case of very shallow bed applications such as rapid pressure swing adsorption (RPSA).

With above choices, the model is mathematically two-dimensional – bed length and time. In the language of process engineering, it is a dynamic one-dimensional model.

3.1.2. Material balance

Changing of material in a control volume is caused by convection, diffusion and interface mass transfer. Flow pattern inside granular bed is complex but can be expressed in several terms:

- Radial flow: Radial flow is assumed to make an ideal mixing, allowing lumping along radius as said above.

- Axial flow: Axial flow is divided into two parts: a plug flow through the bed and dispersion which includes both molecular diffusion and various self-induced axial mixing process. Dispersion is less significant in gas adsorption than liquid adsorption. It is not written explicitly in material balance equation but the effect is accounted by numerical diffusion as described later.

Balance equation for component *i* is written as:

$$\frac{\partial c_i}{\partial t} = -\frac{\partial (uc_i)}{\partial x} - \frac{1-\varepsilon}{\varepsilon}\frac{\partial q_i}{\partial t} \tag{3.1}$$

3.1.3. Heat balance

The heating effects of compression and friction are insignificant and ignored. Temperature changing is assumed only due to inlet/outlet flow and adsorption/desorption heat which means column wall is completely isolated. Temperatures of solid and fluid phases are different because of limit heat transfer rate. However it is impossible to measure these temperatures separately with our experiment facility. A common temperature in between is then assigned to both phases. In real process solid temperature will be higher than fluid temperature during adsorption and lower during desorption. Heat capacity of sorbent is considered make up the whole heat capacity of a control volume because gas heat capacity is relatively very small. Heat capacity of column wall is also ignored, which is acceptable in large diameter column. Temperature of a control volume is regulated by the equation:

$$mCp_s \frac{\partial T}{\partial t} = \frac{\varepsilon}{1-\varepsilon}\left(u\sum_{i=1}^{n_c} c_i Cp_i\right)\frac{\partial T}{\partial x} + \sum_{i=1}^{n_c}\frac{\partial q_i}{\partial t}\Delta H_i \tag{3.2}$$

3.1.4. Fluid dynamic

Fluid velocity plays an important role in the process as shown in above equations. Because velocity estimation is required many times during process simulation, it must be accurate for a meaningful simulation result but at the same time must be simple, otherwise simulation will takes ages to finish. Several alternatives are frequently used:

- Pre-calculation: Velocity is calculated before simulation. This alternative is usually coupled with constant velocity along the bed because it is difficult to calculate velocity change along the bed without simulation. Velocity can be calculated from flow rate, which is known a priori. This alternative is suitable for liquid adsorption or gas purification where adsorption does not affect velocity significantly. In bulk separations such as our case, the amount of adsorbed gas is relatively big and flow rate change remarkably along the bed. Constant velocity assumption is then not accurate.
- From pressure drop, first order polynomial: It is easy to notice that there is no flow rate without pressure drop and flow rate increases with pressure drop as long as there is no bed deformation. Consequently comes a simple but useful assumption: velocity is proportional to pressure drop. The classical equation by Darcy is well-known:

$$u = B\frac{-\Delta p}{\mu l} \tag{3.3}$$

  Although more detail ones such as Kozeny-Carman equation are available, this simple equation seems more effective with permeability coefficient B determined empirically.

- From pressure drop, second order polynomial: Velocity can be estimated more accurate by increase the order of the polynomial. This semi-empirical equation was developed by Ergun for column packed with rings:

$$\frac{-\Delta P}{l} = 150\frac{(1-\varepsilon)^2}{\varepsilon^3}\frac{\mu u}{d_p^2} + 1.75\frac{(1-\varepsilon)}{\varepsilon^3}\frac{\rho u^2}{d_p} \tag{3.4}$$

Ergun equation was later extended to other type of packing and even fluidised bed.

Considering the trade-off between accuracy and computational cost, Darcy law is adopted for this work with permeability coefficient taken from (Richardson, et al., 2002). Pressure is calculated from gas concentration using ideal gas law.

3.1.5. Mass transfer rate

During adsorption a molecule is motivated by chemical potential to diffuse from bulk fluid through laminar boundary around a solid particle to its outer surface. From there it diffuses through the pores into the particle until being adsorbed. The process is reserved during desorption. An extensive summary of mass transfer model can be found in (LeVan & Carta, 2008) with many theories developed for extraparticle and intraparticle transportation. Complete rate equations which consider external mass transfer, pore diffusion, solid diffusion,… are necessary for simulation to exactly follow real processes. Such exhaustive rate equations are impractical due to not only limitation on simulation time but also the lack of parameters. Linear driving force approximation based on adsorbed-phase concentration is therefore chosen to solve the first problem:

$$\frac{\partial q_i}{\partial t} = s_i(q^* - q) \tag{3.5}$$

In order to overcome the lack of parameters, the rate coefficient s_i is calculated based on the slowest transportation step, which is intra-crystal diffusion (micropore diffusion) in case of zeolite 4A:

$$s_i = \frac{15D_i}{r^2} \tag{3.6}$$

Or intra-particle diffusion (macropore diffusion) in case of activated carbon:

$$s_i = \frac{15 D_i}{r_p^2} \tag{3.7}$$

Diffusion coefficient depends on temperature:

$$D_i = D_{i0} e^{-\frac{Ea_i}{RT}} \tag{3.8}$$

3.1.6. Sorption equilibrium

Sorption equilibrium is the first thing to be considered when designing adsorption process. It is standard to describe sorption equilibrium via isotherms – the equilibrium between fluid-phase concentrations (partial pressure when fluid is gaseous) and adsorbed-phase concentrations at a fixed temperature. Isotherms can be qualitatively classified into five types according to Brunauer (Brunauer, et al., 1940) or quantitatively estimated by various models: Henry isotherm (linear isotherm), Freundlich isotherm, Langmuir isotherm, BET isotherm,… Within a certain range real isotherm can be fitted to any model with certain accuracy. However it is important to select the model which does not only match the real isotherms over the entire range of process condition but also represents the relationship between components, in particular interaction and order of affinity. Langmuir model is suitable for microporous adsorbents like zeolite as it matches the favourable isotherm – type I in Brunauer's classification – thanks to the analogy between Langmuir's mechanism and pore filling mechanism. The difference is Langmuir assumed homogeneous adsorption site while zeolite pore size, and consequently adsorption characteristic, distributes in a wide range. To fill in this gap, multi-sites Langmuir isotherm can be used with each site represent a pore size or a range of size. Once again, the number of sites should be chosen to balance model accuracy and complexity. Considering components in this application, dual-site Langmuir (often called Dual-Langmuir) model is selected for zeolite 4A with one site represents big pores which are accessible to all molecules and the other represents small pores which are

inaccessible to hydrocarbons. Multi-component Dual-Langmuir isotherm is described by the equation:

$$q_i^* = Q_{1i}\frac{b_{1i}p_i}{1+\sum_{i=1}^{n_c} b_{1i}p_i} + Q_{2i}\frac{b_{2i}p_i}{1+\sum_{i=1}^{n_c} b_{2i}p_i} \tag{3.9}$$

Parameters of the multi-component isotherm can be approximated by pure gas isotherms. Since adsorption sites are representative of pores with different sizes, adsorption capacity Q_i varies among components. Pore volume is assumed to be constant and adsorption capacity is inverse proportional to the specific volume of adsorbate. The dependence of specific volume on temperature is linearly approximated:

$$\frac{Q_i(T)}{Q_i(T_0)} = \frac{1}{1+\alpha_i(T-T_0)} \tag{3.10}$$

The Langmuir adsorption coefficient represents the affinity of sorbent for component. Its dependence on temperature is given by equation (Butt, et al., 2003):

$$b_i = \frac{b_i^0}{\sqrt{T}} e^{\frac{\Delta H_i}{RT}} \tag{3.11}$$

For the first site, b_{1i}^0 and ΔH_{1i} can be estimated if the values of b_{1i} at two different temperatures T_1 and T_2 are known:

$$\begin{gathered} \Delta H_{1i} = R\frac{T_1T_2}{T_2-T_1} ln\left(\frac{b_{1i}(T_1)}{b_{1i}(T_2)}\sqrt{\frac{T_1}{T_2}}\right) \\ b_{1i}^0 = b_{1i}(T_1)\sqrt{T_1}e^{\frac{\Delta H_{1i}}{RT_1}} \end{gathered} \tag{3.12}$$

Calculation of the second site is similar.

In case of activated carbon, Langmuir model is selected since the pores are accessible to all gases.

3.1.7. Operation

Process operation sets the boundary conditions for the simulation problem. Flow rate, molar fraction and temperature of inlet gas are controlled. That means $T|_{x=0}$ and $(uc_i)|_{x=0}$ are set as boundary conditions:

$$T|_{x=0} = T_{in}(t) \tag{3.13}$$

$$(uc_i)|_{x=0} = f_{in}(t) \tag{3.14}$$

Column wall is completely isolated and does not raise any boundary conditions. Column outlet is connected to a fixed pressure environment (p_{out}) through a one-way control valve. Outlet flow depends on pressures at both side of the valve. Boundary condition at outlet is:

$$u = \begin{cases} 257 k_V R \sum_{i=1}^{n_c} c_i \sqrt{\dfrac{T}{\sum_{i=1}^{n_c} M_i c_i}} & RT \sum_{i=1}^{n_c} c_i > 2p_{out} \\ 514 k_V \sqrt{\dfrac{p_{out}\left(RT \sum_{i=1}^{n_c} c_i - p_{out}\right)}{T \sum_{i=1}^{n_c} M_i c_i}} & p_{out} < RT \sum_{i=1}^{n_c} c_i < 2p_{out} \\ 0 & RT \sum_{i=1}^{n_c} c_i < p_{out} \end{cases} \tag{3.15}$$

In equation (3.15) concentration and temperature are at the end of adsorption column but velocity is at the valve, velocity at the end of column can be calculated by multiplying with the ratio between column cross area and valve orifice. Flow coefficient k_V in supercritical and subcritical cases is available in valve datasheets. The last case represents the one-way property of the valve – no flow when inlet pressure is less than outlet pressure.

Initial condition can be chosen freely by setting the initial gas phase concentration, adsorbed phase concentration and temperature at each node of the spatial mesh as desired. In this work, simulations are conducted with column initially full of nitrogen and in equilibrium state.

3.2. Simulation

3.2.1. Numerical solution

The process model is a set of PDEs with $2n_c+1$ unknown functions: fluid-phase concentrations, adsorbed-phase concentrations and temperature. Finding its analytical solutions is in general impossible and the better choice is solving it numerically via computer simulation. While numerical solutions are only calculated at finite number of points on a mesh within function domain, the number of numerical methods is virtually infinite for any individual to study. They can be classified into three categories:

- Finite difference: These methods convert derivative terms into approximated difference terms. The differential equations of unknown function are converted to algebraic equations of unknown variables which are the values of function at grid points. Algebraic equations are then solved analytically (if possible) or numerically. Finite difference methods are straight forward in term of mathematic and therefore are the first methods invented. Difference formulas and techniques such as variable step have been developed to improve the accuracy of the methods.
- Finite element: These methods approximate solution by simple functions whose parameters are unknown. Substituting these simple functions into the differential equations produces residual because they are only approximate solution. The parameters are then calculated to minimise residuals, which mean solving an optimisation problem. This optimisation step makes finite element methods more accurate but also computationally demanding.
- Finite volume: In these methods, the differential equations are first converted into integral equations by integrating over the whole control volumes around grid points. Volume integrals contain divergence term are then convert into fluxes using divergence theorem. Function values at grid

points are considered average values of the control volumes. Once the formulas relating fluxes and average values are selected and substituted into the integral equations, algebraic equations with these values as unknown are achieved. These algebraic equations are solved as in case of finite difference methods. Finite volume methods are straight forward in term of physic with conservation laws guaranteed thanks to the nature of the methods.

Each approach has its own advantages/disadvantages and may overlap the others in a particular problem. In general no one can tell which approach is better than the others. With a given mesh elaborated methods can produce more accurate solution at the cost of computational demand. Meanwhile, simple methods can also produce more accurate solution by using a finer mesh. Considering our problem where differential equations and geometry are quite simple, the second policy is more efficient in term of accuracy versus computational cost. Finite volume method with fixed step is selected for spatial discretisation and numerical differentiation formulas with variable steps are employed to replace time derivative. The later job is done by standard ODE solver supplied in Matlab.

A common problem with adsorption simulation is stiffness, which arises because of parallel processes with very different rates. In order to overcome this difficulty the whole simulation time is divided into small periods. Temperature is considered constant during a period and updated at the end of each period using equation (3.2) in integral form. Physical properties such as viscosity or isotherms are also updated. The assumption of constant temperature is quite close to the real process when each period lasts only few seconds.

3.2.2. Components

Zeolite 4A is chosen first because it is the most intensively studied material for olefin/paraffin separation. The characteristics of zeolite 4A are given in Table 3-1. Seven gases which are major reactants and products are considered in the simulation: nitrogen, hydrogen, methane, ethane, ethylene, carbon monoxide and carbon dioxide. Two main other components are omitted: water is considered to be completely separated – this is the requirement when a strongly hydrophilic material like zeolite is used; oxygen behaviour during adsorption/desorption is very similar to nitrogen – replacing it by nitrogen significantly reduces computational cost without losing much accuracy. Gas properties such as specific heat capacities or viscosities are taken from (Poling, et al., 2008).

Table 3-1: Zeolite 4A characteristics

Properties	Symbol	Value	Unit
Pellet form		Pellet	
Average size	d_P	0.0032	m
Fractional voidage	ε	0.5	
Density	m	1500	kg/m^3
Specific heat capacity	C_{ps}	1000	J/kg.K
Permeability coefficient	B	2.8×10^{-9}	m^2

Simulation with activate carbon is later conducted. The characteristics of activated carbon are given in Table 3-2. The particle size distribution of activated carbon is assumed to be wider than zeolite 4A. This results in lower fractional voidage and permeability coefficient (higher pressure drop).

Table 3-2: Activated carbon characteristics

Properties	Symbol	Value	Unit
Average size	d_P	0.002	m
Fractional voidage	ε	0.2	
Surface area		1000	m^2/g
Density	*m*	900	kg/m^3
Specific heat capacity	C_{ps}	1000	J/kg.K
Permeability coefficient	*B*	6.2×10^{-10}	m^2

3.2.3. Adsorption characteristics of zeolite 4A

1. Hydrogen:

   Hydrogen is hardly adsorbed on zeolite as well as many other sorbents (Bart & von Gemmingen, 2005).

2. Carbon dioxide:

   Carbon dioxide is the gas with highest affinity toward zeolite. Dual-Langmuir models of carbon dioxide adsorption at 20^OC and 50^OC are available in (Romero-Perez & Aguilar-Armenta, 2010). Thermal expansion coefficient is calculated from adsorption capacities at different temperatures. Diffusion coefficient and activation energy are calculated from (Meng, 1984).

Table 3-3: Adsorption of carbon dioxide on zeolite 4A

T	Q_1	b_1	ΔH_1	Q_2	b_2	ΔH_2	α	D_0	E_a
20^OC	2.024	5.46e-3	-46570	1.303	7.31e-5	-9320	3.48E-3	2.75E-12	11789
50^OC	1.804	8.80e-4	-46570	1.172	4.88e-5	-9320	3.48E-3	2.75E-12	11789

3. Carbon monoxide:

   Dual-Langmuir models of carbon monoxide adsorption at 0^OC and 50^OC are attained by fitting experiment results in (Harper, et al., 1969).

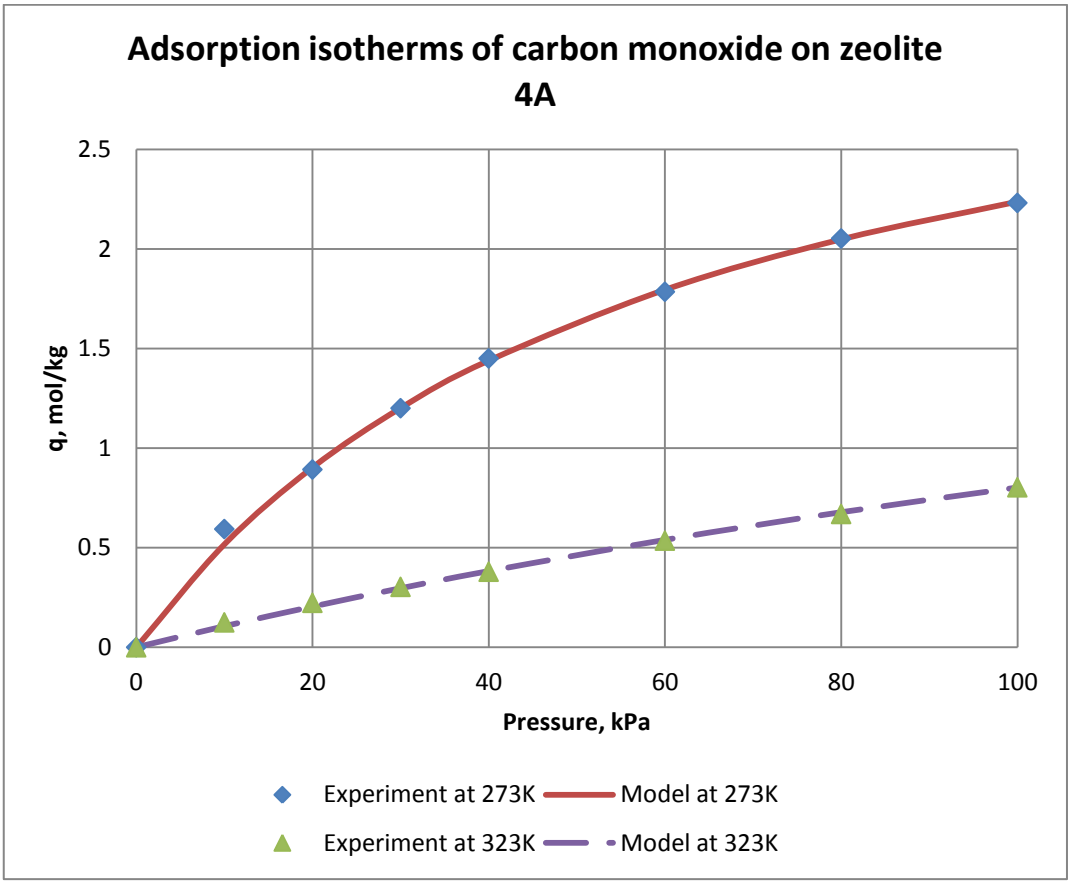

Figure 3-1: Adsorption isotherms of carbon monoxide on zeolite 4A

Thermal expansion coefficient is calculated from adsorption capacities at different temperatures. Heat of adsorption, diffusion coefficient and activation energy are from (Triebe & Tezel, 1995).

Table 3-4: Adsorption of carbon monoxide on zeolite 4A

T	Q_1	b_1	ΔH_1	Q_2	b_2	ΔH_2	α	D_0	E_a
0^OC	2.160	1.71e-5	-20624	1.391	1.71e-5	-20624	3.17E-3	1.21E-10	23312
50^OC	1.810	3.84e-6	-20624	1.175	3.84e-6	-20624	3.17E-3	1.21E-10	23312

4. Ethane:

   Sips models of ethane adsorption at 20^OC and 50^OC are available in (Romero-Perez & Aguilar-Armenta, 2010). They are replaced by fitting Langmuir models.

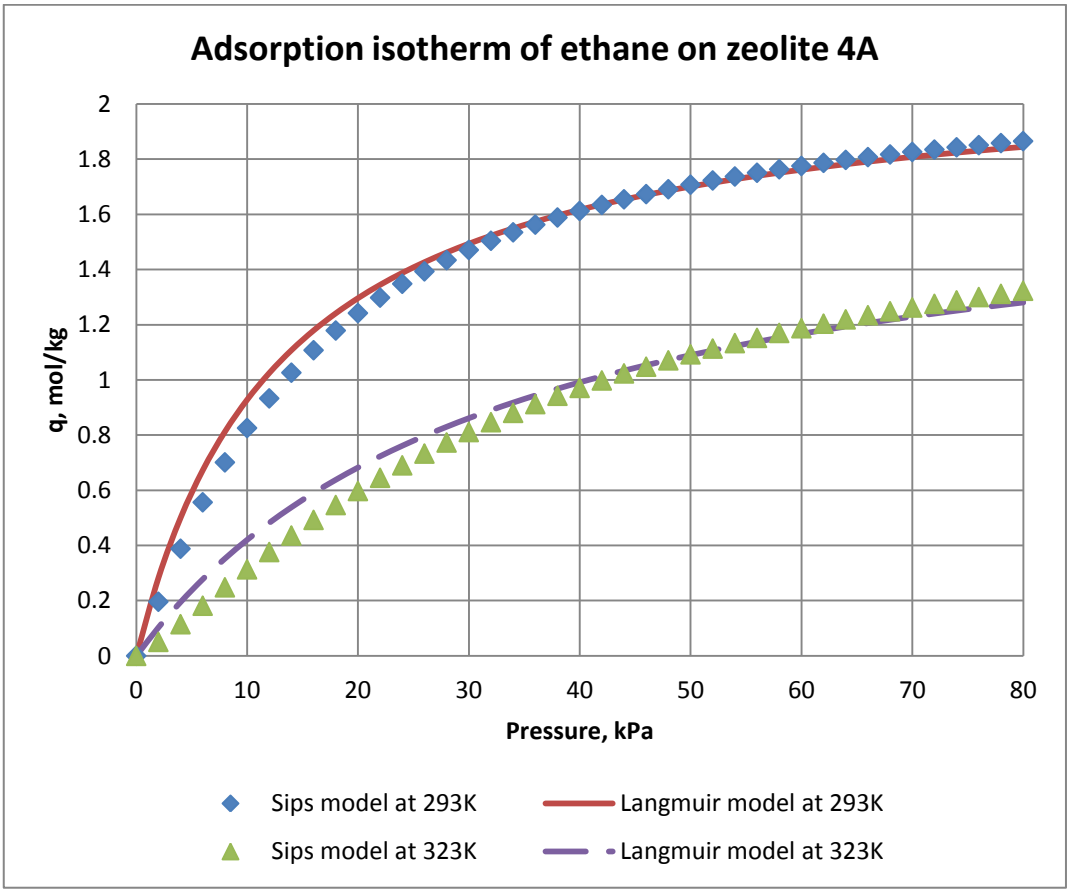

Figure 3-2: Adsorption isotherms of ethane on zeolite 4A

Thermal expansion coefficient is calculated from adsorption capacities at different temperatures. Diffusion coefficient and activation energy are calculated from (Meng, 1984).

Table 3-5: Adsorption of ethane on zeolite 4A

T	Q_1	b_1	ΔH_1	Q_2	b_2	ΔH_2	α	D_0	E_a
20^{O}C	2.147	7.62e-5	-22908	0	0	0	5.26E-3	9.06E-13	14600
50^{O}C	1.808	3.03e-5	-22908	0	0	0	5.26E-3	9.06E-13	14600

5. Ethylene:

Sips models of ethylene adsorption at 20^{O}C and 50^{O}C are available in (Romero-Perez & Aguilar-Armenta, 2010). They are replaced by fitting Langmuir models.

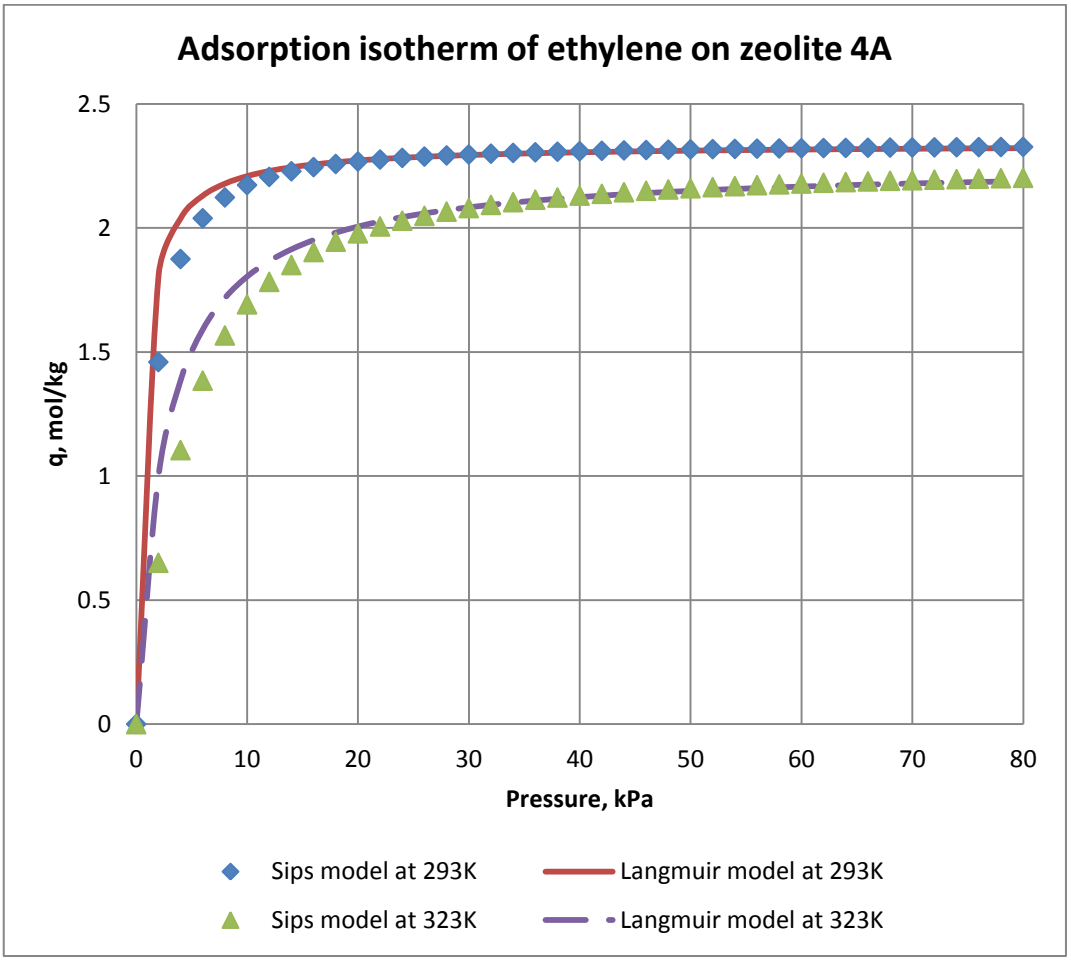

Figure 3-3: Adsorption isotherms of ethylene on zeolite 4A

Thermal expansion coefficient is calculated from adsorption capacities at different temperatures. Diffusion coefficient and activation energy are calculated from (Meng, 1984).

Table 3-6: Adsorption of ethylene on zeolite 4A

T	Q_1	b_1	ΔH_1	Q_2	b_2	ΔH_2	α	D_0	E_a
20^{O}C	2.339	1.70e-3	-36837	0	0	0	1.16E-3	4.75E-12	13800
50^{O}C	2.258	3.98e-4	-36837	0	0	0	1.16E-3	4.75E-12	13800

6. Methane:

Langmuir model of methane adsorption at 35^{O}C is available in (Moore & Koros, 2007). Thermal expansion coefficient is calculated from adsorption

capacities at different temperatures (Harper, et al., 1969). Diffusion coefficient and activation energy are calculated from (Yucel & Ruthven, 1980).

Table 3-7: Adsorption of methane on zeolite 4A

T	Q_1	b_1	ΔH_1	Q_2	b_2	ΔH_2	α	D_0	E_a
0^OC	2.677	4.02e-6	-16720	0	0	0	5.92E-3	3.6E-9	34276
35^OC	2.123	1.64e-6	-16720	0	0	0	5.92E-3	3.6E-9	34276

7. Nitrogen:

   Langmuir model of nitrogen adsorption at 35^OC is available in (Moore & Koros, 2007). Thermal expansion coefficient is calculated from adsorption capacities at different temperatures (Harper, et al., 1969). Diffusion coefficient and activation energy are calculated from (Yucel & Ruthven, 1980).

Table 3-8: Adsorption of nitrogen on zeolite 4A

T	Q_1	b_1	ΔH_1	Q_2	b_2	ΔH_2	α	D_0	E_a
0^OC	2.903	2.66e-6	-23826	0	0	0	5.92E-3	5.3E-10	24244
35^OC	2.302	7.6e-7	-23826	0	0	0	5.92E-3	5.3E-10	24244

3.2.4. Adsorption characteristics of activated carbon

Langmuir isotherms of nitrogen and hydrogen are available in (Choi, et al., 2003).

Langmuir isotherms of methane, ethane, ethylene and carbon dioxide are attained by fitting experiment result in (Reich, et al., 1980) as shown in Figure 3-4, Figure 3-5, Figure 3-6 and Figure 3-7.

Langmuir isotherm of carbon monoxide is available in (Park, et al., 1998).

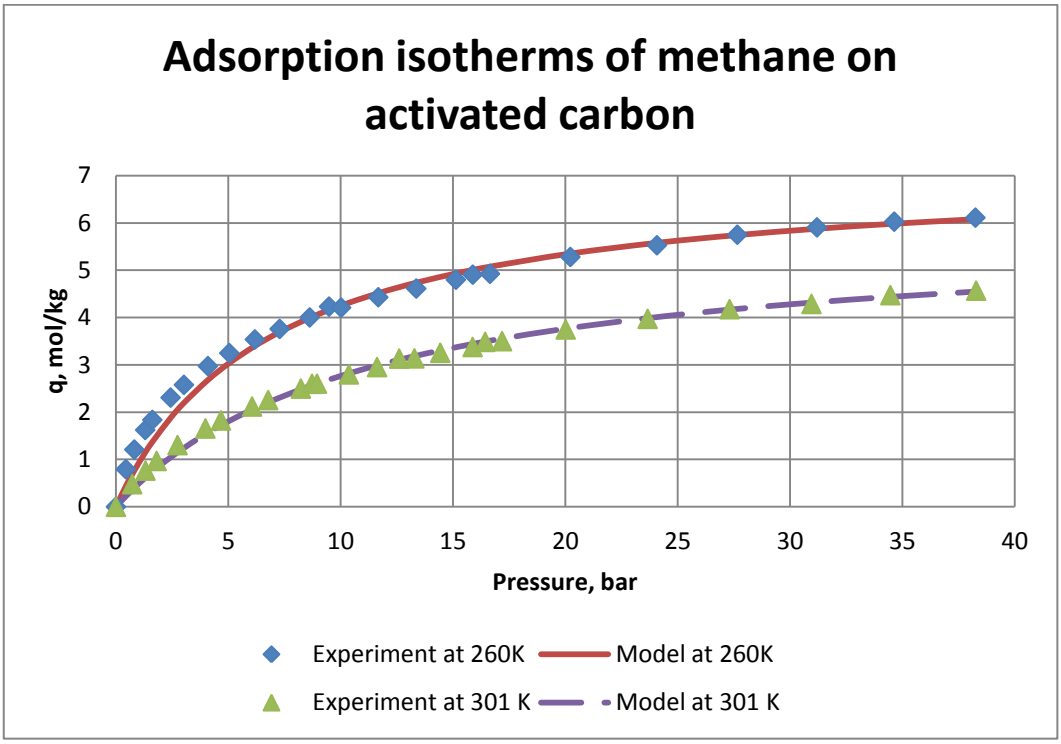

Figure 3-4: Adsorption isotherms of methane on activated carbon

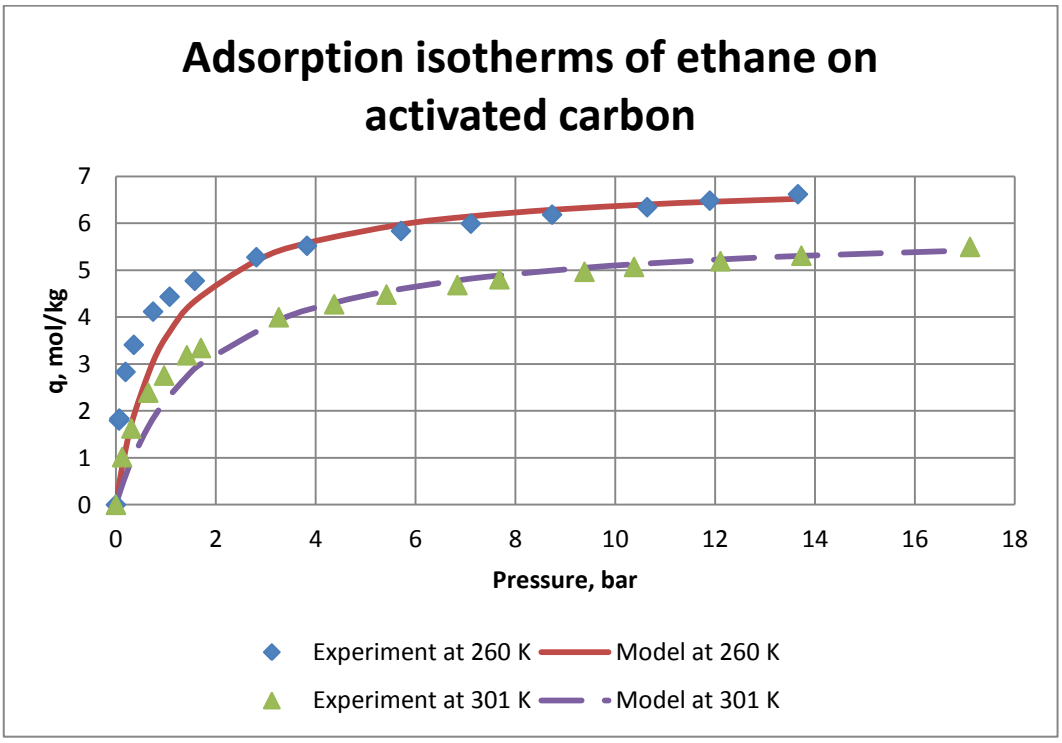

Figure 3-5: Adsorption isotherms of ethane on activated carbon

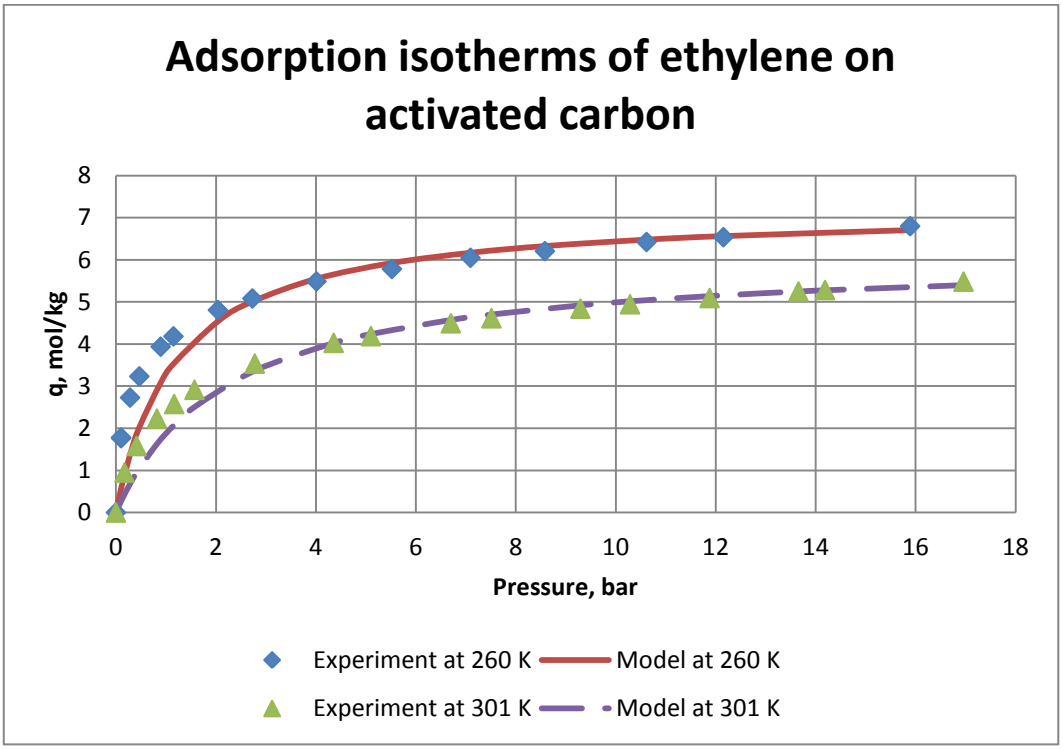

Figure 3-6: Adsorption isotherms of ethylene on activated carbon

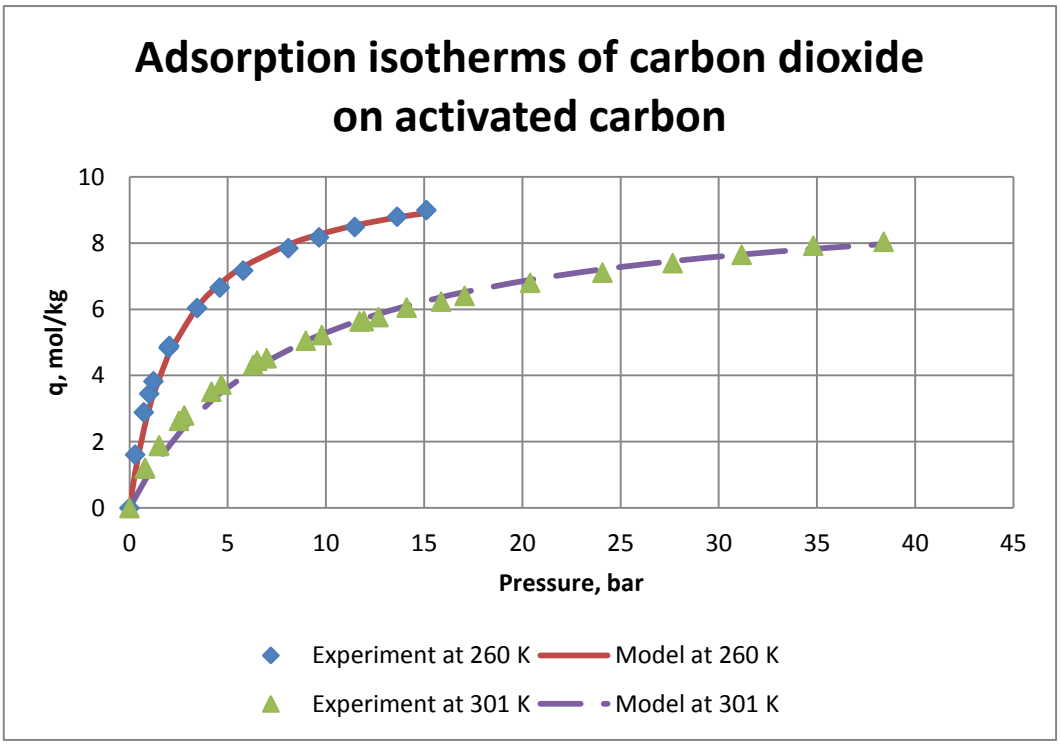

Figure 3-7: Adsorption isotherms of carbon dioxide on activated carbon

Adsorption parameters of activated carbon are summarised in Table 3-9. Because simulation with activated carbon is carried out in a narrow range of temperature, diffusion coefficients are assumed constant for the sake of simplicity.

Table 3-9: Adsorption on activated carbon

Gas	Q * mol/g	b^0 $Pa^{-1}K^{1/2}$	ΔH J/mol	α 1/K	D m^2/s
Nitrogen	3.596	1.48e-7	-11402	6.99e-3	4.00e-6
Methane	5.853	1.04e-6	-6740	4.31e-3	7.60e-8
Ethane	5.918	4.91e-6	-7638	3.58e-3	1.35e-7
Ethylene	6.087	2.18e-6	-8912	3.66e-3	1.44e-7
Carbon monoxide	2.636	1.70e-6	-13118	2.08e-3	5.00e-6
Carbon dioxide	9.672	1.44e-8	-18248	1.52e-3	2.20e-6
Hydrogen	10.153	3.33e-7	0	4.21e-3	1.80e-5

* Adsorption capacity at 303^{O}C

3.3. Numerical diffusion

Numerical diffusion is the known difficulty with computer simulation. High order methods tend to reduce numerical diffusion but might cause unrealistic oscillation. Special techniques such as total variation diminishing (TVD) or flux-corrected transport (FCT) try to minimise numerical diffusion and eliminate oscillation at the same time. These methods however require much more elaboration and, consequently, computation effort. In this work another strategy is applied: physical dispersion is taken out of the original continuous model, the effect of this modification is compensated by numerical diffusion. That means instead of putting much effort to eliminate numerical diffusion we try to match it

with the missing physical dispersion. The matching is not perfect but the difference between physical dispersion and numerical diffusion is tolerable since the influence of dispersion is quite small in gas adsorption processes. In addition we also try to damp oscillation instead of eliminating it completely, which will require much computation effort. This is done by setting a decaying factor *a*: the oscillation amplitude decreases *a* times after each step. Although oscillation still exist, it will be reduced to nearly zero after a short time if decaying factor *a* is large enough. Oscillation can be eliminated (at the cost of more numerical diffusion) if a is set to infinity. Combing two ideas mentioned above, numerical diffusion can be tuned to match physical dispersion by changing spatial discretisation mesh or decaying factor *a* in the equation:

$$\frac{dc_i^{k-1}}{dt} + a\frac{dc_i^k}{dt} = \frac{a+1}{\Delta x}\left(u^{k-1}c_i^{k-1} - u^k c_i^k\right) - \frac{1-\varepsilon}{\varepsilon}\left(\frac{dq_i^{k-1}}{dt} + a\frac{dq_i^k}{dt}\right) \qquad (3.16)$$

The effect of numerical diffusion is tested by simulating inert bed. Figure 3-8 shows the simulation results when methane is fed to an inert column initially full of nitrogen for 2 seconds at a velocity of 0.5 m/s. Without diffusion methane concentration should drop suddenly to zero and nitrogen concentration should rise suddenly to maximum at the middle of column. Instead, when spatial discretisation step size and decaying factor are chosen as 0.5 cm and 1.5 respectively, a 15 cm transitional zone is observed. This is equivalent to physical dispersion with dispersion coefficient D_L in the range of 10^{-4} – 10^{-3} m^2/s, which is compatible with calculation by (Aris & Amundson, 1957) or (Prausnitz, 1958). The simulation took less than 5 seconds to run (on a 3 GHz Core 2 Duo processor) and no artificial oscillation is observed. The implementation was done at Matlab® and the code ode15s was used.

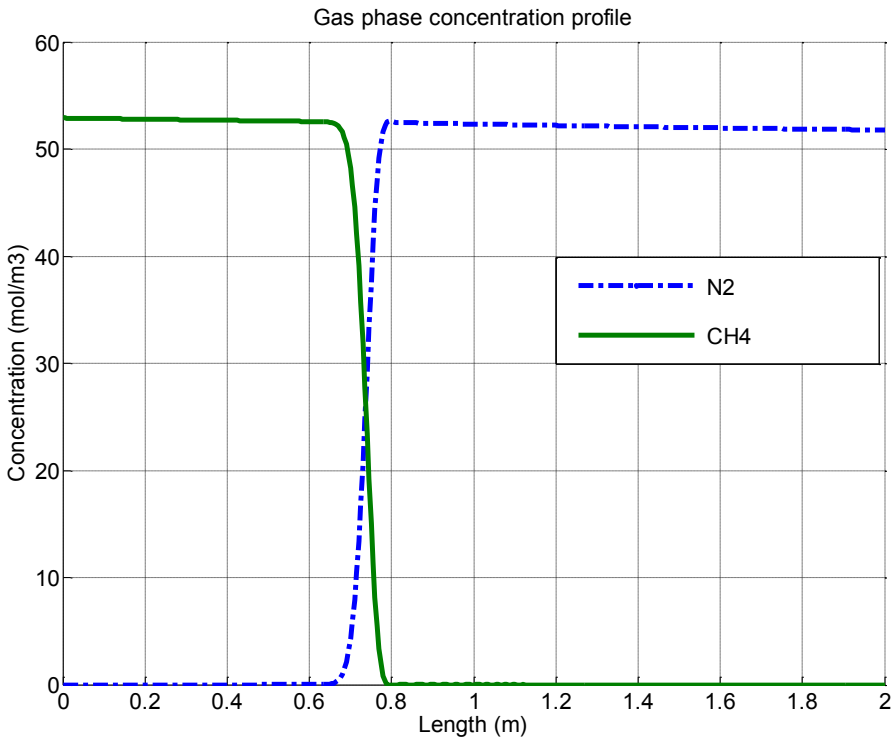

Figure 3-8: Numerical diffusion test

3.4. Simulation result with zeolite 4A

Reactor outlet composition is taken from (Salerno, 2013), where OCM reactions are simulated based on Stansch's kinetic (Stansch, et al., 1997). After being desiccated and cooled down to 40^{O}C the gas composition is:

Table 3-10: Feed composition for simulation

Gas	N_2	H_2	CH_4	C_2H_6	C_2H_4	CO	CO_2
Mol. fraction, %	0.6	19.1	48.5	0.5	8	2.5	20.8

3.4.1. Breakthrough

Since bed radius and cross sectional area do not appear in the model, it can change for scaling up or down the process without affecting simulation result. There is of course technical limitation but it is not necessary to be considered at this stage. For convenience bed cross sectional area is assumed to be 1 m^2 for the whole simulation.

Reactor outlet is fed into a 2-metre adsorption column full of nitrogen at a velocity of 0.5 m/s. Feed temperature and initial bed temperature are both 320 K and outlet pressure is fixed at 1.03 bar – slightly higher than atmospheric pressure. Void fraction is assumed to be 50%. The breakthrough curve is depicted in Figure 3-9. The initial amount of nitrogen is flushed out of the column in few minutes. Methane and hydrogen appear at the outlet almost immediately while carbon monoxide and ethane concentrations increase gradually. Ethylene and carbon dioxide break through after 12.5 minutes.

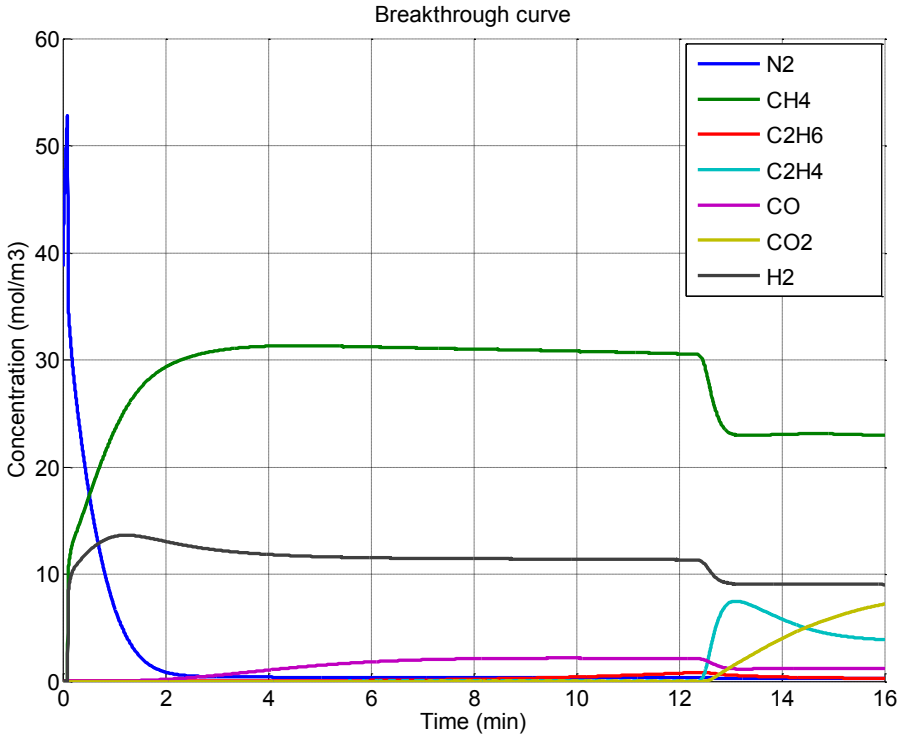

Figure 3-9: Breakthrough simulation

Because outlet pressure is fixed, total concentration is almost constant (a little variation due to temperature change): methane and hydrogen concentrations drop when ethylene and carbon dioxide concentrations rise. The breakthrough curve however does not reflect the actual amount of gases: total flow rate increases along with velocity when adsorption front reaches the outlet as shown in Figure 3-10. If online concentration monitoring is not available in real process,

flow or velocity meter can help detecting when adsorption front approach. In order to avoid ethylene lost adsorption step must finish few minutes before it breaks through. This amount of time is necessary for co-current blowing, which improve ethylene purity.

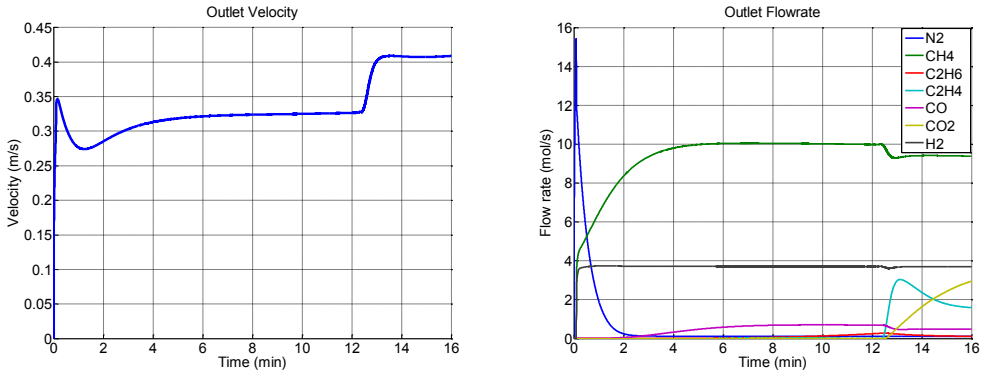

Figure 3-10: Outlet velocity and flow rates

3.4.2. Separation

Two important criteria of a separation process are purity and recovery. Ethylene is usually required in high purity. The goal of separation is producing ethylene at CP grade – 99% (carbon dioxide is ignored). Because ethylene is expensive, losing it during separation is very undesirable. This work aims at 99% ethylene recovery in the separation, which means about 1% increase of production costs compare to complete recovery. The separation procedure, based on conceptual design in chapter two, consists of 4 steps:

1. Adsorption: Reactor outlet is fed to adsorption column after cooling and drying. With above operating conditions, this step is chosen to last 10 minutes. As separation process involves multi columns, the duration of other steps are chosen to be multiple of ten minutes so that a synchronous switching between columns can be achieved.
2. Co-current blow: The purpose of this step is wiping out all the unwanted gases (methane, carbon monoxide,…) in the void of column as well as on the surface of sorbent. This step is essential to achieve high purity when

selectivity is limited and void fraction is high. Purge gas can be carbon dioxide, ethylene it self or a mixture of both. Sweeping away unwanted gases needs only short time and too long blow will lead to ethylene lost. This step is however extended to ten minutes to match adsorption step without losing ethylene. The extension is done by adjusting flow rate.

3. Ethylene desorption: Carbon dioxide is fed to adsorption column until all ethylene is collected at outlet. Carbon dioxide flow rate can be adjusted so that duration is multiple of ten minutes. The trade-off between bed inventory and amount of carbon dioxide is considered when specifying duration.
4. Carbon dioxide desorption: Carbon dioxide is desorbed by purging with air because it is free and diluted effluent can be emitted directly to environment at the end of this step. The duration of this step is also a multiple of ten minutes. Hot air is used first for faster desorption. Cool air is used later to cool down adsorption bed simultaneously with carbon dioxide desorption.

All steps are performed at low pressure to save compression cost. Adsorption takes place at 320 K – around the reactor outlet temperature after cooling. Since carbon dioxide is strongly adsorbed to zeolite, hot air is necessary at the beginning of step 4. Cool air is needed later to cool down adsorption column for the next cycle. In steps 2 and 3 ‘heavier’ gases can displace ‘lighter’ gases without high temperature. However heating time in step 4 can be shortened if the column is preheated in these steps. Higher temperature also means higher volumetric flow rate and faster desorption. Because temperature limit for ethylene – according to ATEX directive – is $300^{O}C$, purge gases in steps 2 and 3 are also heated up to 550 K.

The following simulations are done with a 15 cm^2 cross sectional area column and Bürkert valve type 2836 is installed at the outlet. Valve characteristic is taken

from manufacturer's datasheet (code: 154 553). Flow rates are then scaled up to match 1 m^2 cross sectional area column for convenience. Two schemes are analysed to compare the effect of using ethylene and carbon dioxide in co-current blow step: ethylene in scheme 1 and carbon dioxide in scheme 2. The fourth step – carbon dioxide desorption – is not shown here because it is the same for both schemes as we will see later. After that, the third scheme with real production criteria – 99% recovery and purity – is presented. The general flow sheet for all schemes with two adsorption columns is presented in Figure 3-11, ethylene circulation is only required in scheme 1. The real number of adsorption columns depends on the duration ratio between total cycle and adsorption step. Heaters are hidden for a clearer view.

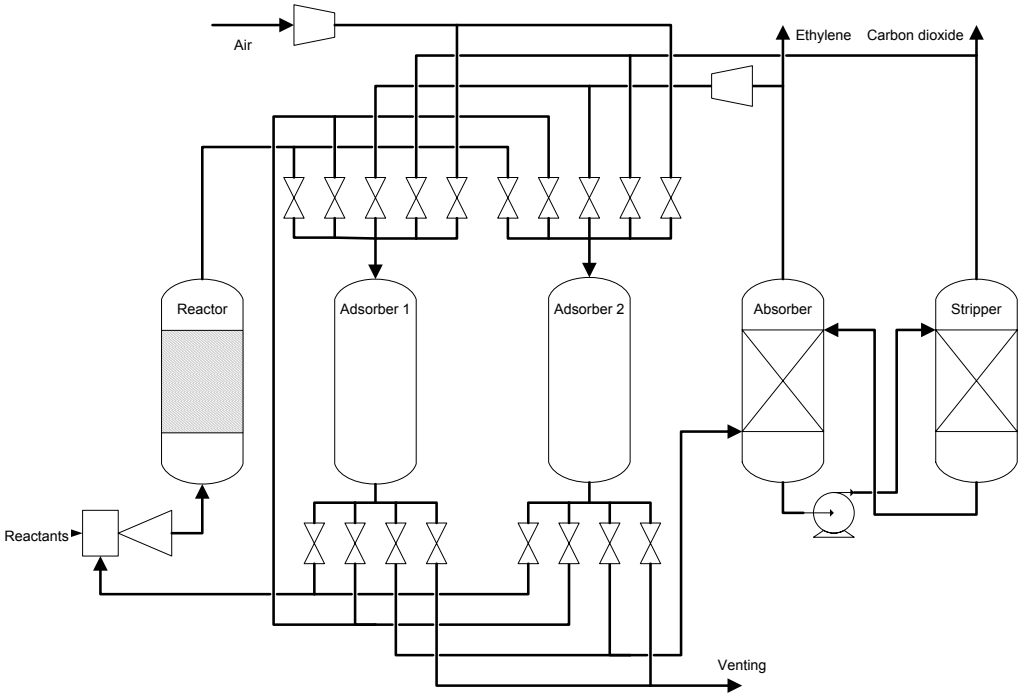

Figure 3-11: Flow sheet for schemes 1, 2, 3

Outlet gas concentrations, velocity and flow rates of adsorption step are in Figure 3-9 and Figure 3-10. State of the column at the end of adsorption step is depicted in Figure 3-12. Methane, ethane and carbon monoxide are displaced by

carbon dioxide and ethylene; they concentrate at the end of column. There is still some methane adsorbed at the beginning of the column due to its high concentration in the feed. Ethane is adsorbed more strongly than methane and carbon monoxide so its front is less steep than the others, which means displacement of ethane is not as effective as the ones with methane and carbon monoxide. Ethane is therefore the main concern in co-current blow step. Ethylene is also partly displaced by carbon dioxide and forms a peak right at carbon dioxide front. Carbon dioxide profile forms two plateaus corresponding to the temperature wave: saturated concentration is more than 3 kmol/m^3 at the beginning of column, where temperature is only 320 K but less than 1.5 kmol/m^3 at the middle of column, where temperature rises to more than 380 K. This dependence means heating is the appropriate measure for desorbing carbon dioxide from zeolite.

Temperature near inlet quickly rises to a peak then drops to feed gas temperature. Temperature far from inlet increases slowly at first but sharply when adsorption front arrives. In real process where online measurement of adsorbate concentration is impossible, temperature monitor can help locate adsorption front. With the assumption of temperature equilibrium between gas and solid phase, temperature front almost coincides with concentration front. However a small oscillation can be notice in case of temperature. This is due to the decoupling of heat and mass balance said in section *Numerical solution* above. The magnitude of oscillation is only few centigrade and does not affect concentration calculation but simulation is much faster. The ratio of run time over simulation time is around 2 – a quite impressive number considering the nonlinear property of the model and the number of components.

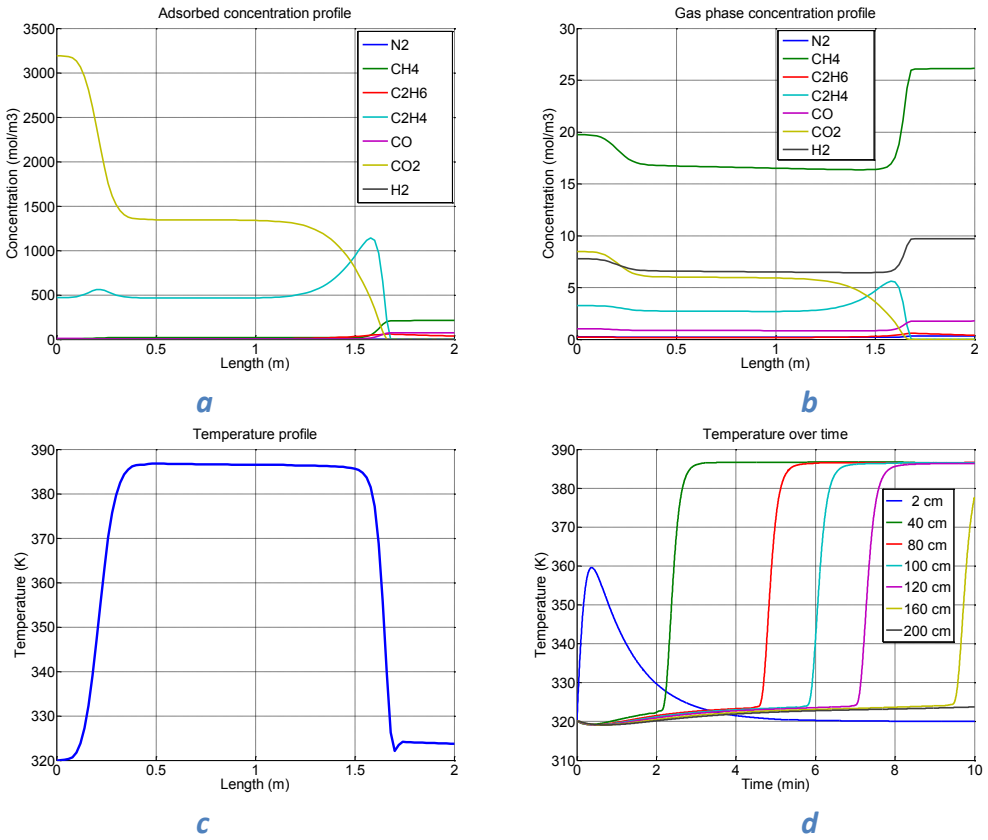

Figure 3-12: Simulation result of adsorption step

Profiles at the end of adsorption step: concentration in adsorbed phase (*a*), concentration in gas phase (*b*), temperature profile (*c*); and temperature over time at different distances from bed inlet (*d*)

After adsorption step there is still a significant amount of unwanted gases in column, both adsorbed and gas phases. Co-current blow is necessary to obtain ethylene with high purity. Simulation results of this step with ethylene and carbon dioxide as purge gases are in Figure 3-13 and Figure 3-14 respectively, profiles along the column are at the end of steps.

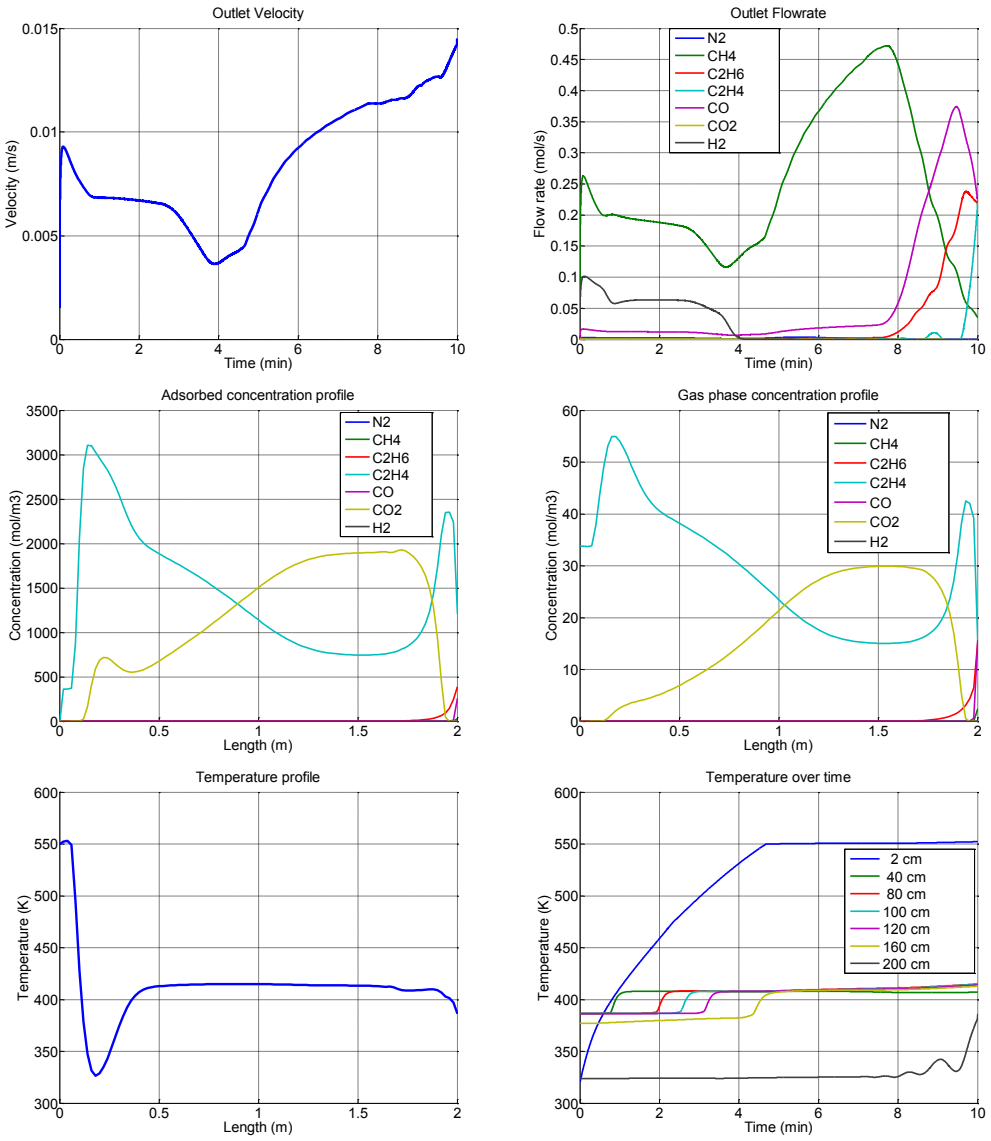

Figure 3-13: Co-current blow with ethylene – scheme 1

The outlets of two cases are very similar but concentration profiles are different. It can be seen from concentration profile in adsorbed phase that carbon dioxide in feed gas displaces ethylene more effectively than ethylene in feed gas displace carbon dioxide. The reason is that ethylene can only displace carbon dioxide in one site. For the other site with smaller pore sizes it acts as inert gas.

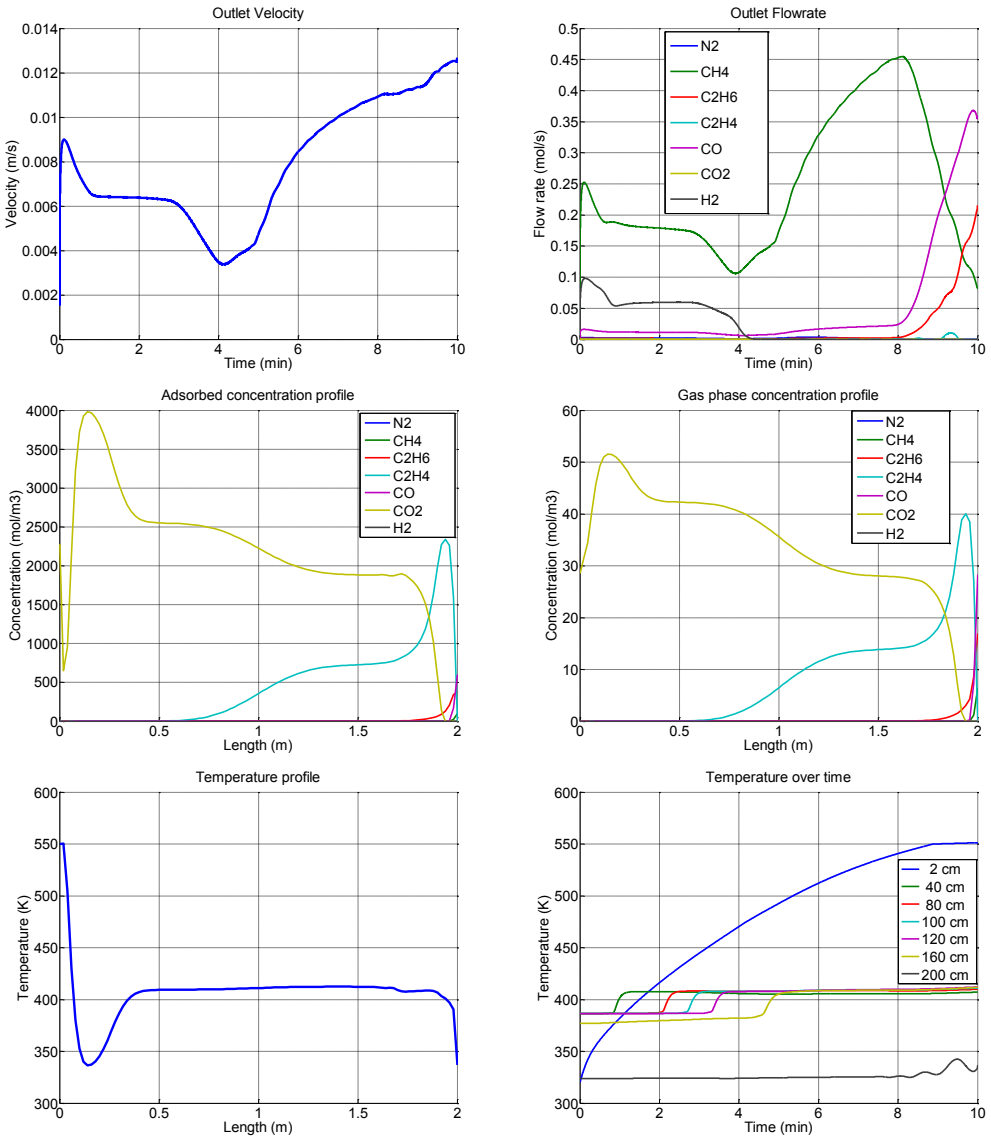

Figure 3-14: Co-current blow with carbon dioxide – scheme 2

In scheme 1, adsorption column is purged by carbon dioxide with a velocity of 0.6 m/s after ethylene blow. The result is in Figure 3-15. After ten minutes there is no ethylene in column, both adsorbed and gas phases. Outlet composition is given in Table 3-11. After carbon dioxide removal, ethylene can be recovered at 99% purity.

Table 3-11: Outlet composition of ethylene desorption step in scheme 1

Gas	N_2	H_2	CH_4	C_2H_6	C_2H_4	CO	CO_2
Mol. fraction, %	0	0	0.005	0.234	33.15	0.041	66.57

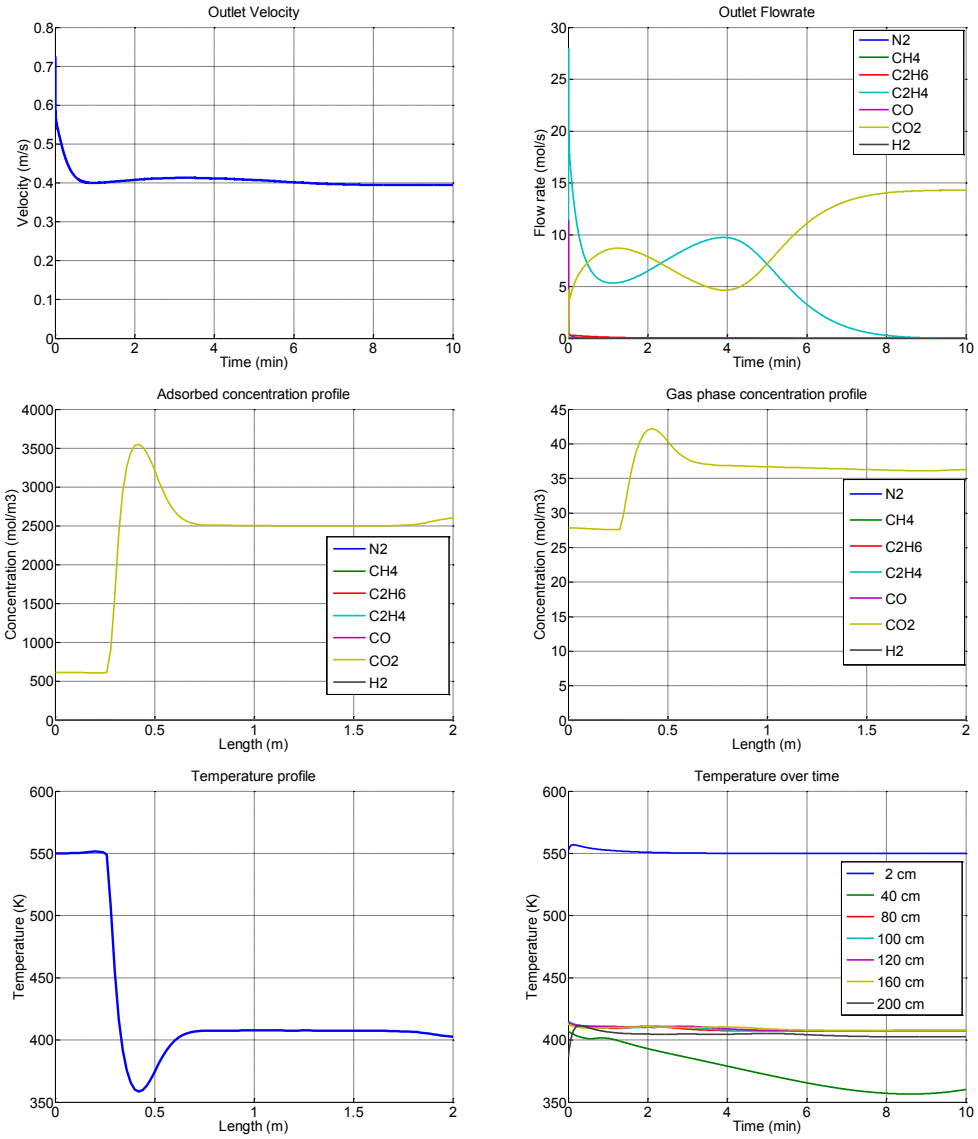

Figure 3-15: Purging by carbon dioxide in scheme 1

In scheme 2, adsorption column is purged by carbon dioxide with a velocity of 0.35 m/s after carbon dioxide blow. The result is in Figure 3-16. After ten minutes there is no ethylene in column, both adsorbed and gas phases. Outlet composition is given in Table 3-12. After carbon dioxide removal, ethylene can be recovered at 96% purity.

Table 3-12: Outlet composition of ethylene desorption step in scheme 2

Gas	N_2	H_2	CH_4	C_2H_6	C_2H_4	CO	CO_2
Mol. fraction, %	0	0	0.033	0.504	17.98	0.213	81.27

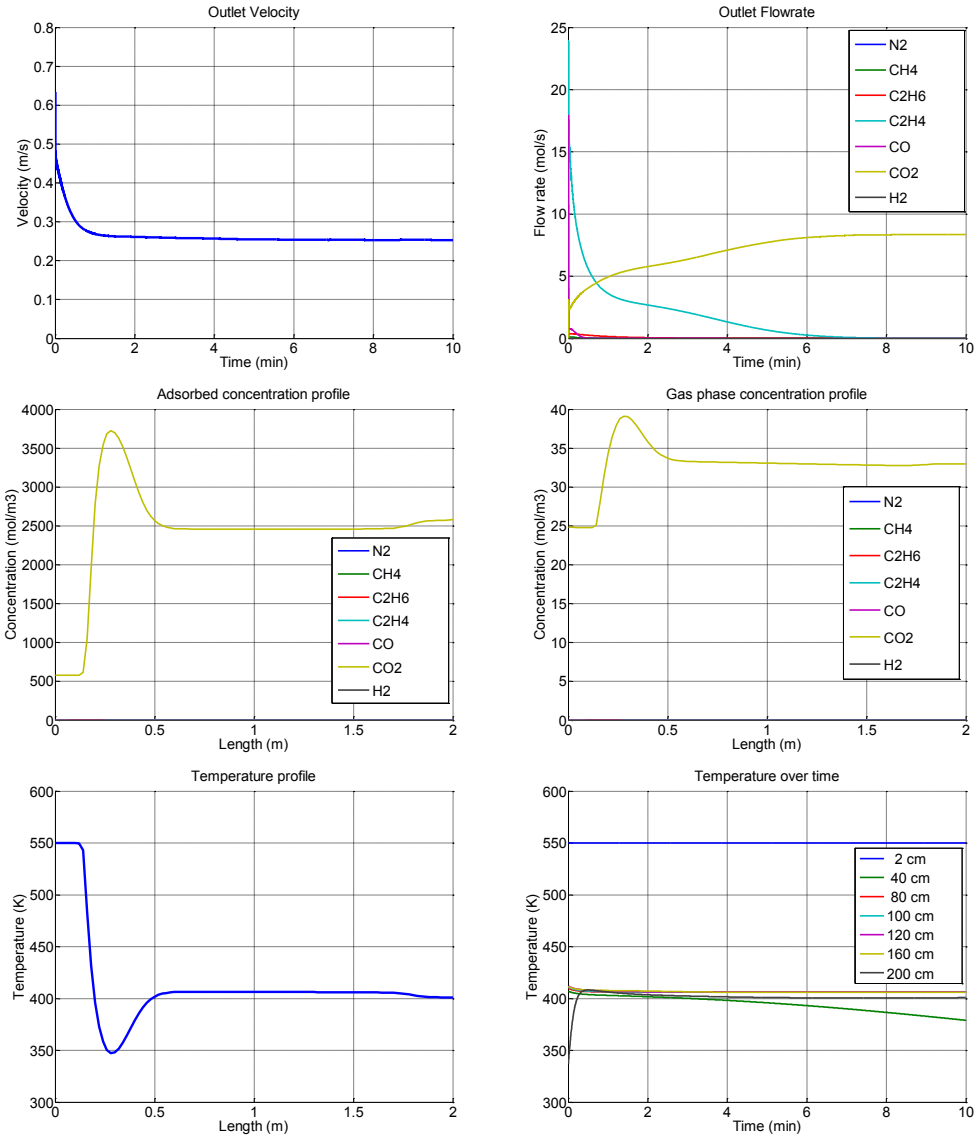

Figure 3-16: Purging by carbon dioxide in scheme 2

Unlike the previous step, the states of adsorption column after purging are similar in two cases but outlets are different. Scheme 1 requires almost double sweep gas flow rate, which in turn results in higher outlet flow rate and more carbon dioxide needs removing although it is fed only in one step. The advantage of using ethylene for co-current blow is higher purity because more paraffin is

blown out before ethylene appears at the outlet. However operation is simpler and less equipment are required if carbon dioxide is used.

Considering all the pros and cons mentioned above, carbon dioxide is the better choice for co-current blow. The source of carbon dioxide for both steps is stripper column in carbon dioxide removal section as stated in *Process flow development*. Because ethylene helps increase purity, a mixture of ethylene and carbon dioxide can be used in co-current blow step instead of pure carbon dioxide. Therefore a portion of effluence of ethylene desorption step is recycled for co-current blow without going through carbon dioxide removal section. This solution reduces carbon removal duty. The simulation of scheme 3 with this design is presented below. Operating parameters such as feeding flow rate are tuned to achieve the set performance.

The separation routine of scheme 3 lasts one hour. Adsorption (step 1) and co-current blow (step 2) each last ten minutes. Ethylene desorption (step 3 and 4) and carbon dioxide desorption (step 5 and 6) are lengthen to twenty minutes so that the effluent can be recycled to purge previous steps. This extension increases the required bed inventory but reduces the amount of gases needed for operation. The inlet and outlet of steps are given in Table 3-13.

Table 3-13: Inlets and outlets in scheme 3

Step	Feed gas		Usage of effluent
	Source and flow rate	T, K	
1	Reactor outlet at a velocity of 0.5 m/s	320	To reactor or other processes
2	46% of effluent from step 3	550	To reactor or other processes
3	Effluent from step 4	550	To step 2 and CO_2 removal
4	Carbon dioxide at a velocity of 0.29 m/s	550	To step 3
5	Effluent from step 5	370	To CO_2 removal and vent
6	Dry air at a velocity of 4 m/s	310	To step 5

The effluent of adsorption column through six steps, achieved after nearly 90 minutes running simulation, is illustrated in Figure 3-17. “Light” components are collected during the first twenty minutes, mostly in the first ten minutes. The second ten minutes contributes little to methane and hydrogen recoveries due to very small flow rate but is crucial to ethylene purity. This small flow rate is typical with displacement purge but it also gives a hint that co-current blow duration and bed inventory can be significantly reduced. Ethylene is desorbed during the second twenty minutes but only collected in the first half and recycled in the second. This circulation does not only halve carbon dioxide consumption as sweep gas but also avoids the expensive retrieval of ethylene from highly diluted mixture. The composition of ethylene-rich stream is given in Table 3-14. After carbon dioxide removal, 98.9% ethylene is recovered with 98.9% purity and the main contaminate is ethane – 1%. Carbon dioxide is desorbed in the last twenty minutes with the effluent during second half is also recycled. Although highly diluted carbon dioxide can be emitted directly to atmosphere, this recirculation is very beneficial because it help save a lot of air blowing duty.

Table 3-14: Composition of ethylene-rich stream in scheme 3

Gas	N_2	H_2	CH_4	C_2H_6	C_2H_4	CO	CO_2
Mol. fraction, %	0	0	2e-4	0.381	35.19	0.008	64.42

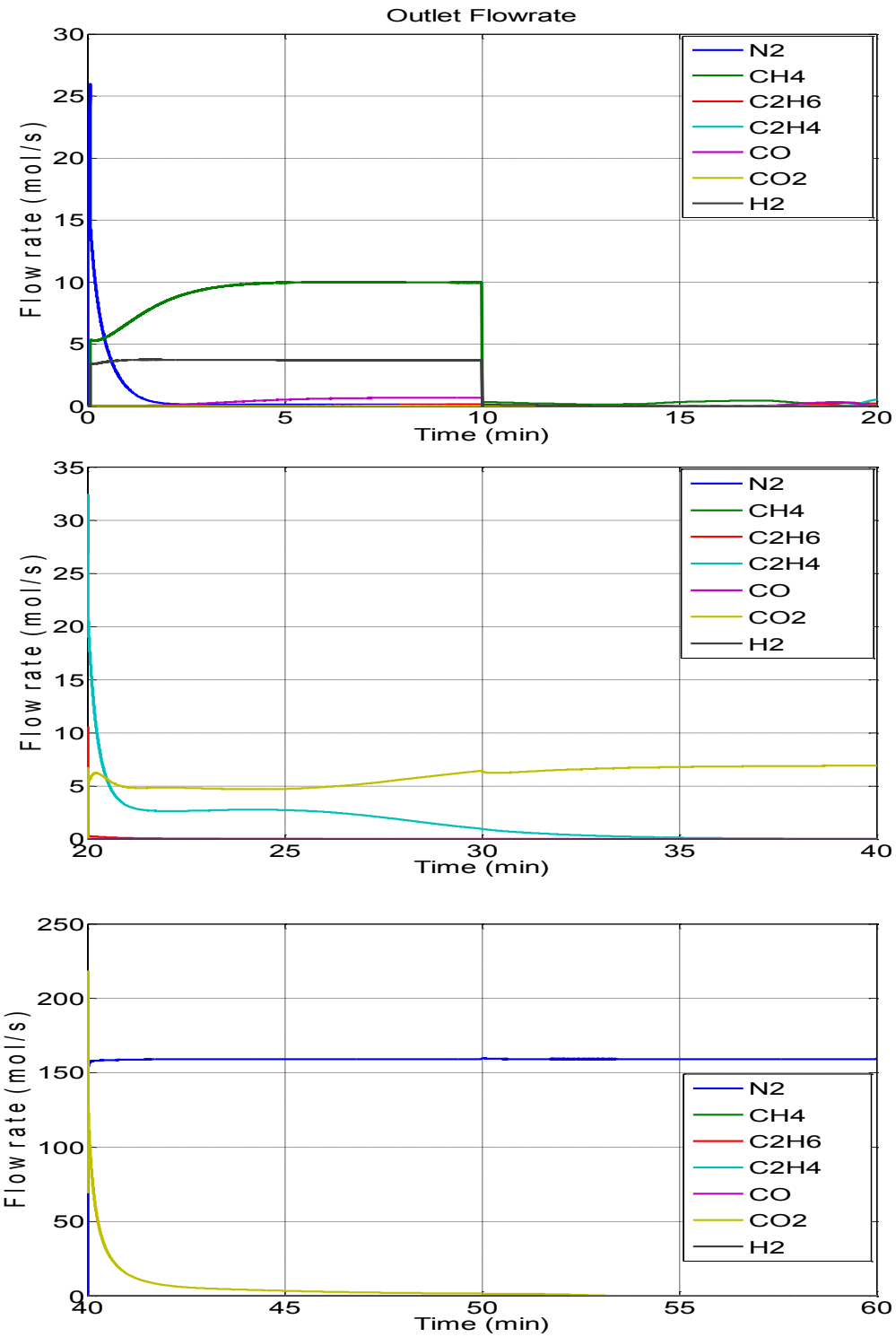

Figure 3-17: Effluent of entire cycle in scheme 3

3.4.3. Discussion

The reactor performance from (Salerno, 2013) is 45.4% methane conversion with 39.7% ethylene selectivity and 2.5% ethane selectivity. When this reactor is combined with conventional downstream process, the operating cost is 834 €/t ethylene according to equation (2.4). This high operating cost is due to low selectivity: only raw material already cost 645€. The consequence is a payout period longer than 15 years when ethylene price is 1135 €/t (Salerno, 2013). When separating one tonne of ethylene with scheme 3, nearly 11 tonnes of carbon dioxide pass through adsorption column. Among them 2.9 tonnes need separating from ethylene, 3.8 tonnes need separating from air for recirculation and about 4 tonnes are diluted by air – less than 4% – and can be emitted to atmosphere. Desorption steps also consume 84000 m^3 air and 5.9 GJ heating for each tonne of ethylene produced. Beside air blower, the other major equipments required in scheme 3 are adsorption columns. Bed inventory is 4.8 tonne of zeolite for per tonne/day or 115 kg of zeolite for per kg/h ethylene production. The utilities consumption per tonne ethylene for downstream process in scheme 3 is summarised in Table 3-15. Costs of major equipments in adsorption section are given in Table 3-16. For comparison, investment on compressor and demethanizer in case of conventional downstream solution is €21 million (Salerno, 2013).

Simulation shows that adsorptive (scheme 3) and conventional downstream solutions require about the same initial investment (refrigerant compressors are excluded as it is already accounted in utilities cost). Scheme 3 is slightly better as a few percents of operating cost can be saved. Overall this particular adsorptive separation scheme improves the profitability of OCM technology but not enough to change its economic status. The biggest advantage of this scheme in comparison with conventional solution is the robustness against inert diluents such as nitrogen. No matter how much nitrogen presents in reactor outlet it will

get out of adsorption column together with methane and hydrogen and does not affect ethylene adsorption thanks to the big difference between their affinities.

Table 3-15: Operating cost summary

Item	Unit	Amount	Price*, €	Total price, €
CO_2 removal				
Pumping	kWh	5.4	0.075	0.41
Steam	tonne	6.7	5.67	37.99
Caustic soda	kg	0.08	3	0.24
Adsorption				
Heating	GJ	5.9	2	11.8
Air blowing	kWh	1680	0.075	126
Total				**176.44**

* Utilities prices are calculated according to (Ulrich & Vasudevan, 2006) at CE PCI = 588.8 and fuel price at 2 $/GJ

Table 3-16: Equipment cost

Item	Specification	Unit	Amount	Price*, x1000€	Total price, x1000€
Sorbent	Zeolite 4A	tonne	1940	2	3880
Column	8x10 (DxH)	pcs.	6	597.2	3583.2
Blower**	64500 m^3/h	pcs.	22	492.5	10835
Total					**18298.2**

* The prices of equipments are estimated by Aspen Process Economic Analyzer

** Only small blowers are available in the database of Aspen Process Economic Analyzer. Lower price when one big blower is installed instead of 22 small ones.

Although only one of the goals set for adsorptive solution is achieved, the studied case is far from optimal and there are points that can be improved for a better process:

- Proper reactor performance: Reactor can operate at different conditions and performance. Low selectivity means waste of raw materials and no separation technique can help it. High selectivity however couples with low conversion and increasing cost of methane separation may overshadow raw material save. As adsorption can separate methane at a lower price, it should be combined with highly selective performance.
- Air blower: A major advantage of adsorptive separation is avoidance of expensive compression (gas and refrigerant). In scheme 3, it is however replaced by air blowing. Air blowing makes up half of initial investment (in adsorption section) as well as 70% of separation cost and cancels the above mentioned advantage. Although cost of air blowing can be reduced by lowering pressure drop with bigger sorbent particles and pipes, adsorptive separation can only be really superior when the need for air blowing is eliminated or significantly reduced. This means it is necessary to find another sorbent where carbon dioxide desorption is easier, even with the sacrifice of adsorption capacity and selectivity.

One more point should be concerned with adsorptive separation is collection of effluent. Unlike distillation, absorption or membrane processes where separated components come out at the same time from different outlets, components separated by adsorption come out from the same outlet at different time. This feature enables the chance that separated component mix back together. Simulation shows the composition at the end of adsorption column and back mixing in column is already accounted. Out of column back mixing can still occur in connecting pipes where Reynold number increases due to diameter reduction and at local obstacle such as valves or pipe connections. This matter must be taken into consideration during process design. In scheme 3, the sequence of components come out of column matches their order of affinity: hydrogen, methane, carbon monoxide, ethane, ethylene and carbon dioxide. Hence, back mixing may contaminate ethylene with ethane and carbon monoxide. If the

order of affinity can be changed so that carbon dioxide comes between ethylene and other components, separation performance will be improved and the process will be more robust toward pipe layout and switching time. All these points will be covered in the next part.

3.5. Simulation result with activated carbon

In this simulation, a smaller outlet valve is selected (Bürkert valve type 2833, code: 175 900) because there is no high flow rate air blowing.

Reactor outlet composition is chosen as case three (Pan, et al., 2010) in Table 2-1. Compare to the performance from (Salerno, 2013), methane conversion is lower but selectivity is higher resulting in a little lower yield (16.5% compare to 18%). The gas composition is:

Table 3-17: Feed composition for simulation

Gas	N_2	H_2	CH_4	C_2H_6	C_2H_4	CO	CO_2
Mol. fraction, %	0	6.4	65.5	3.7	8.8	6.5	9.1

3.5.1. Separation

The separation cycle in case of activated carbon, scheme 4, lasts half an hour with adsorption, co-current blow and desorption each last ten minutes. A part of the effluent from desorption step is recycled for co-current blow. The inlet and outlet of steps are given in Table 3-13. Because all gases are easier to desorb, neither heat up nor air blow are required. It can be noticed that adsorption with activated carbon is performed at lower temperature in comparison with zeolite 4A. Low temperature is usually desired since it favours adsorption. However, in case of zeolite 4A, mass transfer rate is restricted by small pore structure and temperature must be high enough for a reasonable diffusion rate. This problem does not occur with the large pore structure of activated carbon and a lower operating temperature can be chosen.

Table 3-18: Inlets and outlets in separation with activated carbon

Step	Feed gas		Usage of effluent
	Source and flow rate	T, K	
1	Reactor outlet at a velocity of 0.625 m/s	300	To reactor or other processes
2	26% of effluent from step 3	300	To reactor or other processes
3	Carbon dioxide at a velocity of 1 m/s	300	To step 2 and CO_2 removal

The flow sheet for scheme 4 is presented in Figure 3-18. It is easy to notice that two-step adsorption (scheme 4) requires less switching valves than three-step adsorption (schemes 1, 2, 3). This does not only result in less investment but also simpler operation.

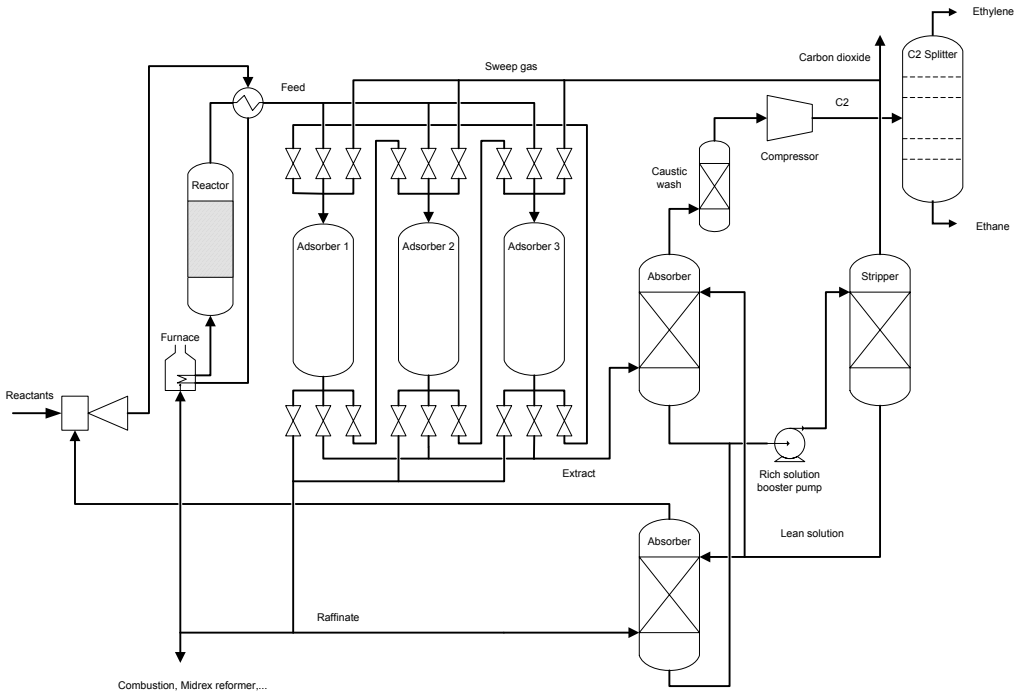

Figure 3-18: Flow sheet for scheme 4

The effluent of adsorption column through three steps is illustrated in Figure 3-17. “Light” components are collected during the first twenty minutes, mostly in the first ten minutes. Ethylene is desorbed during the last ten minutes with 99.9% recovery. Without a dedicated carbon dioxide desorption step, there are

considerable amounts of carbon dioxide in both extract and raffinate streams. Therefore each stream is fed to its own absorber to remove carbon dioxide as depicted in Figure 3-18. The absorber for raffinate can be however omitted if methane and carbon dioxide are processed together, for example in burner or Midrex methane reformer. The compositions of ethylene-rich stream before carbon removal, after carbon removal and after ethane removal are given in Table 3-19.

Table 3-19: Composition of ethylene-rich stream in scheme 4

Gas	N_2	H_2	CH_4	C_2H_6	C_2H_4	CO	CO_2
Before carbon dioxide removal							
Mol. fraction, %	0	0	0.0191	2.8136	7.4323	1e-4	89.735
After carbon dioxide removal							
Mol. fraction, %	0	0	0.1854	27.41	72.404	0.0006	0
After 98% ethane removal							
Mol. fraction, %	0	0	0.25	0.75	99	0.0008	0

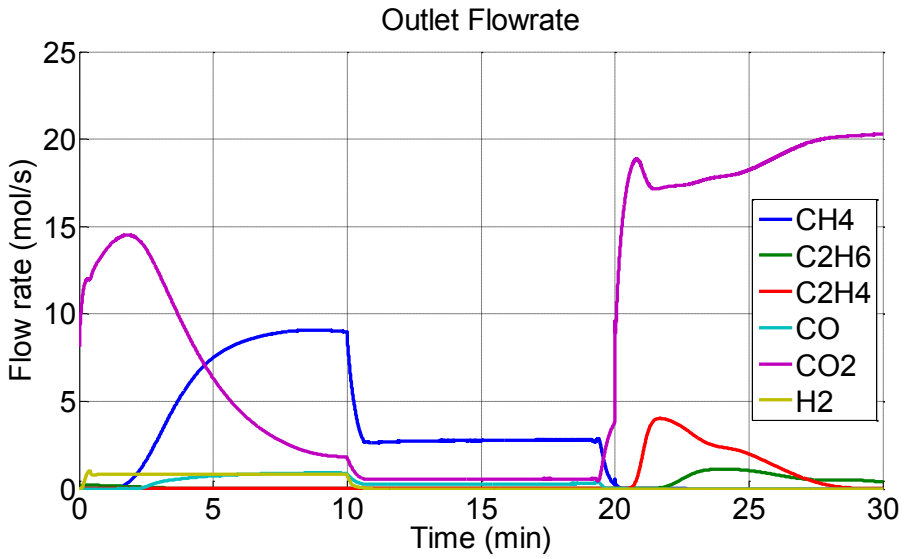

Figure 3-19: Effluent of entire cycle in scheme 4

3.5.2. Discussion

Operating cost with conventional downstream processing is 817 €/t ethylene in case three, somewhat less than the case from Salerno thanks to lower raw material cost – 583 €/t ethylene. Compare to zeolite 4A, activated carbon works faster with cycle duration reduced by a half but separation performance is worse with almost no ethane/ethylene separation. However neither compressor nor blower is necessary.

Although heating and air are not required for operation, carbon removal duty is 28.6 tonne CO_2 per tonne ethylene – more than double as in scheme 3. Separation cost in scheme 4 is therefore solely cost of carbon dioxide removal – 166 €/t ethylene. Compare to scheme 3, separation cost is lightly reduced. Compare to conventional downstream process, separation cost is reduced by 25%. Since separation makes up about 30% operating cost (in conventional downstream process), total operating cost is reduced by 7%.

Bed inventory in scheme 4 is 3.9 tonne of activated carbon per tonne/day or 94 kg of activated carbon per kg/h ethylene production. Compare to scheme 3, bed inventory is reduced by 18% but reduction of cost of sorbent is much more because activated carbon can be ten times cheaper than zeolite 4A.

Based on simulation result, it can be said that methane removal with activated carbon is more economic than conventional distillation as well as methane and ethane simultaneous removal with zeolite 4A. The achieved result can still be improved by:

- Increasing reaction selectivity: Although separation cost is remarkably saved (compare to conventional downstream process), total operating cost is only reduced by a few percent as separation only makes up a small portion of production. If reaction selectivity is increased (although conversion may

decrease), operating cost will shift from raw material to separation and the benefit of adsorptive separation will be amplified.

- Lengthening desorption duration: When desorption duration is lengthened, total cycle time will increase along with bed inventory. This means more initial capital is required. However by lengthening desorption duration it is possible to lower sweep gas flow rate and carbon dioxide consumption can be saved by recirculation of diluted ethylene (the last minutes in desorption step). Taking into consideration that operating cost contribute more than initial capital to the final price, this compromise is likely to bring more befit.

These judgements will be implemented on experimental study.

Chapter 4. Experimental study

Simulation has revealed important aspects of adsorption and useful guidelines for designing downstream process. In the next step, single column experiment is conducted to give more accurate information on adsorptive separation and more concrete conclusion about the proposed solution.

4.1. Experiment setup

Adsorption experiment setup is integrated into an existing OCM mini-plant, which already consisted of OCM fluidised-bed reactor, membrane reactor and an absorption unit for carbon dioxide removal. The inlet of adsorption unit is connected to the outlet of fluidised-bed reactor so that it can process reactor effluent as described in Chapter 2. The reactor is fed with methane, oxygen and nitrogen from cylinders installed outside mini-plant. Beside the real reactor effluent, it is necessary to experiment on artificial ones, which may be taken from literature or modified to test the flexibility of adsorption process. Therefore methane, oxygen and nitrogen are also connected directly to adsorption unit together with ethane, ethylene and carbon dioxide – the main reaction products. Two other remarkable products – carbon monoxide and hydrogen – are either highly toxic or explosive. For the safety reason, carbon monoxide is replaced by nitrogen and hydrogen is replaced by helium. These replacements are acceptable because the substitutions are similar in regard of adsorption characteristic compare to the components of main concern – ethylene Figure 4-1.

Because both reactant and products are explosive, safety is of major concern when setting up experiment. The mini-plant is classified as zone 2 according to ATEX directive 94/9/EC. HAZard and OPerability (Hazop) study has been conducted for adsorption experiment without the presence of oxygen. Therefore oxygen will also be substituted by nitrogen in experiment. In Figure 4-2 is the flow sheet of adsorption experiment setup in combination with fluidised-bed

reactor. Gas flow rates are regulated by Mass Flow Controller (MFC) and one Mass Flow Meter (MFM) is installed at outlet, all are manufactured by Bronkhorst with operating range given in Table 4-1. All MFCs are calibrated at 20^{O}C with 1% tolerance. The system is designed to operate at pressure up to 6 bar, pressure is regulated by Bürkert proportional valve type 2835 (code 175 996) installed at the outlet. For protection, a mechanical pressure relief valve is installed at the inlet. Two three-way valves are installed at both ends of adsorption column so that gas flow can be reversed when desired.

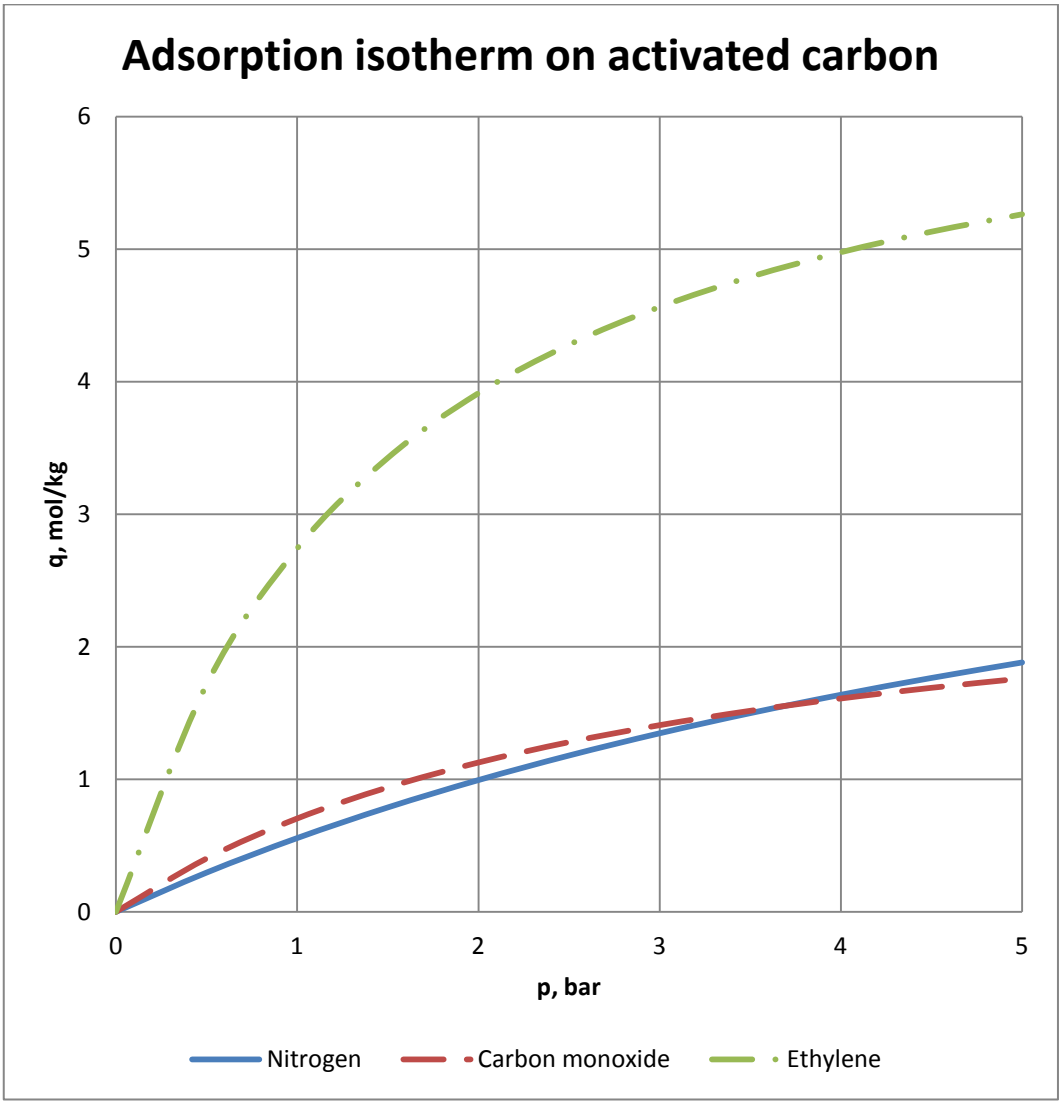

Figure 4-1: Adsorption isotherms on activated carbon at 0^{O}C

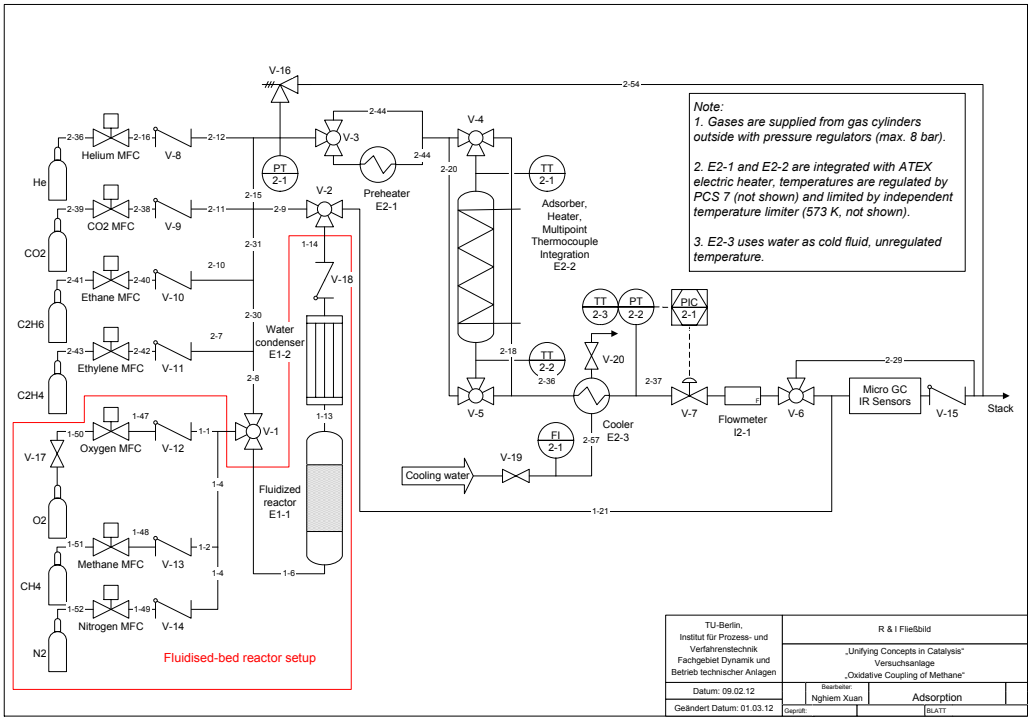

Figure 4-2: Flow sheet of adsorption experiment setup

Effluent of adsorption unit flows through gas analyser. Gas analyser is very crucial to experiment result. Gas chromatography is the typical technique in laboratory. Although it is accurate, the sampling time (few minutes at least) is too long in comparison with adsorption cycle. Hence online infrared (IR) gas analyser S700 by SICK is employed for measurement. The analyser can measure continuously because there is no separation as with chromatography. However this feature limits the number of components can be monitored and causes interaction between results. Careful calibration is then needed to ensure correct results. The tolerance of infrared gas analyser using UNOR modules is less than 1% but can drift up to 1% per week and also depends on flow rate with deviation up to 0.1% per 10 l/h. In order to minimise tolerance, weekly calibration is performed on gas analyser and daily software calibration is performed on control system. The measuring ranges of methane, ethane, ethylene and carbon dioxide are 0 – 100, 0 – 30, 0 – 30 and 0 – 50 %mol respectively. They cover operating ranges of all gases except carbon dioxide. During desorption, carbon dioxide

concentration can go up to 100% and cannot be measured directly. In those cases, carbon dioxide concentration is calculated by subtracting other gas concentration from 100%. Since carbon dioxide will be removed by absorption, this calculation does not affect separation performance.

Table 4-1: Operating ranges of mass flow controllers

Gas	Flow rate	Inlet pressure	Outlet pressure
Nitrogen	0.4 – 20 l/min	2 – 11 bar	1 – 8.8 bar
Oxygen	0.2 – 10 l/min	2 – 11 bar	1 – 8.8 bar
Helium	0.4 – 20 l/min	2 – 11 bar	1 – 8.8 bar
Methane	0.2 – 10 l/min	2 – 11 bar	1 – 8.8 bar
Ethane	0.1 – 5 l/min	2 – 11 bar	1 – 8.8 bar
Ethylene	0.2 – 10 l/min	2 – 11 bar	1 – 8.8 bar
Carbon dioxide	0.2 – 8 l/min	2 – 11 bar	1 – 8.8 bar
Outlet MFM	0.4 – 20 l/min	1 – 8.8 bar	1 – 8.8 bar

Adsorption column (Figure 4-3) is made of stainless column and can be heated up to 400^{O}C using a 1kW EMK heating cable by Bartec. The column is 1100 mm long, inner and outer diameters are 45 and 50 mm. Heating power and consequently temperature are regulated via pulse width modulation (PWM) unit. In addition, temperature is limited under 280^{O}C via standalone BTB temperature limiters by Bartec to follow ATEX directive. The column and heating cable are insulated by mineral wool. A multipoint thermocouple (18 measuring points) by Wika is implemented inside column to measure bed temperature. As mentioned before, it is however impossible to discriminate between solid and gas phase temperatures.

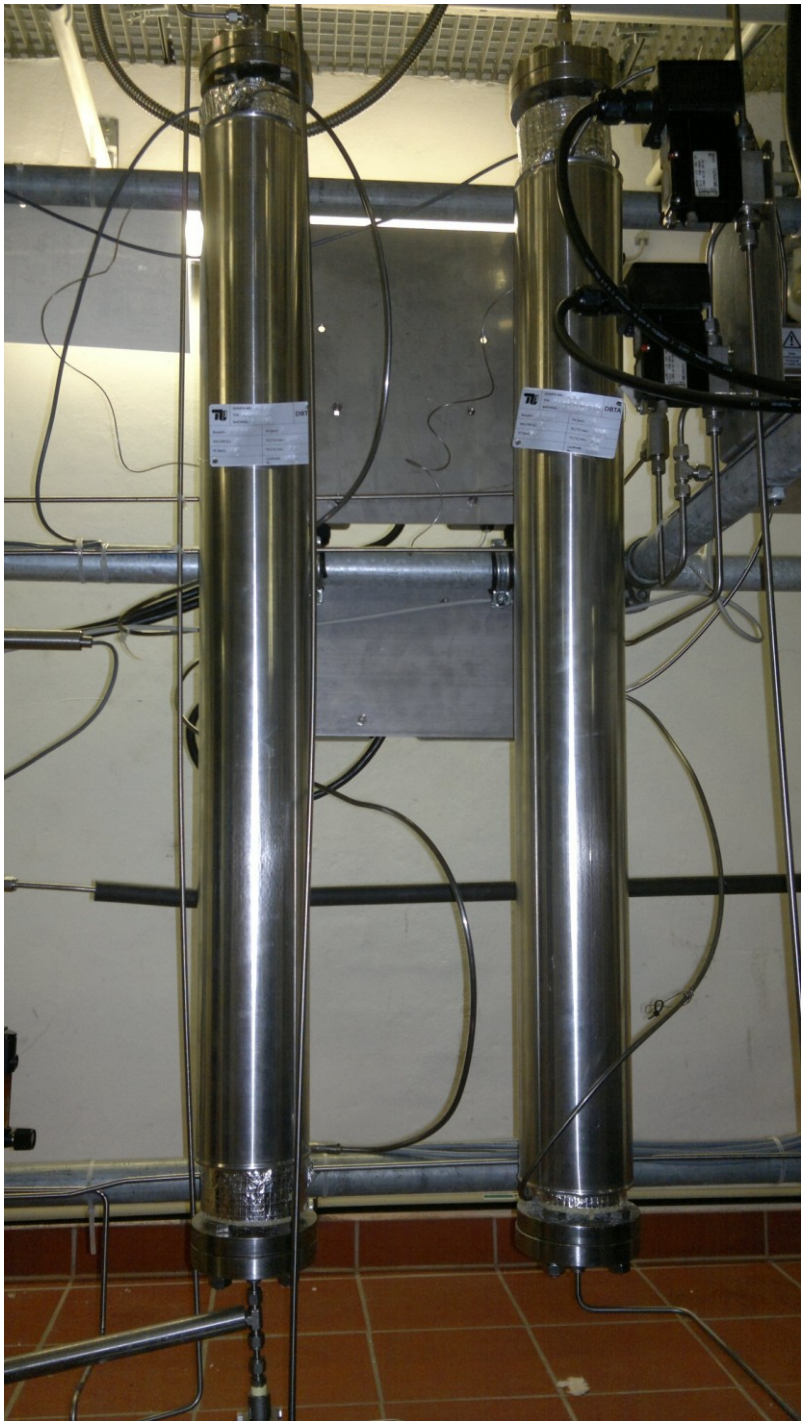

Figure 4-3: Adsorption column

The adsorption setup as well as the whole mini-plant is connected to PCS 7 control system by Siemens, which based on PLC S7-400. Measurement data are stored in the computer based Operator Station (OS). Equipments are operated

via the graphical human machine interface depicted in Figure 4-4. Measured values are illustrated at the symbols of the corresponding equipments. Special visual effects are used to catch the attention of operator when temperatures are higher than limits as depicted in Figure 4-5. Feeding of oxygen and flammable gases is automatically stopped in those cases. Gas feeding is also stopped in over pressure situation.

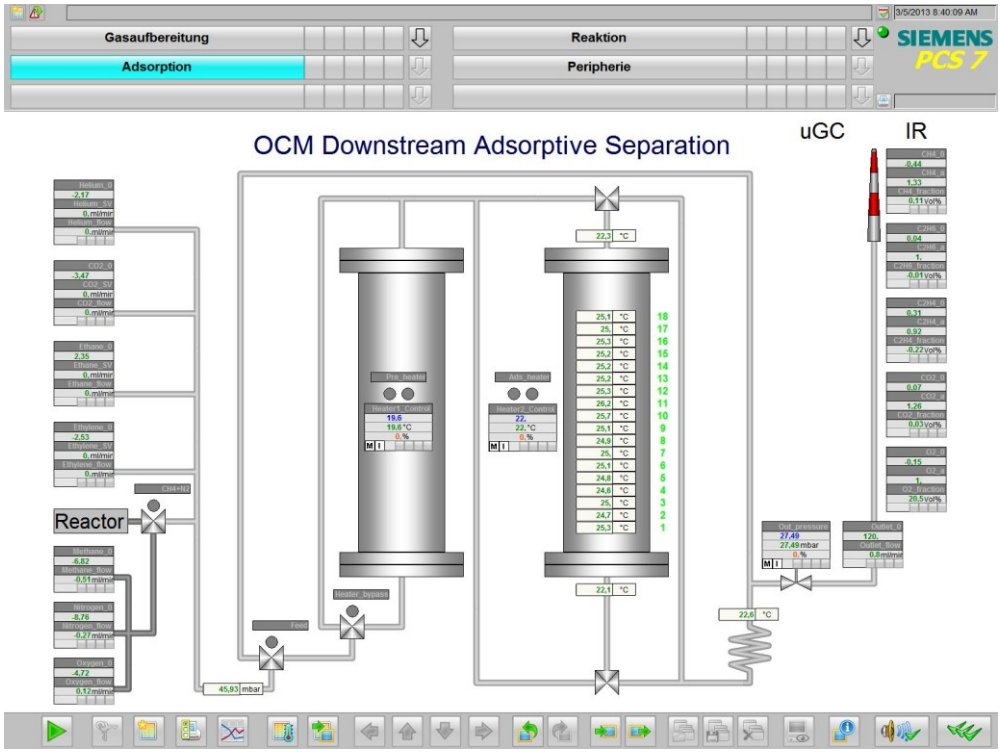

Figure 4-4: Human machine interface

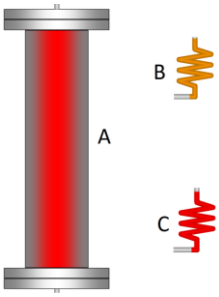

Figure 4-5: Special states of system

A – Column over heated (>300^{O}C)

B – Insufficient cooling (>40^{O}C)

C – Cooling failure (>50^{O}C)

4.2. Material selection

Simulation result shows that zeolite 4A can be used for separation but its high affinity toward carbon dioxide is a big drawback (see Appendix D for experimental result). The ideal sorbent should adsorb carbon dioxide more than other gases except ethylene. In that case not only operating cost is saved but ethylene purity is also increased. Although such an ideal sorbent has not been found yet, our simulation revealed that the adsorption characteristic of activated carbon is more desirable than that of zeolite 4A. Adsorption isotherms of carbon dioxide and hydrocarbons on activated carbon at 28^{O}C are drawn in Figure 4-6 based on experimental data from (Reich, et al., 1980). It can be seen that up to 7 bar using carbon dioxide as purge gas effectively help separating ethylene from methane. However carbon dioxide does not help in ethylene/ethane separation as it is adsorbed less than both of them in that pressure range. This means using activated carbon as sorbent reduces cost of methane separation but requires extra C_2-splitter. Other desired qualities of activated carbon are low price and hydrophobicity. The later one means normal water condensing is enough and there is no need for desiccation. Considering the relative cost of demethanizer and C_2-splitter, activated carbon is chosen as the sorbent.

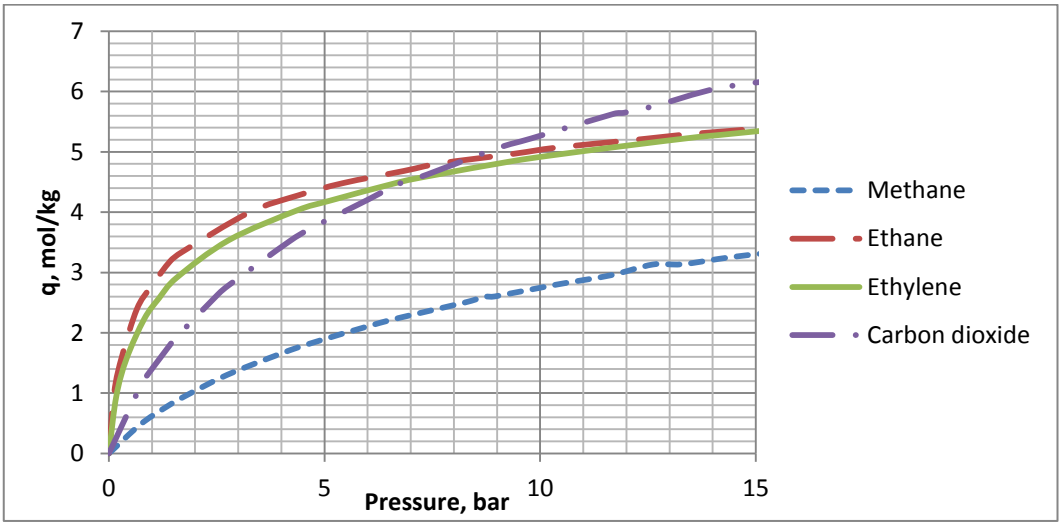

Figure 4-6: Adsorption isotherms on activated carbon

After choosing sorbent the second decision is choosing feed composition. As discussed in the previous chapter, adsorptive separation should be combined with high selectivity reactor performances to minimise production cost. One of such performances is presented in (Culp, et al., 2003) with 60% ethylene selectivity but only 20% methane conversion. The reactor outlet composition is given in Table 4-2. The artificial feed of adsorption unit is based on this composition. Modifications are replacing propylene by ethylene, oxygen and carbon monoxide by nitrogen and hydrogen by helium. Composition of the feed used for adsorption unit is given in Table 4-3.

Table 4-2: Original reactor outlet composition

Gas	N_2	O_2	CH_4	C_2H_6	C_3H_8	C_2H_4	C_3H_6	CO	CO_2	H_2	H_2O
Mol fraction, %	3.53	1.54	69.84	1.77	0.08	6.66	0.39	0.98	5.65	9.14	0.41

Table 4-3: Composition of the feed of adsorption unit

Gas	N_2	CH_4	C_2H_6	C_2H_4	CO_2	He
Mol fraction, %	6.06	69.96	1.88	7.26	5.67	9.17

4.3. Calibration

Although calibration is performed weekly on infrared gas analyser, validation is always performed at the beginning of the day when experiment is conducted. First of all, pure helium is passed through gas analyser and zero point drift is read from measured value. Then different mixtures with known composition are passed through gas analyser and sensitivity drift is determined. Finally, measured value is corrected by linear equation (4.1) with parameters a and b calculated from two point measurement.

$$y = a(x + b) \tag{4.1}$$

In Table 4-4 is the result of calibration procedure.

Table 4-4: Gas analyser calibration

Flow	Actual value	Measured value	a	b
Methane calibration				
4000 mln/min He	0%	-0.07%		
4000 mln/min CH_4	100%	99.6%		
			1	0.07
Ethane calibration				
4000 mln/min He	0%	0.04%		
3800 mln/min He + 200 mln/min C_2H_6	5%	5.02%		
			1	-0.04
Ethylene calibration				
4000 mln/min He	0%	-0.35%		
3600 mln/min He + 400 mln/min C_2H_4	10%	10.66%		
			0.91	0.35
Carbon dioxide calibration				
4000 mln/min He	0%	0.07%		
2000 mln/min He + 2000 mln/min CO_2	50%	47.82%		
			1.05	-0.07

4.4. Separation

Adsorption column is loaded with 800g activated carbon from ChemPur (Nr. 009074). The packing density is 500 kg/m^3 and surface area is 300 m^2/g. Feed flow rate is set at 0.4 g/min ethylene. With the composition as in Table 4-3, the feed flow is given in Table 4-5.

Table 4-5: Feed flow

Gas	N_2	CH_4	C_2H_6	C_2H_4	CO_2	He
Flow, mln/min	267	3083	83	320	250	404

A separation cycle consists of five steps: one adsorption and four desorptions. Sweep gas used in desorption steps is the effluent of the next step except the last desorption step when 4000 mln/min carbon dioxide is used as sweep gas. Each step lasts ten minutes. Because there is only one column available, real recycled effluents are replaced by artificial mixtures of ethylene and carbon dioxide. During experiment bed temperature varies between 25^{O}C and 31^{O}C while feed temperature is fixed at 22^{O}C. This variation is solely due to adsorption/desorption heat as heating cable was turn off. Temperature variation of a representative point (point 9 in the multipoint thermocouple) is depicted in Figure 4-7. During adsorption step, temperature drop as the bed is cooled down by fed methane. After that temperature rises because of adsorption enthalpy of carbon dioxide. During 12th minute, temperature rises sharply, indicate the arrival of adsorption front. It then goes down slowly to the initial value. Operating pressure varies from 0.2 bar to 1.4 bar. The high pressure is because of gas analyser, pressure drop across adsorption column is always less than 0.1 bar. Inlet and outlet pressures are also depicted in Figure 4-7. The sudden drop of pressure between 10th and 15th minutes indicates co-current blow step.

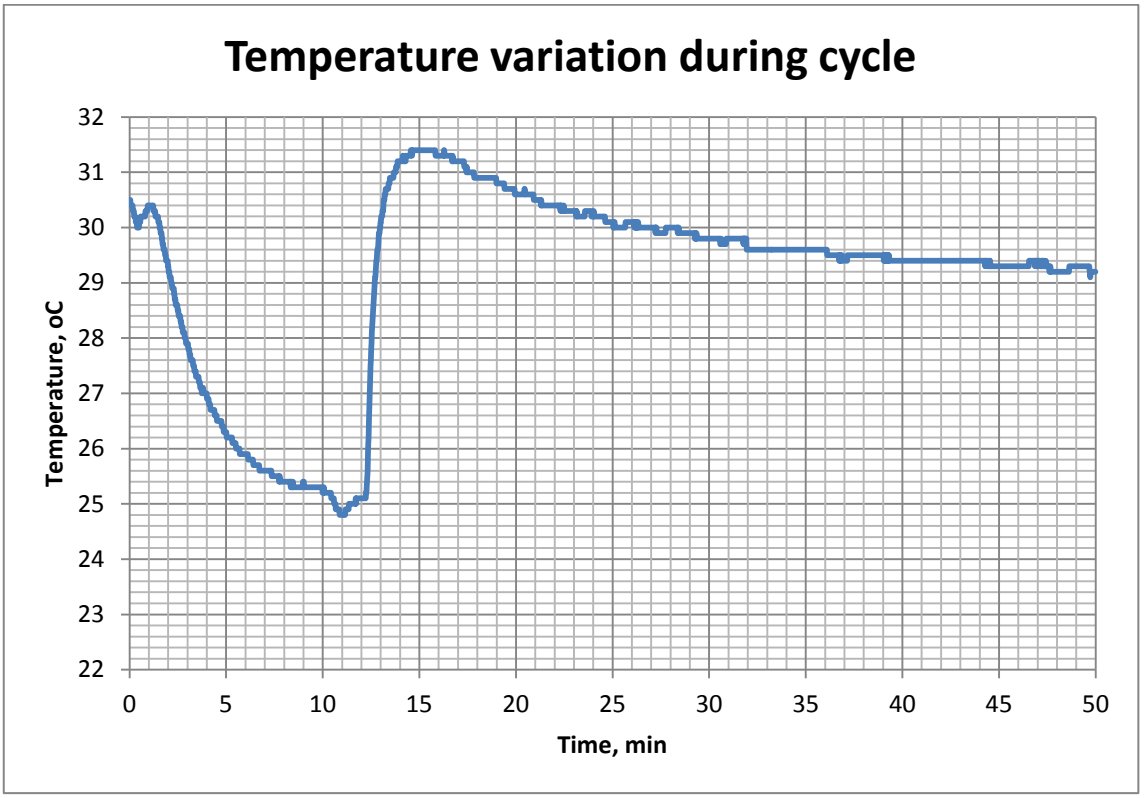

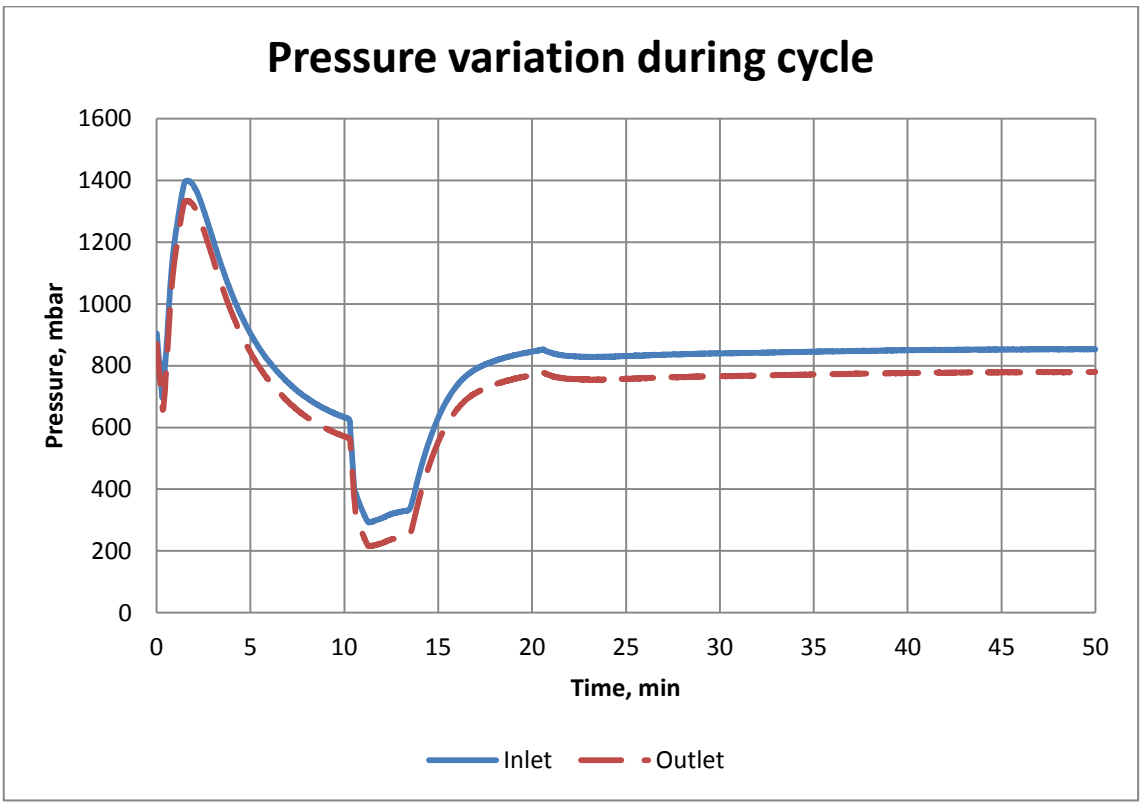

Figure 4-7: Column temperature and pressure

The breakthrough curve is illustrated in Figure 4-8. Carbon dioxide fraction went out of measurement range and measured value stay fixed at the maximum. One important notice is measured methane fraction varied between 0.17 and 0.53 at the end of cycle, when it should be 0 because all methane had been desorbed. This wrong information is caused by the interaction between gases. In this case, high concentrated carbon dioxide increases the measured values of methane by infrared analyser. In order to calculate methane accumulation correctly, the measured values of methane must be subtracted by the average value, 0.35%.

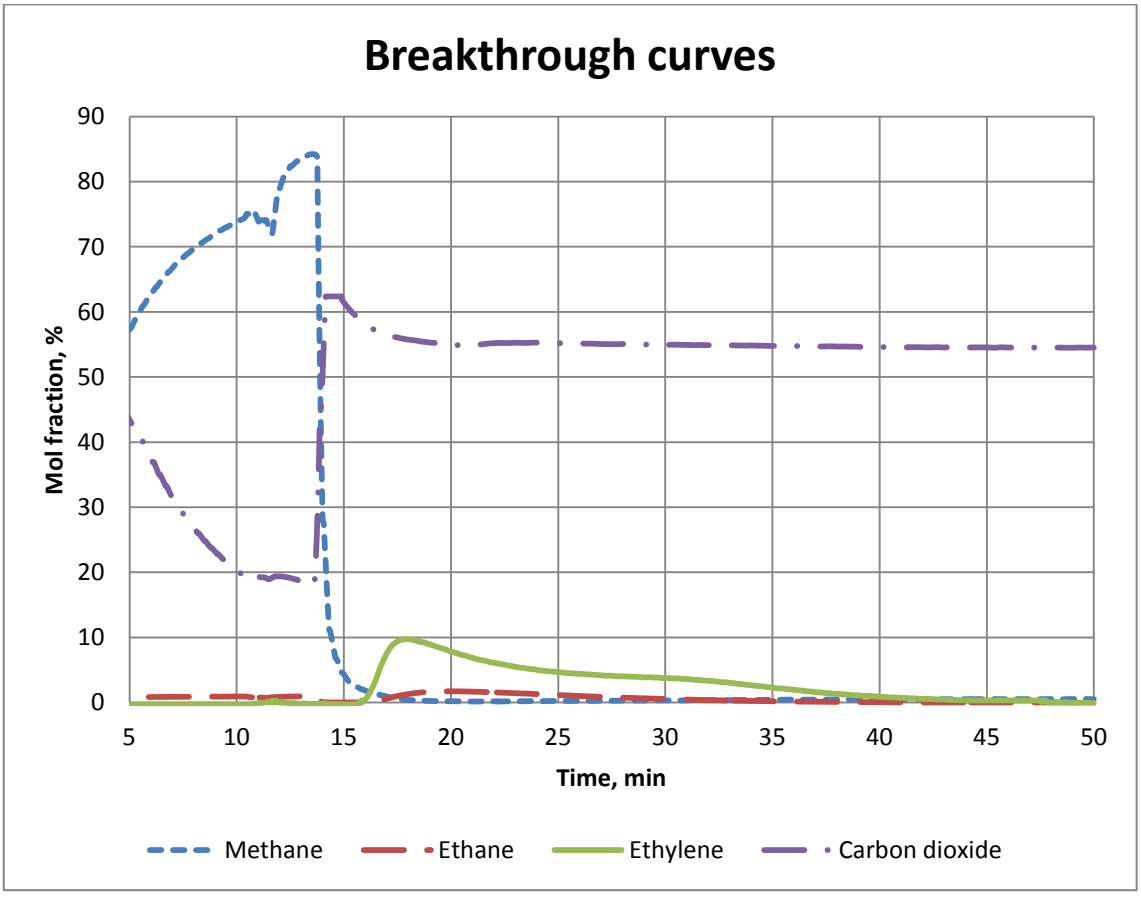

Figure 4-8: Breakthrough curve

The outlet flow rates of adsorption unit after correction is depicted in Figure 4-9. It can be seen from both figures that outlet flow can be clearly divided into two parts. The first part came out in the first 16 minutes (10 min. adsorption and 6 min. co-current blow) consists of methane, carbon dioxide, unmeasured nitrogen

and helium. The second contain mostly carbon dioxide, ethylene, ethane and some methane as contaminant. Ethylene fraction rose quickly to nearly 10% then declined gradually to 0%.

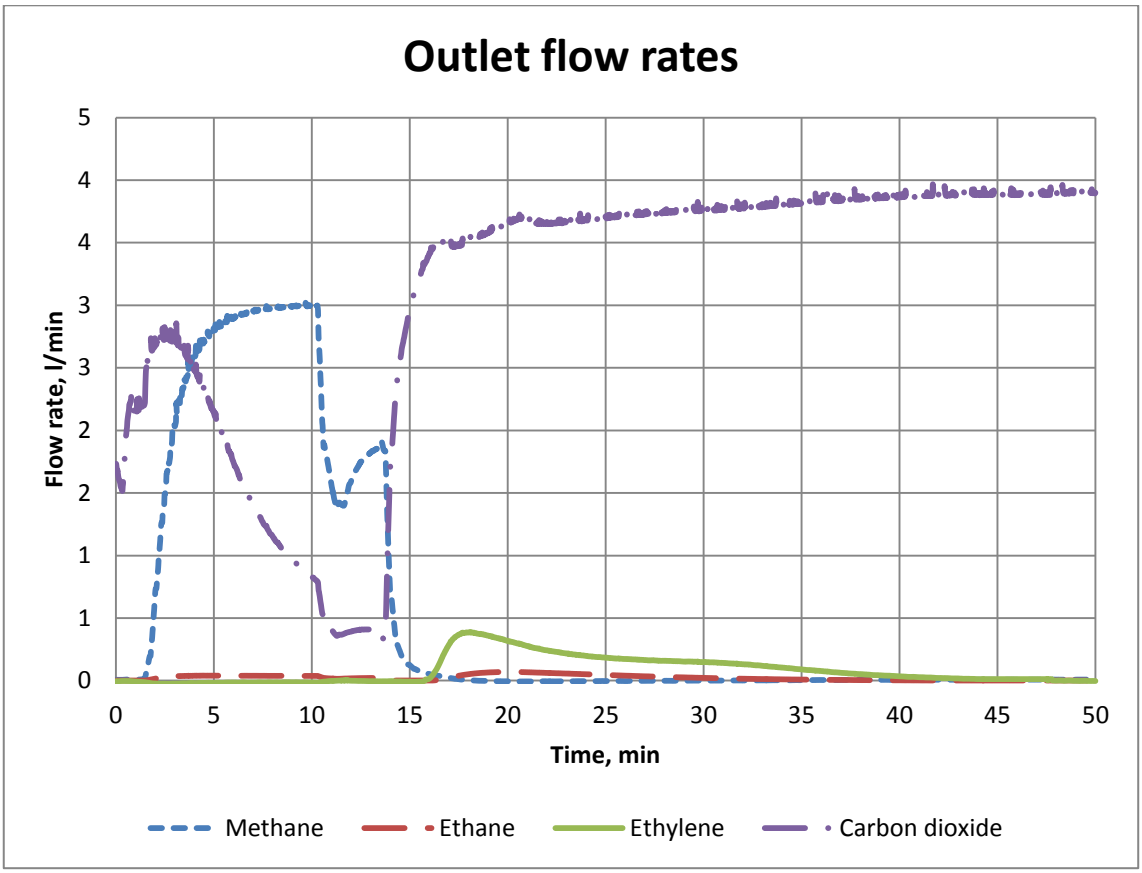

Figure 4-9: Outlet flow rate

Experiment shows that ethylene/ethane separation is ineffective. This was predicted by simulation in section 3.5. On the other hand ethylene/methane separation is excellent. Methane fraction had already dropped to 1.7% when ethylene appeared at the outlet and approached 0% after a few minutes. The composition of ethylene-rich stream is given in Table 4-6.

Table 4-6: Composition of experimental ethylene-rich stream

Gas	CH_4	C_2H_6	C_2H_4	CO_2
Mol. fraction, %	0.02	1.11	5.73	93.14

4.5. Discussion

4.5.1. Simulation – experiment comparison

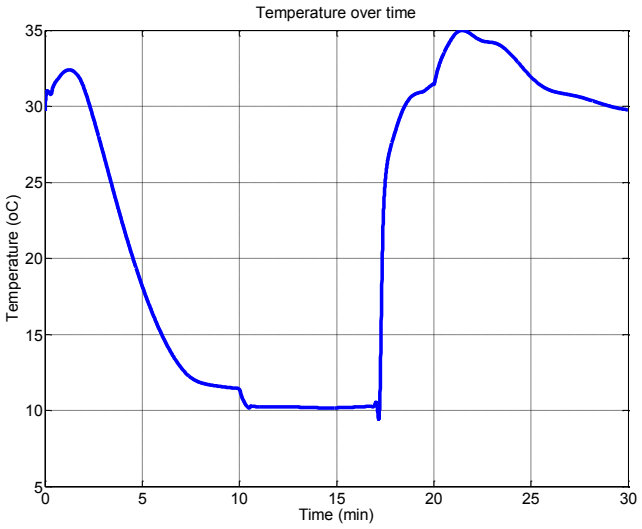

Figure 4-10: Simulated temperature variation during cycle

In comparison with experiment, the trend of simulated temperature variation (Figure 4-10) is similar but the amplitude is four times bigger. This is easy to understand since simulation was conducted with higher adsorption capacity (surface area is 3.3 times larger than experiment) and perfect heat insulation of column wall is assumed. Incomplete insulation in experiment makes the process closer to isothermal condition and causes a slight difference between temperatures at the beginning and the end of cycle (approx. $1^{O}C$). For a detailed comparison between experiment and simulation, the adsorption isotherm and adsorption enthalpy for activated carbon Nr. 009074 by ChemPur is needed.

The trends of outlet flow in simulation (Figure 3-19) and experiment (Figure 4-9) are also similar. Compare to simulation, experimental cycle was lengthened from 30 minutes to 50 minutes on purpose. This increases bed inventory by 40% but allow effluent recirculation, which reduces carbon dioxide removal duty from 28.6 t/t ethylene to 25 t/t ethylene. Consider the low price of activated carbon, long cycle is more economical.

4.5.2. Economic evaluation

The gas analyser did not detect any ethylene loss. Therefore it can be claimed, within confidence level and tolerance of the device, that ethylene is completely recovered. When carbon dioxide is removed from the composition in Table 4-6, a mixture of 83.5% ethylene + 16.2% ethane + 0.3% methane retrieved. Ethylene with 99% purity can be obtained if C_2-splitter can remove 97% of ethane.

Compare to simulation with zeolite 4A, the whole cycle time is only five times of adsorption time thanks to short co-current blow. This means minimum five columns instead of six are needed for continuous processing. However inlet and outlet switching no longer match each other. If co-current blow is lengthened to synchronise inlet and outlet switching, six columns are again required and bed inventory is 6.7 tonne of activated carbon for per tonne/day or 160 kg of activated carbon for per kg/h C_2 product. As operating cost, carbon dioxide consumption is 25 t/t C_2 production. Bigger bed inventory and carbon dioxide consumption is the consequence of weaker carbon dioxide adsorption: it takes more carbon dioxide and time to displace the same amount of ethylene. They are however small drawbacks in comparison to the benefit gained with using activated carbon. Despite increased bed inventory sorbent cost is reduced thanks to cheap price.

Lower carbon dioxide affinity makes the separation robust against not only inert diluents but also C_2 selectivity. Since carbon dioxide cannot compete with ethylene and ethane during adsorption, it does not affect ethylene adsorption capacity of the bed and more carbon dioxide caused by lower C_2 selectivity will not increase bed inventory. Carbon dioxide removal duty is also tied to adsorption selectivity instead of reaction selectivity as recycled stream is larger than the amount produced by reactor. This means 6.7 tonne of activated carbon for per tonne/day C_2 product and 25 tonne of carbon dioxide per tonne of C_2 are common numbers for typical reactor performances except ones with very low

selectivity, which should never been considered. The huge amount of carbon dioxide certainly imposes a big operating cost but no other cost is required. In other word operating cost of adsorption unit has been shifted to carbon dioxide removal section.

In the following is the evaluation of the studied case:

The artificial reactor effluent used in experiment is corresponding to the reactor performance in Table 4-7 (with nitrogen and helium replace carbon monoxide and hydrogen)

Table 4-7: Artificial reactor performance

X_{CH4}, %	S_{C2H4}, %	S_{C2H6}, %	S_{CO}, %	S_{CO2}, %	Consumption per tonne C_2H_4	
					CH_4	O_2
30.02	48.38	12.53	20.19	18.9	2.36 tonne	3.79 tonne

The operating cost when combining this reactor performance with conventional downstream processing is given in Table 4-8. The high operating cost is in agreement with previous work (Suzuki, et al., 1996) where 30% methane conversion and 80% C_2 selectivity are required for profitability. Raw materials make up 60% operating cost while compression and refrigerant for demethanizer make up more than 90% of utilities cost. It is worthy notice that operating cost of C_2-splitter is quite small despite the difficulty of ethylene/ethane separation. The reason is C_2 account for less than 10% of the whole stream and C_2-spliter work at -20^{O}C, much closer to ambient temperature than demethanizer. The expense of ethylene fractionation lies in very high distillation column rather than utilities consumption.

Table 4-8: Operating cost with conventional downstream process

Item	Unit	Amount	Price*, €	Total price, €
Reaction				
Methane	tonne	2.36	140	330.4
Oxygen	tonne	3.79	30	113.7
Heating	GJ	8.13	2	16.26
Cooling	GJ	45.3	0.05	2.27
Compression	Nm^3	11019	0,009	99.17
CO_2 removal				
Pump**	tonne	1.23	0,9	1.11
Steam	tonne	1.23	5.67	6.97
Caustic soda	kg	1.1	3	3.3
Demethanizer				
Refrigerant	GJ	4.5	38	171
C_2-splitter				
Refrigerant	GJ	1.05	1.6	1.68
Total				**745.86**

* Utilities prices are calculated according to (Ulrich & Vasudevan, 2006) at CE PCI = 588.8 and fuel price at 2 $/GJ

** Pumping cost per tonne carbon dioxide

The operating cost when combining this reactor performance with the proposed downstream processing is summarised in Table 4-9. Total operating cost is reduced by more than 100€ thanks to the new proposal. Although carbon dioxide removal cost increases almost fifteen times, it is still less than the refrigerant cost for demethanizer that we get rid of. The important improvement is nearly twelve times reduction of compression duty. This does not only result in the corresponding reduction of electricity consumption but also a big save of capital cost for compressor.

Table 4-9: Operating cost with proposed downstream process

Item	Unit	Amount	Price*, €	Total price, €
Reaction				
Methane	tonne	2.36	140	330.4
Oxygen	tonne	3.79	30	113.7
Heating	GJ	8.13	2	16.26
Cooling	GJ	45.3	0.05	2.27
CO_2 removal				
Pump**	tonne	25	0,9	22.5
Steam	tonne	25	5.67	141.75
Caustic soda	kg	0.1	3	0.3
C_2-splitter				
Compression	Nm^3	955	0,009	8.6
Refrigerant	GJ	1.05	1.6	1.68
Total				**637.46**

* Utilities prices are calculated according to (Ulrich & Vasudevan, 2006) at CE PCI = 588.8 and fuel price at 2 $/GJ

** Pumping cost per tonne carbon dioxide

In spite of all the improvement said above, total operating cost is still 50€ higher than the threshold given in Chapter 2 – 580€. According to global cost curve of 2011 (source: Dow), this performance is only competitive in Northeast Asia or Western Europe, where fifteen refineries have shut down since 2008 due to weak profit margin (Kent & Werber, 2013) and 33% of crackers are expected to be uneconomical by 2015 (Wanichko, 2014). This means adsorption alone is not enough to make OCM profitable. However it opens big chance for other savings that ensure a profitable OCM. Two of them are described below:

- Oxygen cost: Adsorption process is more robust to the presence of nitrogen. If the "light" stream is not recycled back to OCM reactor, dilution by nitrogen instead of excess methane will not affect production cost significantly. In that case enriched oxygen or even air can be used instead of pure oxygen and oxygen price will be greatly reduced. Even when pure oxygen is selected, an ASU can be installed. The surplus energy released by

reactor is enough to cover electricity demand from ASU, gas compressor and refrigerator. In any case, oxygen cost can be reduced by a half at least.

- Steam cost: Steam accounts for more than 75 of utilities cost but it is already available from reactor cooler. Extra piping is the only work required to make use of this free steam. With a modest estimation, reactor cooler can supply half of steam demand by carbon dioxide stripper.

With two saving options above, operating cost can be reduce to ca. 500 €/t and operating cost by OCM is in the range of production cost in United States, where is selected for economic evaluation. The only question left is the capital cost of the proposed solution. Compare to conventional downstream process, compressor size is reduced more than ten times and cryogenic equipments are taken away. The trade-off is bigger absorption column and investment in adsorption unit. Unlike raw materials or utilities cost, this initial expense depend considerably on process scale. At the scale of 135 000 t/y, demethanizer costs €6.8 million and carbon dioxide removal section (duty: 4.09 tonne CO_2 per tonne ethylene) costs €15.3 million according to (Salerno, 2013). Using six-tenths rule, cost of carbon dioxide removal section will rise to €45.9 million with the proposed process. A comparison between two alternatives is given in Table 4-10 with equipment costs estimated by Aspen Process Economic Analyzer. Units such as reactor are the same in both cases and not shown.

Table 4-10: Fixed cost comparison

Item	Conventional, mil. €	Proposal, mil. €
Compressor	25.4	3.1
CO_2 removal	15.3	45.9
Demethanizer	6.8	0
Adsorption columns	0	6.1
Sorbent	0	0.5
Total	**47.5**	**55.6**

The proposed required about €8 million more fixed cost than the conventional one. This difference is small compare to the investment the whole plan and can be pay back within a year by the saving from operating cost. As conclusion we can say that the proposed downstream process is superior to the conventional one and makes OCM technology profitable. The whole process can be designed as described in Figure 2-5 with composition of streams given in Table 4-11.

Table 4-11: Stream compositions

Stream	Fraction, % mol					
	CH_4	C_2H_4	C_2H_6	CO	CO_2	H_2
Feed	69.96	7.26	1.88	6.06	5.67	9.17
Sweep gas	0	0	0	0	100	0
Extract	0.02	5.73	1.11	0	93.14	0
Raffinate	40.08	0	0.55	9.67	35.07	14.63
C2	0.29	83.53	16.18	0	0	0
C2H4	0.35	99.46	0.19	0	0	0
C2H6	0	4.96	95.04	0	0	0

Chapter 5. Conclusions and outlook

The idea of OCM started in 1970s, after the oil crisis. Since then it has been developed together with other alternative solutions such as renewable energy. In recent years, when oil price again roses to the new record, new technologies such as bio-ethanol has find theirs application and helped mitigate the impact on economy. In ethylene industry, advances of hydraulic fracturing and horizontal drilling technology leaded to shale gas boom and ethane is replacing naphtha as the main raw material: the global share of ethylene from ethane and liquefied petroleum gas (LPG) will rise from 40% in 2008 (Seddon, 2010) to nearly 50% by 2023 (Energy Security Analysis, Inc., 2013). When this feed stock is not available, CTO technology, which comprises coal gasification followed by methanol synthesis and MTO, and GTL technology are chosen to utilise coal and methane from natural gas. MTO alone can also be utilised to produce ethylene from imported methanol. It is getting popular in China with a 300 000 t/y plant operating in Nanjing and three more planned to operate by 2015 with capacities of 295 000 t/y, 600 000 t/y and 833 000 t/y. GTL plants are operated and planned in North America and Middle East, where methane is abundant. These plants are all expensive because of many conversion steps. For example a GTL plant can cost three times as much as a traditional refinery. Despite that fact, these technologies are still more competitive than such a direct conversion technology as OCM, which requires less capital cost.

It is easy to point out that poor reactor performance is the weak point of OCM technology. The trade-off between methane conversion and ethylene selectivity leads to high direct cost due to either large raw materials consumption or large separation duty. There is however another distinctive feature of OCM: reactor effluent contains much more methane and carbon dioxide than any other technology: MTO, GTL or ethane cracking. This specialty makes conventional downstream process unsuitable to OCM and results in more direct cost. In this

thesis, a new downstream process based on adsorption is proposed. It ties separation cost to the amount of ethylene instead of methane and carbon dioxide. Therefore it is more appropriate for the low ethylene fraction in OCM downstream and makes this technology profitable with the current reactor performances. Furthermore, tying separation cost to ethylene fraction makes the proposed process more robust and flexible with reactor performance. Together with the absent of cryogenic conditions it makes plan design and operation are easier. Another advantage of the new proposal is the ability of utilising all the heat released by reaction. This energy economisation, in combination with highly selective reactor performance, can reduce carbon footprint to a point where it is lower than for ethane cracking – a significant advantage in locations with strict emission regulation. Overall, there is a big chance that OCM with the proposed downstream process is competitive enough to find its industrial application in the near future.

Beside the improvement with adsorptive separation there are still others needed for successful commercialisation of OCM. The first of all is OCM reactor – the heart of the process. New downstream solution has made current reactor performances profitable. Some of them such as case 1 in Table 2-1 are even better than the one used in experiment. However they are all nominal performance achieved in small scale within short duration. The longest test in Table 2-1 is case 4 with 100 hours, its performance is comparable to the one used in experiment. The longest tests found in literature are conducted by Cantrell et al. (Cantrell, et al., 2003) in 30 days. Their performances are however poorer with less than 30% ethylene selectivity and less than 14% methane conversion. In the future more tests with longer time are required before any industrial application.

Catalyst and reactor developments are both crucial to performance stability. Fixed-bed reactor is the most popular type and yields acceptable performances.

Heat management is of great importance to long time performance as overheated catalysts may degrade. Inert dilution or extra methane is essential to maintain heat dissipation rate when specific heat transfer area is reduced by scaling up. Learning from case 4, steam dilution may be a good choice as it does not only carry out reaction heat but also prevent coke formation over catalyst surface.

Fluidised-bed reactor is a useful solution for temperature control and can provide nearly isothermal condition. Fluidisation required more mechanically stable catalyst and ethylene selectivity may decrease due to back mixing. With both pros and cons, further study should be conducted to quantitatively evaluate this option in comparison with the standard fixed-bed reactor.

Membrane reactor also attracts interest from scientist with the potential of improving performance. Highest C_2 yield has been achieved with catalytic membrane reactor (case 7 in Table 2-1) but ethane/ethylene ratio is quite high, leading to low ethylene selectivity. Short contact time due to the thin catalyst layer may be the cause of this drawback. Combination with packed catalytic bed for further dehydrogenation of ethane should be considered. Non-catalytic membranes were also used for the purpose of achieving the optimal oxygen profile along reactor. Some improvements have been achieved but the complication with membrane material poses a real difficulty for industrial application. On the other hand, fixed-bed reactor with secondary feed point also gives the ability to manipulate oxygen profile. Since membrane reactor is a new concept in industry, time is needed for finding its application.

No matter which catalyst and reactor used, it is reasonable to expect selectivity far below 100% and a large amount of by-products. Therefore the next improvement should be utilising them to increase the profitability of the whole process. All major by-products of OCM have their application and can be put in other processes and converted to valuable products. This task is however much

easier on paper than in the real world. Several challenges must be considered for practical application:

- Technical challenge: Connecting multiple process increases complexity, safety concern and operation difficulty. Flexibility is significantly reduced thanks to the requirement of not only main product quality but also by-product quality. Comprehensive study of any proposal must analyse not only nominal performance but also deviation from that point. The proposed downstream solution produces two streams of by-product: ethane and mixture of methane, carbon dioxide, carbon monoxide, hydrogen. Extra separation is then necessary prior to processing any pure component except ethane. Processes which can consume methane, carbon dioxide, carbon monoxide and hydrogen together such as combustion are preferred.
- Financial challenge: Adding extra equipments needs more investment. This matter may be simple from academic perspective but of great importance in real application.
- Market challenge: Product value can be easily calculated by multiplying price with productivity. Realising this value is however not so simple. The broader product range the more cost of distribution network and other marketing measure are required. For example, co-generation of electricity as in (Hugill, et al., 2005) requires expensive power transmission network in remote area. Another matter with expanding product range is supply/demand mismatch. Productivity ratios are fixed by technology but demands of different products vary independently. Supply/demand mismatch is thus inevitable and chance is higher with more products.

These challenges signify that further study is necessary for accurate evaluation of by-product value. As preliminary result, we suggest convert all by-products to ethylene or higher hydrocarbons and avoid the challenges with expanding product range. Ethane retrieved at high purity and pressure can be converted by

mature ethane crackers and the mixture of methane, carbon dioxide, carbon monoxide and hydrogen can be converted by Midrex reformer and Fischer-Tropsch reactor (which is a part of GTL technology). Conversion of syngas via methanol is also possible but requires more steps and higher pressure. Light hydrocarbons from both additional processes can be separated in the same units with OCM downstream while heavy ones need extra separation equipments. Part of mixture stream will also be burnt to supply energy to fired heater or compressor if necessary. Since all technology mentioned above are already commercialised, the chance of successful combination is quite high. The economic feasibility of Midrex reformer and low pressure Fischer-Tropscher reactor combination has not been proved. However the ecologic effect is definitely positive with the reduction of carbon footprint. Anyway further intensive study is essential as profitability depends on many other factors such as production scale or region

Last but not least is the further improvement of downstream process. The synthesis of adsorptive process was based on available materials but there is always the possibility to develop better ones. Apart from common qualities such as capacity, stability, important criteria of the new sorbents include order of affinity and the easiness of carbon dioxide desorption as discussed. For the process itself, some analysis has been performed (see Appendix E) but there is still the room for optimisation, which depends on the particular sorbent and reactor performance. Another step that plays an important role in downstream process is carbon dioxide separation. Carbon capture technology is currently an attractive topic with much progress. However further study is necessary to tailor these technologies for the low pressure but highly concentrated stream in the proposal. With comprehensive development of the whole process, it is strongly believed that oxidative coupling of methane will be a practical choice for producing ethylene in the future.

Appendix A. Material calculation

Assuming that only two reactions take place in reactor and oxygen reacts completely:

$$2CH_4 + O_2 \rightarrow C_2H_4 + 2H_2O \quad (1.1)$$

$$CH_4 + 2O_2 \rightarrow CO_2 + 2H_2O \quad (1.2)$$

Then 1 mol of methane fed in the reactor will produce $Y/2$ mol of ethylene and $X-Y$ mol of carbon dioxide while $(1\text{-}X)$ mol of methane remains unconverted.

1 mol of oxygen is consumed to produce 1 mol of ethylene. 2 mol of oxygen is consumed to produce 1 mol of carbon dioxide. Assuming total oxygen conversion, $(2X\text{-}1.5Y)$ mol of oxygen must be fed along with 1 mol of methane to produce $Y/2$ mol of ethylene and $X-Y$ mol of carbon dioxide.

Assuming complete water removal, inlet and outlet compositions are calculated and summarised in Table A-1.

Table A-1: Inlet and outlet composition

	Methane	Oxygen	Ethylene	Carbon dioxide	Total
Molecular mass	16	32	28	44	
Amount per mol methane feed, mol					
Inlet	1	$2X - 1.5Y$	0	0	$1 + 2X - 1.5Y$
Outlet	$1 - X$	0	Y/2	$X(1 - S)$	$1 - Y/2$
Consumption	X	$2X - 1.5Y$	0	0	$3X - 1.5Y$
Amount per mol ethylene production, mol					
Inlet	2/Y	$\frac{4 - 3S}{S}$	0	0	$\frac{2 + 4X - 3Y}{Y}$
Outlet	$\frac{2 - 2X}{Y}$	0	1	$2\frac{1 - S}{S}$	$\frac{2 - Y}{Y}$
Consumption	2/S	$\frac{4 - 3S}{S}$	0	0	$\frac{6 - 3S}{S}$
Molar fraction, %					
Outlet	$\frac{200 - 200X}{2 - Y}$	0	$\frac{100Y}{2 - Y}$	$\frac{200X - 200Y}{2 - Y}$	100
Weight per mol ethylene production, g					
Inlet	$\frac{32}{Y}$	$\frac{128 - 96S}{S}$	0	0	$\frac{32 + 128X - 96Y}{Y}$
Outlet	$\frac{32 - 32X}{Y}$	0	28	$88\frac{1 - S}{S}$	$\frac{32 + 56X - 60Y}{Y}$
Consumption	32/S	$\frac{128 - 96S}{S}$	0	0	$\frac{160 - 96S}{S}$
Weight per gram ethylene production, g					
Inlet	$\frac{8}{7Y}$	$\frac{32 - 24S}{7S}$	0	0	$\frac{8 + 32X - 24Y}{7Y}$
Outlet	$\frac{8 - 8X}{7Y}$	0	1	$\frac{22 - 22S}{7S}$	$\frac{8 + 14X - 15Y}{7Y}$
Consumption	$\frac{8}{7S}$	$\frac{32 - 24S}{7S}$	0	0	$\frac{40 - 96S}{7S}$

* S and Y are selectivity and yield of ethylene, the subscript C_2H_4 is omitted for the sake of brevity.

** The difference between inlet and outlet weights corresponds to the condensed water.

Appendix B. Utility calculation

1. Reactant heating

As calculated in Appendix A, reactor feed per tonne ethylene production consists of $\frac{8}{7Y}$ tonne of methane and $\frac{32-24S}{7S}$ tonne of oxygen. It is assumed that feed stream will be heated to 300^{O}C below reaction temperature by waste heat exchanger. A furnace is then needed to heat up the feed stream 300^{O}C more. Specific heat capacity is fixed at 40 J/mol.K for both gases. This translates into 2.5 MJ/t.K for methane (16 g/mol) and 1.25 MJ/t.K for oxygen (32 g/mol). Heat required for each gas is calculated according to the simple equation $\mathrm{Q}=\mathrm{m}.\mathrm{C_p}.\Delta\mathrm{T}$

With furnace efficiency is chosen as 90%, total fuel consumption of the furnace is $\frac{1+2\mathrm{X_{CH_4}}-1.5\mathrm{Y_{C_2H_4}}}{\mathrm{Y_{C_2H_4}}}$

2. Reactor cooling

As calculated in Appendix A, $2\frac{1-S}{S}$ kmol of carbon dioxide are produced along with 1 kmol of ethylene. 280 MJ are released when producing 1 kmol of ethylene via reaction (1.1) and 890 MJ are released when producing 1 kmol of carbon dioxide via reaction (1.2). In total, $\frac{1780-1500\mathrm{S_{C_2H_4}}}{\mathrm{S_{C_2H_4}}}$ MJ are released by both reactions when 1 kmol of ethylene is produced. This translates into $\frac{63.6-53.6\mathrm{S_{C_2H_4}}}{\mathrm{S_{C_2H_4}}}$ GJ/t ethylene production.

3. Compression

As calculated in Appendix A, total flow rate per ethylene flow rate is $\frac{2-Y}{Y}$ mol/mol at reactor outlet. This means production of 1 kmol of ethylene (28k g) requires compression of $\frac{2-Y}{Y}$ kmol gases, which is equivalent to $22.4\frac{2-Y}{Y}$ Nm^3. In other words, $800\frac{2-Y}{Y}$ Nm^3 need to be compressed to produce 1 tonne of ethylene.

4. Caustic soda

In the feed stream of caustic wash tower 1 kmol of ethylene is accompanied by $\frac{2-2X}{Y}$ kmol of methane. The standard volume is then $\frac{44.8-44.8X_{C_2H_4}+22.4Y_{C_2H_4}}{Y_{C_2H_4}}$ Nm^3 per kmol ethylene, which is equivalent to $\frac{1.6-1.6X_{C_2H_4}+0.8Y_{C_2H_4}}{Y_{C_2H_4}}$ Nm^3 per tonne ethylene. Since each Nm^3 needs about 0.1 g caustic soda, caustic soda consumption is $\frac{0.16-0.16X_{C_2H_4}+0.08Y_{C_2H_4}}{Y_{C_2H_4}}$ kg/t ethylene production.

Appendix C. Utility price

Utilities prices are calculated according to equation (C.1) (Ulrich & Vasudevan, 2006):

$$C_u = a\,(CE\,\mathrm{PCI}) + b\,(C_f) \qquad (C.1)$$

where C_u is the price of the utility in USD, C_f is the price of fuel in $/GJ, CE PCI is the dimensionless index issued monthly by Chemical Engineering (Chemical Engineering, 2013), and a and b are coefficients whose units depend on utility type.

In this work, CE PCI is chosen as 588 (December 2011). Natural gas is chosen as fuel with price about 2 $/GJ in April 2012 (U.S. Energy Information Administration, 2013). The utility prices are converted from USD to EUR with exchange rate at 1.3.

1. Cooling water

For cooling water, $a = 0.0001 + 3\text{x}10^{-5}q^{-1}$ and $b = 0.003$ with q is capacity in m^3/s (maximum 10). q is chosen as 10 concerning the scale of OCM plant. The price of cooling water is 0.05 €/GJ

2. Electricity

For electricity, $a = 1.3\text{x}10^{-4}$ and $b = 0.01$. Electricity price calculated by equation (C.1) is 0.0965 $/kWh or 0.0743 €/kWh. The round up value of 0.075 €/kWh is used for cost calculation.

3. Steam

For steam, $a = 2.7\text{x}10^{-5}m^{-0.9}$ and $b = 0.0034p^{0.05}$ with m is capacity in kg/s (maximum 40) and p is pressure in barg. p is chosen as 1 since reboiler works at low temperature and m is chosen as maximum value 40. Steam price calculated by equation (C.1) is 7.37 $/t or 5.67 €/t.

4. Refrigerant

For refrigerant, $a = 0.6Q^{-0.9}T^{-3}$ and $b = 1.1x10^{6}T^{-5}$ with Q is cooling capacity in kJ/s (maximum 1000) and T is absolute temperature. Q is chosen as 1000 concerning the scale of OCM plant. Refrigerant prices at different temperature are given in Table C-1.

Table C-1: Refrigerant price

Temperature, ^{O}C	Price, €/GJ	Application
-30	2	Deethanizer
-138	38	Demethanizer
-153	68	Demethanizer with excess uncondensed gas

Appendix D. Experiment with zeolite 4A

Adsorption column was loaded with 800g zeolite 4A, which was supplied by Carl Roth GmbH (article number: 8471) in the form of 1.6 – 2.6 mm pellets. The same flow as the experiment with activated carbon (Table 4-5) was fed to the column in ten minutes (totally 44072 mln of gases). Then 26250 mln of carbon dioxide were fed to the column in 20 minutes. Finally the column is purged by 235563 mln of nitrogen in 170 minutes. This extreme long time is to ensure the maximum desorption efficient. In other words, it ensures that nitrogen consumption will be minimised. In order to accelerate desorption, the column is heated up and later cooled down to the original temperature. Due to the limited nitrogen flow rate, it is only heated up to 70^{O}C instead of more than 200^{O}C as in simulation. As the result, nitrogen consumption is 58890 Nm^3/t ethylene – more than double of the simulation result. The carbon dioxide outlet flow rate and column temperature is depicted in Figure D-1. Experiment confirmed that the high affinity toward carbon dioxide make zeolite unsuitable of the application.

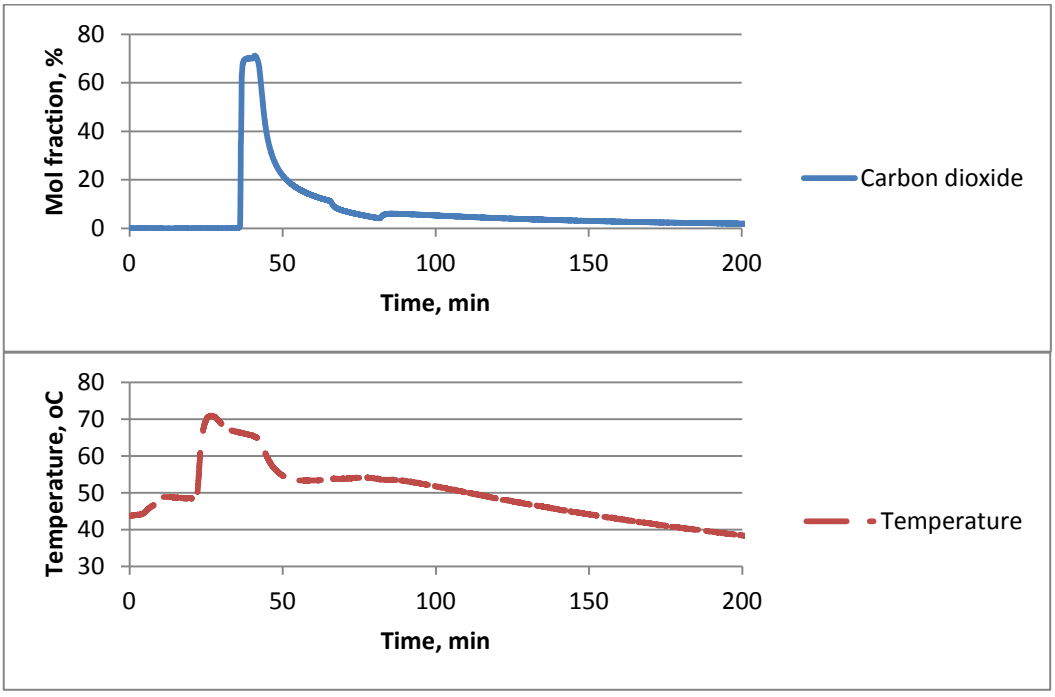

Figure D-1: Carbon dioxide desorption with zeolite 4A

Appendix E. Three-step scenario

As said in the conceptual development section, the adsorptive separation process involves two essential steps, adsorption and ethylene desorption, and one optional step – carbon dioxide desorption. Two-step scenario is discussed in Chapter 4. Here three-step scenario is investigated. The extra step lasts twenty minutes. 8000 mln/min air is used to purge carbon dioxide; the effluent of the last ten minutes is recycled (artificially) to save air consumption. Breakthrough curve and outlet flow rate are depicted in Figure E-1, the values of carbon dioxide measurement at the beginning of the third step are approximate. Ethylene separation performance is similar to two-step scenario but 'light' stream contains much less carbon dioxide. The prices of carbon dioxide separation are longer cycle, which means bigger bed inventory, and air consumption at 20000 m^3/t ethylene production. Although air consumption is four times less than the case of zeolite thanks to the lower affinity of carbon dioxide, it still requires significant compressing effort.

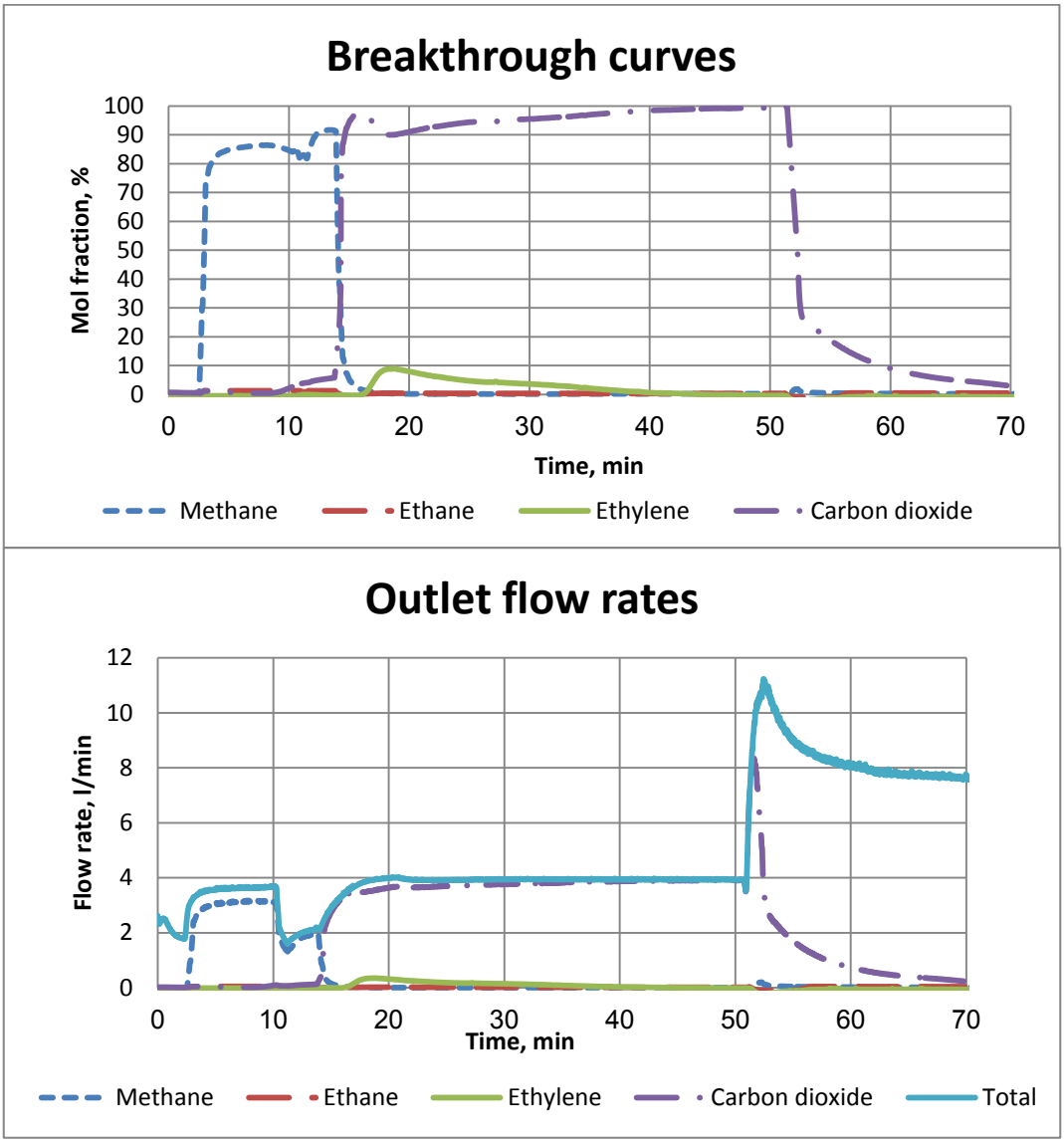

Figure E-1: Breakthrough curve and outlet flow rate – three-step scenario

Another problem arises with the third step is revamping. In comparison with zeolite, activated carbon has bigger pore and consequently faster mass transfer rate. Therefore the durations of adsorption/desorption steps are inverse proportional to gas flow rates. For example if feed flow rate from reactor is doubled, adsorption time will be halved. Carbon dioxide flow rate is doubled together with feed flow rate and ethylene desorption time will be also halved. This means, in two-step scenario, the same adsorption unit can process double amount of feed gas just by reducing duration of all steps by a half. The only

limitation is the switching rate between columns. The same practice in three-step scenario will require also double air flow rate. When air blower is already at full capacity, either extra blower or extra columns need to be installed to handle higher feed flow rate. Figure E-2 demonstrates a case study of revamping for double feed flow rate but sweep gases flow rates are fixed. Adsorption step is shortened but total cycle duration stays almost the same. The number of columns, which is equal to cycle duration – adsorption duration ratio, must be increased for continuous processing.

In general, two-step scenario is more recommended.

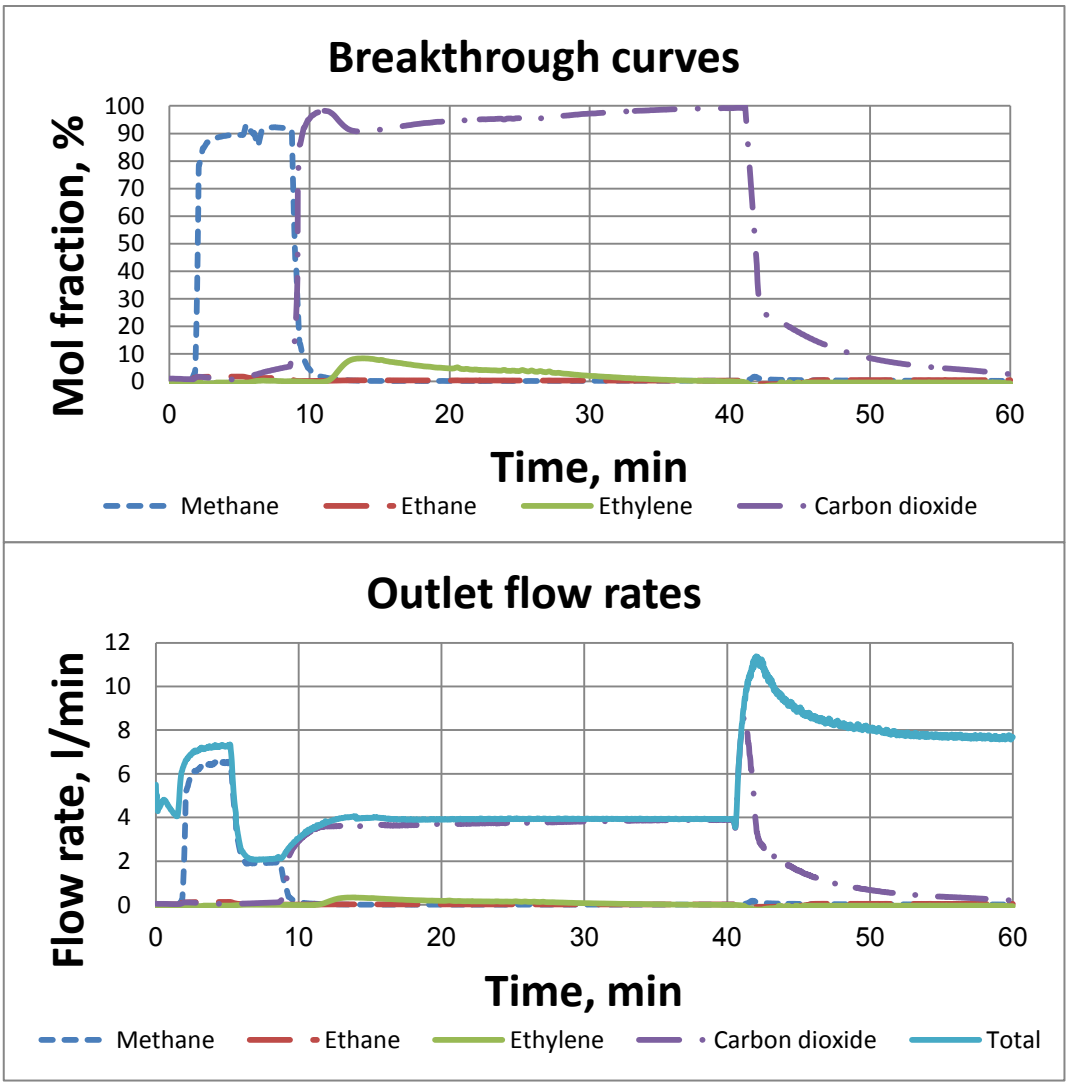

Figure E-2: Revamp for double feed flow rate in three-step scenario

References

Aika, K. & Nishiyama, T., 1988. Utilisation of CO2 in the Oxidative Coupling of Methane over PbO-MgO and PbO-CaO. *J. Chem. Soc., Chem. Commun.*, pp. 70 - 71.

Alter, E. & Bruns, L., 1982. *Process for Separating off Olefins from Gases Containing Olefins.* USA, Patent No. 4328382.

Aris, R. & Amundson, N. R., 1957. Some Remarks on Longitudinal Mixing or Diffusion in Fixed Bed. *AIChE Journal*, 3(2), pp. 280 - 282.

Asami, K. et al., 1995. Conversion of methane with carbon dioxide into C2 hydrocarbons over metal oxides. *Applied Catalysis A: General*, Volume 126, pp. 245-255.

Asami, K., Kusakabe, K.-i., Ashi, N. & Ohtsuka, Y., 1997. Synthesis of ethane and ethylene from methane and carbon dioxide over praseodymium oxide catalysts. *Applied Catalysis A: General*, Volume 156, pp. 43-56.

Baker, B. B. & Knaack, D. F., 1961. *Process for the Separation of Hydrocarbons.* USA, Patent No. 3007981.

Barchas, R., McCue, R., Wallsgrove, C. & Whitney, M., 1999. *Chemical Absorption Process for Recovering Olefins from Cracked Gases.* USA, Patent No. 5859304.

Barghezadeh, E., Hassan, A. & Hassan, A., 2004. *Preparation of Catalyst and Use for High Yield Conversion of Methane to Ethylene.* USA, Patent No. US20040220053A1.

Baronskaya, N. A., Woldman, L. S., Davydov, A. A. & Buyevskaya, O. V., 1996. Ethylene Recovery from the Gas Product of Methane Oxidative Coupling by Temperature Swing Adsorption. *Gas Sep. Purif.*, 10(1), pp. 85 - 88.

Bart, H.-J. & von Gemmingen, U., 2005. Adsorption. In: *Ullmann's Encyclopedia of Industrial Chemistry.* s.l.:Wiley-VCH, pp. 1 - 75.

Baxter, W. N., 1963. *Process for the Separation of Hydrocarbons.* USA, Patent No. 3101381.

Baxter, W. N., 1965. *Process for the Separation of Hydrocarbons.* USA, Patent No. 3218366.

Bernard, G. G. & Bond, D. C., 1948. *Separation of Olefins from Hydrocarbon Mixtures.* USA, Patent No. 2451376.

Beysel, G., 2009. *Enhanced Cryogenic Air Separation - a Proven Process applied to Oxyfuel.* Cottbus, s.n.

Bhatia, S., Thien, C. Y. & Mohamed, A. R., 2009. Oxidative Coupling of Methane (OCM) in a Catalytic Membrane Reactor and Comparison of its Performance with other Catalytic Reactors. *Chemical Engineering Journal*, Volume 148, pp. 525 - 532.

Bjorklund, M. C., Kruglov, A. V. & Carr, R. W., 2001. Further Studies of the Oxidative Coupling of Methane to Ethane and Ethylene in a Simulated Countercurrent Moving Bed Chromatographic Reactor. *Ind. Eng. Chem. Res.*, Volume 40, pp. 2236-2242.

Brown, R. E. & Hair, R. L., 1993. *Monoolefin/Paraffin Separation by Selective Absorption.* USA, Patent No. 5202521.

Brunauer, S., Deming, L. S., Deming, W. E. & Teller, E., 1940. On a Theory of the van der Walls Adsorption of Gases. *J. Am. Chem. Soc.*, 62(7), pp. 1723 - 1732.

Butt, H., Graf, K. & Kappl, M., 2003. Adsorption. In: *Physics and Chemistry of Interfaces.* Weinheim: Wiley-VCH.

Cai, Y. et al., 2003. Selective conversion of methane to C2 hydrocarbons using carbon dioxide over Mn–SrCO3 catalysts. *Catalysis Letters*, 86(4), pp. 191-195.

Cantrell, J. et al., 2013. Consider GTL as an Economic Alternative for Stranded Natural Gas and Ethane. *Hydrocarbon Processing.*

Cantrell, R. D. et al., 2003. *Catalysts for the Oxidative Dehydrogenation of Hydrocarbons.* USA, Patent No. US6576803B2.

Chemical Engineering, 2013. *Chemical Engineering Plant Cost Index.* [Online] Available at: http://www.che.com/pci/

Chen, C., Xu, Y., Li, G. & Guo, X., 1996. Oxidative coupling of methane by carbon dioxide: a highly C2 selective La203/ZnO catalyst. *Catalysis Letters*, Volume 42, pp. 149-153.

Choi, B.-U., Choi, D.-K., Lee, Y.-W. & Lee, B.-K., 2003. Adsorption Equilibria of Methane, Ethane, Ethylene, Nitrogen, and Hydrogen onto Activated Carbon. *Journal of Chemical Engineering and Data*, Volume 48, pp. 603 - 607.

Chu, P. & Landis, E., 1990. *Selective Oxidative Coupling.* USA, Patent No. US4914252.

Cobb, J. R., 1958. *Recovery of Olefin Hydrocarbons.* USA, Patent No. 2855433.

Cole, R. M., 1950. *Solvent Extraction of Unsaturated Hydrocarbons.* USA, Patent No. 2523681.

Cooper, J. B. & Small, K., 1997. *Process for Recovering Olefins from Gaseous Mixtures.* USA, Patent No. 5639935.

Culp, G. L. et al., 2003. *Methods for Manufacturing Olefins from Lower Alkans by Oxidative Dehydrogenation.* USA, Patent No. US6518476B1.

Curtis, T. & Ware, T., 2012. Restricting North Dakota Gas-flaring Would Delay Oil Output, Impose Cost. *Oil & Gas Journal*, 110(11), pp. 96 - 106.

Cymbaluk, T. H., Nowack, G. P. & Johnson, M. M., 1996. *Copper (I) Carboxylate-containing Olefin Complexing Reagents.* USA, Patent No. 5523512.

Cymbaluk, T. H., Tabler, D. C., Johnson, M. M. & Nowack, G. P., 1992. *Method for Preparing Olefin Complexing Reagents and Use thereof.* USA, Patent No. 5104570.

Dautzenberg, F. M. et al., 1992. Catalyst and Reactor Requirements for the Oxidative Coupling of Methane. *Catalysis Today*, 13(4), pp. 503 - 509.

Davis, H. S. & Francis, A. W., 1937. *Method for Recovery of Olefins from Gaseous or Liquid Mixtures.* USA, Patent No. 2077041.

Eldred, B. E., 1923. *Process of Separaing Olefines from Gaseous Mixtures.* USA, Patent No. 1465600.

Eldridge, R. B., 1993. Olefin/Paraffin Separation Technology: a Review. *Ind. Eng. Chem. res.*, 32(10), pp. 2208 - 2212.

Energy Security Analysis, Inc., 2013. *A Perfect Storm: Global Natural Gas Liquids 2013 - 2023,* s.l.: s.n.

Eng, D. & Chiang, P.-H., 1995. Methane Oxidative Coupling: Technical and Economic Evaluation of Chemical Cogenerative Fuel Cell. *Energy & Fuels*, Volume 9, pp. 794 - 801.

Evans, T. W. & Scheibli, J. R., 1945. *Recovery of Olefins.* USA, Patent No. 2376239.

Francis, A. W., 1949. *Separation of Olefins.* USA, Patent No. 2463482.

Francis, A. W. & Reid, E. E., 1948. *Separation of Olefins.* USA, Patent No. 2445520.

Friedman, B. S. & Stedman, R. F., 1945. *Process for the Separation of an Unsaturated Hydrocarbons from a Hydrocarbon Mixture.* USA, Patent No. 2391404.

Gilliland, E. R., 1945. *Concentration of Olefins.* USA, Patent No. 2369559.

Godini, H. R. et al., 2014. Performance Analysis of a Porous Packed Bed Membrane Reactor for Oxidative Coupling of Methane: Structural and Operational Characteristics. *Energy & Fuel*, 28(2), pp. 877 - 890.

Hamilton, J. D., 2009. *Causes and Consequences of the Oil Shock of 2007-08.* Washington, s.n.

Harper, R. J., Stifel, G. R. & Anderson, R. B., 1969. Adsorption of Gases on 4A Synthetic Zeolite. *Canadian Journal of Chemistry*, Volume 47, pp. 4661 - 4670.

Hayashi, J. et al., 1996. Separation of Ethane/Ethylene and Propane/Propylene Systems with a Carbonized BPDA-pp'ODA Polyimide Membrane. *Ind. Eng. Chem. Res.*, 35(11), pp. 4176-4181.

Hoebink, J. H. B. J., Couwenberg, P. M. & Marin, G. B., 1994. Fixed Bed Reactor Design for Gas Phase Chain Reactions Catalysed by Solids: the Oxidative Coupling of Methane. *Chemical Engineering Science*, 49(24), pp. 5453 - 5463.

Hoebink, J. H. B. J. et al., 1995. Economics of the Oxidative Coupling of Methane as an Add-on Unit for Naphtha Cracking. *Chem. Eng. Technol.*, Volume 18, pp. 12 - 16.

Hong, S. U., Kim, J. Y. & Kang, Y. S., 2001. Effect of Water on the Facilitated Transport of Olefins through Solid Polymer Electrolyte Membranes. *Journal of Membrane Science*, Volume 184, pp. 39 - 48.

Ho, W. S. W., Doyle, G., Savage, D. W. & Pruett, R. L., 1988. Olefin Separation via Complexation with Cuprous Diketonate. *Ind. Eng. Chem. Res.*, 27(2), pp. 334 - 337.

Hsiue, G. H. & Yang, J. S., 1993. Novel Methods in Separation of Olefin/Paraffin Mixture by Functional Polymeric Membranes. *Journal of Membrane Science*, Volume 82, pp. 117 - 128.

Hugill, J., Tilemans, J., Dijsktra, S. & Spoelstra, S., 2005. Feasibility Study on the Co-generation of Ethylene and Electricity through Oxidative Coupling of Methane. *Applied Thermal Engineering*, Volume 25, pp. 1259 - 1271.

Ilinich, O. M. & Zamaraev, K. I., 1993. Separation of Ethylene and Ethane over Polyphenylene Oxides Membranes: Transient Increase of Selectivity. *Journal of Membrane Science*, Volume 82, pp. 149 - 155.

Jarvelint, H. & Fair, J. R., 1993. Adsorptive Separation of Proylen-Propane Mixtures. *Ind. Eng. Chem. Res.*, 32(10), pp. 2201 - 2207.

Jaso, S., 2012. *Modeling and Design of the Fluidized Bed Reactor for the Oxidative Coupling of Methane.* s.l.:Technische Universität Berlin.

Joshua, W. P. & Stanley, H. M., 1935. *Separation and Recovery of Olefines from Gases Containing the Same.* USA, Patent No. 2005500.

Kang, Y. S., Char, K. H. & Kang, S. W., 2009. *Silver Nanoparticle/Polymer Nanocomposite Membranes for Olefin/Paraffin Separation and Method of Preparing the same..* USA, Patent No. 7491262 B2.

Keller, G. E. & Bhasin, M. M., 1982. Synthesis of Ethylene via Oxidative Coupling of Methane: I. Determination of Active Catalysts. *Journal of Catalysis*, 73(1), pp. 9 - 19.

Keller, G., Marcinkowsky, M. E., Verma, S. K. & Williamson, K. D., 1992. Olefin Recovery and Purification via Silver Complexation. In: *Separation and Purification Technology.* New York: Marcel Dekker Inc..

Kent, B. & Werber, C., 2013. Refinery Closures Hurt Europe's Energy Security. *Hydrocarbon Processing.*

Kiesskalt, S., 1944. *Process of Adsorbing Gases and Vapours.* USA, Patent No. US2349098.

Kiesskalt, S., 1944. *Process of Adsorbing Gases and Vapours.* USA, Patent No. US2354383.

Kooh, A., Dubois, J.-L., Mimoun, H. & Cameron, C. J., 1990. Oxidative Coupling of Methane: Maximizing the Yield of Coupling Products under Cofeed Operating Conditions. *Catalysis Today*, 6(4), pp. 453 - 462.

Kruglov, A. V., Bjorklund, M. C. & Carr, R. W., 1996. Optimization of the Simulated Countercurrent Moving-Bed Chromatographic reactor for the Oxidative Coupling of Methane. *Chemical Engineering Science*, 51(11), pp. 2945-2950.

Kundu, P. K., Zhang, Y. & Ray, A. K., 2009. Modeling and simulation of simulated counter current moving bed chromatographic reactor for oxidative coupling of methane. *Chemical Engineering Science*, Volume 64, pp. 5143 - 5152.

Labinger, J. A., 1988. Oxidative Coupling of Methane: An Inherent Limit to Selectivity. *Catalysis Letter*, Volume 1, pp. 371 - 376.

Lefebvre, B., 2013. US refiners don’t care if Keystone XL pipeline gets built. *Hydrocarbon Processing.*

LeVan, M. D. & Carta, G., 2008. Adsorption and Ion Exchange. In: *Perry's Chemical Engineer's Handbook.* 8th ed. s.l.:McGraw-Hill.

Lincoln Journal-Star, 2008. TransCanada Proposes Second Oil Pipeline. 12 June.

Liu, H. et al., 2008. Scale up and Stability Test for Oxidative Coupling of Methane over Na2WO4-Mn/SiO2 Catalyst in a 200 ml Fixed-bed Reactor. *Journal of Natural Gas Chemistry*, Volume 17, pp. 59 - 63.

Long, R. B., Caruso, F. A. & de Feo, R. J., 1972. *Bimetallic Salts and Derivatives thereof, their Preparation and Use in the Complexing of Ligands.* USA, Patent No. 3651159.

Lopez-Isunza, F., 2013. *Modelling Fixed-bed Multicomponent Adsorption for Ultra-low Sulphur Diesel.* The Hague, s.n.

Machida, K. & Enyo, M., 1987. Oxidative Dimerization of Methane over Cerium Mixed Oxides and its Relation with their Ion-conducting Characteristic. *J. Chem. Soc., Chem. Commun.*, pp. 1639 - 1640.

Machocki, A., 1996. Methane Oxidative Coupling in an Undiluted Reaction Mixture in a Reactor-Adsorber System with Gas Recirculation. *Applied Catalysis A: General*, Volume 146, pp. 391-400.

Marcinkowsky, A. E., Keller, G. E. & Verma, S. K., 1979. *Olefin Separation Process.* USA, Patent No. 4174353.

Meng, H., 1984. *Sorption Equilibria and Kinetics of Sequential Sorption in Zeolite Molecular Sieves.* McMaster University: s.n.

Miller, S. A., 1969. *Ethylene and its Industrial Derivatives.* London: Ernest Benn.

Miltenburg, A. v., 2007. *Adsorptive Separation of Light Olefin/Paraffin Mixture - Dispersion of CuCl in Faujasite Zeolites.* Technische Universiteit Delft: s.n.

Mleczko, L. & Baerns, M., 1995. Catalytic Oxidative Coupling of Methane - Reaction Engineering Aspects and Process Schemes. *Fuel Processing Technology*, 42(2 - 3), pp. 217 - 248.

Moore, T. T. & Koros, W. J., 2007. Gas Sorption in Polymers, Molecular Sieves and Mixed Matrix Membranes. *Journal of Applied Polymer Science*, Volume 104, pp. 4053 - 4059.

Morisato, A., He, Z., Pinnau, I. & Merkel, T. C., 2002. Transport Properties of PA 12-PTMO/AgBF4 Solid Polymer Electrolyte Membranes for Olefin/Paraffin Separation. *Desalination*, Volume 145, pp. 347 - 351.

Murata, K., Hayakawa, T. & Fujita, K., 1997. Excellent Effect of Lithium-doped Sulfated Zirconia Catalysts for Oxidative Coupling of Methane to Give Ethene and Ethane. *Chem. Commun.*, pp. 221 - 222.

Nijmeijer, D. C., 2003. *Gas-Liquid Membrane Contractors for Olefin/Paraffin Separation.* University of Twente: s.n.

Nölken, E., 1966. *Process for Isolating Olefins from Mixtures by Absorption.* USA, Patent No. 3284530.

Okamoto, K. et al., 1999. Olefin/Paraffin Separation through Carbonized Membranes Derived from an Asymetric Polyimide Hollow Fiber Membrane. *Ind. Eng. Chem. Res.*, 38(11), pp. 4424 - 4432.

Otsuka, K. & Komatsu, T., 1987. Active Catalysts in Oxidative Coupling of Methane. *J. Chem. Soc., Chem. Commun*, pp. 388 - 389.

Pak, S. & Lunsford, J. H., 1998. Thermal Effects during the Oxidative Coupling of Methane over Mn/Na2WO4/SiO2 and Mn/Na2WO4/NgO catalysts. *Applied Catalysis A: General*, Volume 168, pp. 131 - 137.

Pan, D., Ji, S., Wang, W. & Li, C., 2010. Oxidative Coupling of Methane in a Dual-bed Reactor Comprising of Particle/Cordierite Monolithic Catalysts. *Journal of Natural Gas Chemistry*, Volume 17, pp. 600 - 604.

Park, J.-H.et al., 1998. Adsorber dynamics and optimal design of layered beds for multicomponent gas adsorption. *Chemical Engineering Science*, 53(23), pp. 3951 - 3963.

Park, Y. S., Won, J. & Kang, Y. S., 2000. Preparation of Poly(ethylene glycol) Brushes on Polysulfone Membranes for Olefin/Paraffin Separation. *Langmuir*, Volume 16, pp. 9662 - 9665.

Pinnau, I. & Toy, L. G., 2001. Solid Polymer Electrolyte Composite Membranes for Olefin/Paraffin Separation. *Journal of Membrane Science*, Volume 184, pp. 39 - 48.

Pirovano, C., Sanfilippo, D., Saviano, F. & Piovesan, L., 2002. *Process for the Separation of Light Olefins from Paraffins.* USA, Patent No. 6414210.

Poling, B. E. et al., 2008. Physical and Chemical Data. In: *Perry's Chemical Engineer's Handbook.* 8th ed. s.l.:McGraw-Hill.

Prausnitz, J. M., 1958. Longitudinal Dispersion in a Packed Bed. *AIChE Journal*, 4(1), pp. 14M - 22M.

Quinn, H. W., 1965. *Use of Complex Fluoro Salts to Separate Olefins from Paraffins.* USA, Patent No. 3189658.

Rameshni, M., 2002. *Cost Effective Options to Expand SRU Capacity Using Oxygen,* s.l.: s.n.

Ray, G. C., 1952. *Recovery of Olefin Hydrocarbons.* USA, Patent No. 2589960.

Rege, S. U., Padin, J. & Yang, R. T., 1998. Olefin/Paraffin Separations by Adsorption: pi-complexation vs. Kinetic Separation. *AIChE Journal*, 44(4), pp. 799 - 809.

Reich, R., Ziegler, W. T. & Rogers, K. A., 1980. Adsorption of Methane, Ethane and Ethylene Gases and their Binary and Ternary Mixtures and Carbon Dioxide on Activated Carbon at 212 - 301 K and Pressures to 35 atmospheres. *Ind Eng. Chem. Process Des. Dev.*, Volume 19, pp. 336 - 344.

Reine, T. A., 2004. *Olefin/Paraffin Separation by Reactive Absorption.* s.l.:The University of Texas at Austin.

Ren, T., Patel, M. K. & Blok, K., 2008. Steam Cracking and Methane to Olefins: Energy Use, CO2 Emissions and Production Costs. *Energy*, Volume 33, pp. 817 - 833.

Richardson, J. F., Harker, J. H. & Backhurst, J. R., 2002. Particle Technology and Separation Processes. In: *Coulson and Richardson's Chemical Engineering.* 5th ed. Oxford: Butterworth-Heinemann.

Robey, R. F., 1941. *Concentration of Olefins.* USA, Patent No. 2245719.

Robey, R. F., 1941. *Process for Concentrating and Storing Olefins.* USA, Patent No. 2235119.

Romero-Perez, A. & Aguilar-Armenta, G., 2010. Adsorption Kinetics and Equilibria of Carbon Dioxide, Ethylene, Ethane on 4A (CECA) Zeolite. *J. Chem. Eng. Data*, 55(9), pp. 3625 - 3630.

Royal Dutch Shell plc, 2013. *Shell will not pursue US Gulf Coast GTL project,* s.l.: s.n.

Ryu, J. H. et al., 2001. Facilitated Olefin Transport by reversible Olefin Coordination to Silver Ions in a Dry Cellulose Acetate Membrane. *Chem. Eur. J.*, 7(7), pp. 1525 - 1529.

Safarik, D. J. & Eldridge, R. B., 1998. Olefin/Paraffin Separations by Reactive Absorption: a Review. *Ind. Chem. Eng. Res.*, 37(7), pp. 2571 - 2581.

Salerno, D., 2013. *Optimal Synthesis of Downstream Process using the Oxidative Coupling of Methane Reaction.* Technische Universität Berlin: s.n.

Sasol Canada, 2013. *Canada Gas-to-Liquids project,* s.l.: s.n.

Sasol, 2013. *Sasol's world-scale ethane cracker & gas-to-liquids facility,* s.l.: s.n.

Savoy, M., 1951. *Concentration of Olefins.* USA, Patent No. 2561822.

Schweer, D., Mleczko, L. & Baerns, M., 1994. OCM in a Fixed-bed Reactor: Limits and Perspectives. *Catalysis Today*, 21(2 - 3), pp. 357 - 369.

Schwittay, C., Turek, T. & Lintz, H.-G., 2001. Oxidative Coupling of Methane to Ethylene in a Reactor-Separator. *Chemie Ingenieur Technik*, 73(6), p. 670.

Seddon, D., 2010. *PETROCHEMICAL ECONOMICS - Technology Selection in a Carbon Constrained World.* s.l.:Imperial College Press.

Shaw, J. A., 1949. *Treatment of Coke-oven Gas.* USA, Patent No. 2471550.

Shell, 2012. *Pearl GTL - an overview,* s.l.: s.n.

Stansch, Z., Mleczko, L. & Baerns, M., 1997. Comprehensive Kinetics of Oxidative Coupling of Methane over the La2O3/CaO catalyst. *Ind. Eng. Chem. Res.*, Volume 36, pp. 2568 - 2579.

Staudt-Bickel, C. & Koros, W. J., 2000. Olefin/Paraffin Gas Separations with 6FDA-based Polyimide Membranes. *Journal of Membrane Science*, Volume 170, pp. 205 - 214.

Steigelmann, E. F. & Hughes, R. D., 1973. *Process for Separation of Unsaturated Hydrocarbons.* USA, Patent No. 3758603.

Strand, C. P., 1950. *Selective Solvent Separation of Unsaturated Hydrocarbons.* USA, Patent No. 2515140.

Suzuki, S., Sasaki, T. & Kojima, T., 1996. New Process Development of Natural Gas Conversion Technology to Liquid Fuels via OCM Reaction. *Energy & Fuels*, Volume 10, pp. 531 - 536.

Tabler, D. C. & Johnson, M. M., 1977. *Hydrocarbon Separations.* USA, Patent No. 4025574.

Talisman Energy, 2012. *Talisman Energy exits GTL project,* s.l.: s.n.

Taniewski, M., Lachowicz, A., Skutil, K. & Czechowicz, D., 1996. The Effect of Dilution of the Catalyst Bed on its Heat-transfer Characteristics in Oxidative Coupling of Methane. *Chemical Engineering Science*, 51(18), pp. 4271 - 4278.

The Linde Group, 2013. *Research cooperation develops innovative technology for environmentally sustainable syngas production from carbon dioxide and hydrogen,* s.l.: s.n.

Thomas, W. J. & Crittenden, B., 1998. *Adsorption Technology and Design.* Oxford: Butterworth-Heinemann.

Tonkovich, A. L., Carr, R. W. & Aris, R., 1993. Enhanced C2 Yields from Methane Oxidative Coupling by Means of a Separative Chemical Reactor. *Science*, 8 October, Volume 262, pp. 221 - 223.

Trans Canada, 2013. *Keystone XL Pipeline.* [Online]
Available at: http://keystone-xl.com/about/the-project/

Triebe, R. W. & Tezel, F. H., 1995. Adsorption of Nitrogen, Carbon Monoxide, Carbon Dioxide and Nitric Oxide on Molecular Sieves. *Gas. Sep. Purif.*, 9(4), pp. 223 - 230.

U.S. Energy Information Administration, 2013. [Online]
Available at: www.eia.gov

Uebele, C. E., Grasselli, R. K. & Nixon, W. C., 1970. *Olefin Recovery Process.* USA, Patent No. 3514488.

Ulrich, G. D. & Vasudevan, P. T., 2006. How to Estimate Utility Costs. *Chemical Engineering,* pp. 66 - 69.

UOP, 2009. *UOP Amine Guard FS Technology for Acid Gas Removal,* s.l.: s.n.

Vakhshouri, K. & Hashemi, M. M. Y. M., 2008. Simulation Study of Radial Heat and Mass Transfer inside a Fixed Bed Reactor. *International Journal of Chemical and Biological Engineering*, 1(1), pp. 1 - 8.

Van Raay, H. G. & Schwenk, U., 1959. *Process for Separating Olefinic Hydrocarbons using Silver Fluoborate and Silver Fluosilicate Solutions.* USA, Patent No. 2913505.

Wang, S. & Zhu, Z. H., 2004. Catalytic Conversion of Alkanes to Olefins by Carbon Dioxide Oxidative Dehydrogenations - A Review. *Energy & Fuels*, Volume 18, pp. 1126-1139.

Wang, Y. & Ohtsuka, Y., 2000. CaO–ZnO Catalyst for Selective Conversion of Methane to C2 Hydrocarbons Using Carbon Dioxide as the Oxidant. *J. Catal.*, Volume 192, p. 252–255.

Wang, Y. & Ohtsuka, Y., 2001. Mn-based binary oxides as catalysts for the conversion of methane to C2 hydrocarbons with carbon dioxide as oxidant. *Applied Catalysis A: General*, Volume 219, p. 183–193.

Wang, Y., Takahashi, Y. & Ohtsuka, Y., 1998. Carbon dioxide-induced selective conversion of methane to C2 hydrocarbons on CeO2 modi®ed with CaO. *Applied Catalysis A: General*, Volume 172, pp. L203 - L206.

Wang, Y., Takahashi, Y. & Ohtsuka, Y., 1999. Carbon Dioxide as Oxidant for the Conversion of Methane to Ethane and Ethylene Using Modified CeO2 Catalysts. *Journal of Catalysis*, Volume 186, p. 160–168.

Wang, Y., Zhuang, Q., Takahashi, Y. & Ohtsuka, Y., 1998. Remarkable enhancing effect of carbon dioxide on the conversion of methane to C2 hydrocarbons using praseodymium oxide. *Catalysis Letters*, Volume 56, p. 203–206.

Wanichko, J., 2014. The ethane addiction: How long will the US advantage last?. *Hydrocarbon Processing.*

World Bank, 2013. [Online]
Available at: http://go.worldbank.org/016TLXI7N0

Yang, J. S. & Hsiue, G. H., 1997. Selective Olefin Permeation through Ag(I) Contained Silicone Rubber-graft-poly (acrylic acid) Membranes. *Journal of Membrane Science*, Volume 126, pp. 139 - 149.

Yang, R. T., 2003. Sorbents for Applications. In: *Adsorbents: Fundamentals and Applications.* s.l.:John Wiley & Sons.

Yang, R. T., 2003. π-complexation Sorbents and Applications. In: *Adsorbents: Fundamentals and Applications.* USA: John Wiley & Sons.

Yucel, H. & Ruthven, D. M., 1980. Diffusion in 4A Zeolite - Study of the Effect of Crysral Size. *J. C. S. Faraday I*, Volume 76, pp. 60 - 70.

Zarrinpashne, S., Ahmadi, R. & Zekordi, M., 2006. *Catalyst Direct Conversion of Methane to Ethane and Ethylene.* USA, Patent No. US20060155157A1.

Zavyalova, U., Holena, M., Schlögl, R. & Baerns, M., 2011. Statistical Analysis of Past Catalytic Data on Oxidative Methane Coupling for New Insights into the Composition of High-Performance Catalysts. *ChemCatChem*, Volume 3, p. 1935 – 1947.

Zhusheng, X. et al., 1996. Role of Steam on the Reaction Performance of Methane Oxidative Coupling over Basic Catalysts. *Chemical Engineering Science*, 51(4), pp. 515 - 519.

Zimmermann, H. & Walzl, R., 2012. Ethylene. In: *Ullmann's Encyclopedia of Industrial Chemistry.* s.l.:Wiley-VCH, pp. 465 - 529.

List of contribution

Scientific papers

Godini H. R., Jašo S., Martini W., Stünkel S., Salerno D., Nghiem Xuan S., Song S., Sadjadi S., Trivedi H., Arellano-Garcia H., Wozny G., 2012. Concurrent Reactor Engineering, Separation Enhancement and Process Intensification: Comprehensive Unicat Approach for Oxidative Coupling of Methane. *Technical Transaction*, 109 (5), pp. 63 – 74.

Shankui S., Stünkel S., Godini H. R., Nghiem Xuan S., Wozny G., Yuan J., 2012. Investigation on membrane-assisted CO2 removal process for oxidative coupling of methane in mini-plant scale. *Technical Transaction*, 109 (5), pp. 223 – 232.

Nghiem Xuan S., Arellano-Garcia H., Tran T. K., Wozny G., 2012. Oxidative Coupling of Methane: a new process concept for the improvement of the downstream processing by using adsorption, *Technical Transaction*, 109 (5), pp. 233 – 242.

Godini H. R., Xiao S., Jašo S., Stünkel S., Salerno D., Nghiem Xuan S., Song S., Wozny G., 2013. Techno-Economic Analysis of Integrating the Methane Oxidative Coupling and Methane Reforming Processes, *Fuel Processing Technology,* Volume 106, pp. 684–694.

Conferences

Oral presentation at 2nd Doktorandenseminar Adsorption, Braunschweig, Germany, September 15 – 16, 2011. *Adsorption Process in the Downstream of Oxidative Coupling of Methane*.

Oral presentation at AIChE Annual Meeting, Minneapolis, USA, October 16 – 21, 2011. *Adsorptive Separation in the Downstream of the Oxidative Methane Coupling Process*.

Oral presentation at 19th International Conference Process Engineering and Chemical Plant Design, Krakow, Poland, September 25 – 27, 2012. *Oxidative Coupling of Methane: a new process concept for the improvement of the downstream processing by using adsorption*.